Title

Study on the dilute solution properties of poly (Methylmethacrylateco-acrylamide)

Permalink

https://escholarship.org/uc/item/3z81w58x

Author

Oh, Seaung,

Publication Date

1991

Peer reviewed|Thesis/dissertation

Study on the Dilute Solution Properties of Poly (Methylmethacrylate-co-Acrylamide)

by

Seaung Oh

B.S. Seoul National University, 1979
M.S. Seoul National University, 1984

DISSERTATION

Submitted in partial satisfaction of the requirements for the degree of

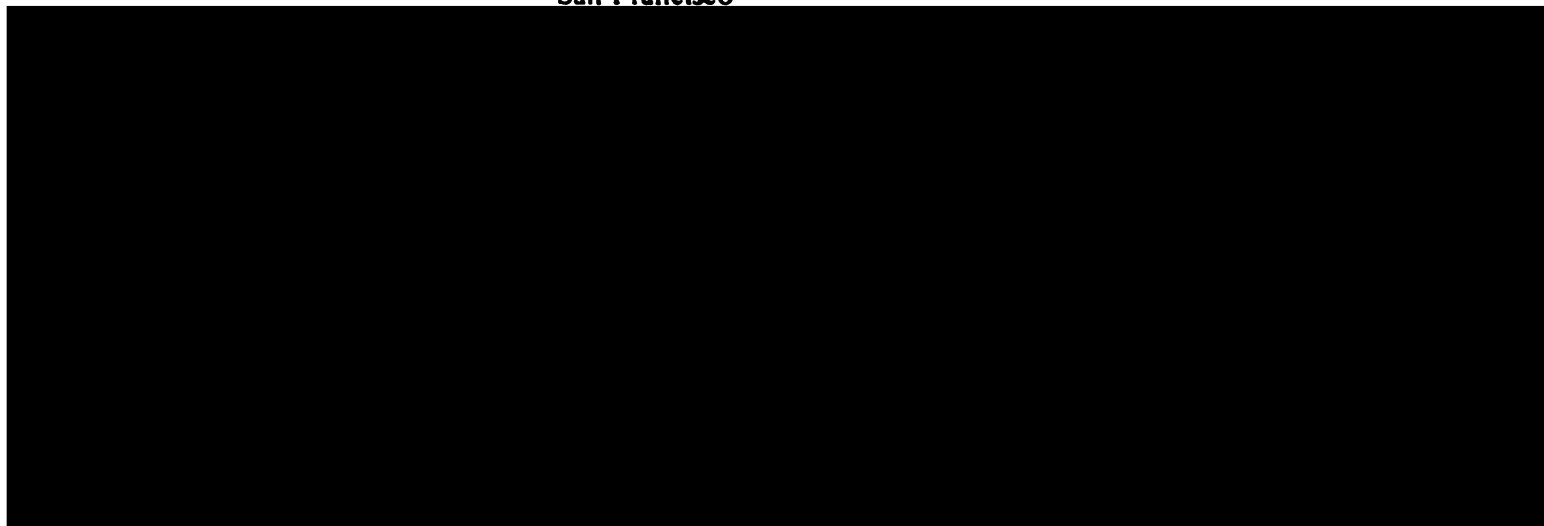## DOCTOR OF PHILOSOPHY

in

Pharmaceutical Chemistry

in the

GRADUATE DIVISION

of the

UNIVERSITY OF CALIFORNIA

San Francisco

Date . . . . University Librarian . . . . . .

Degree Conferred: . . 3/25/91 . . . .

To my parents

ACKNOWLEDGEMENTS

Study on the Dilute Solution Properties of

Poly (Methylmethacrylate -co- Acrylamide)

by

Seaung Y. Oh

Departments of Pharmacy and Pharmaceutical Chemistry

University of California, San Francisco

Abstract

Dilute solution properties of a copolymer of acrylamide(AA) and methylmethacrylate(MMA) (48/52 mole %) in N-methylformamide are studied by static and dynamic light scattering and viscometry. The copolymer was prepared by free radical polymerization in ethanol with 2, 2'-azobisisobutyronitrile as initiator. The reactivity ratios for the monomers were determined (r_{MMA} = 3.20, r_{AA} = 0.31), and they show that the copolymer is random. Fractionation by molecular weight was carried out in N-methyl formamide (solvent) - ethanol (nonsolvent) system. The molecular weights and second virial coefficients of the fractions were determined by measuring the average intensity of scattered light. Intrinsic viscosities were measured using an Ostwald viscometer. The Huggins' constant for each fraction is well within the range usually observed for many species of linear polymers in good solvents. Diffusion coefficients were measured by dynamic light scattering. The coefficient for the first order concentration dependence of diffusion coefficient agrees well with theoretical calculations. The second virial coefficient, intrinsic viscosity, diffusion coefficient are expressed in terms of power of molecular weight and the exponents obtained are -0.260, 0.662, 0.582 , respectively. These exponents are in good agreements with theoretically predicted values for non-draining self-avoiding flexible linear chain molecules. The ratios between equivalent sphere radii calculated from second virial coefficient (R_T), intrinsic viscosity (R_V), diffusion coefficient (R_H) are compared with theoretical predictions

iv

for non-draining self-avoiding linear chain molecules. The ratios obtained, $R_V/R_H = 1.07$, $R_T/R_H = 0.96$, $R_V/R_T = 1.11$ show good agreement with the theoretically predicted ratios, $R_V/R_H = 1.12$, $R_T/R_H = 1.02$, $R_V/R_T = 1.10$. These findings extend results observed for homopolymers and alternating copolymers to random copolymers consisting of comonomers with very different polarities.

Thesis Chairman: _____ Ronald A. Siegel Sc. D

TABLE OF CONTENTS

CHAPTER 4. DIMENSIONAL STUDY IN DILUTE SOLUTION

CHAPTER 5. CONCLUSIONS AND SUGGESTIONS FOR FUTURE WORK

LIST OF TABLES

LIST OF FIGURES

Chapter 1 INTRODUCTION

1.1 Background

Large scale dilute solution properties of flexible chain polymers, such as radius of gyration

(R_G), second virial coefficient (A_2), diffusion coefficient (D_0) and intrinsic viscosity ($[\eta]$), have been

the subject of both theoretical consideration and experimental measurement (Yamakawa, 1971,

Freed, 1987). These properties reflect the polymer size in the solution. R_G is the root-mean-

square distance of the segments of the polymer chain from its center of gravity; A_2 is proportional

to an effective volume excluded to a molecule by another molecule in solution; D_0 is related to

the apparent "hydrodynamic" size of a molecule as it drifts through a solvent; and $[\eta]$ is another

measure of the polymer molecules' hydrodynamic volume influencing the rate of energy

dissipation during shear flow of the polymer solution.

Experimental measurements of these dilute solution properties have been carried out in

various polymer-solvent systems, and the data are used extensively in testing the theories which

predict the influence of chain length and the polymer-solvent thermodynamic interactions

(Yamakawa, 1971, Freed, 1987). Such data have also been used in the study of chain branching

architecture (Douglas et al, 1990, Bauer et al, 1989, Rey et al, 1987) and chain conformation

(Murakami et al, 1980, Krigbaum et al, 1988).

Theoretical considerations of these properties had been carried out since 1930's, since

Staudinger (1930) found that the molecular weight of a polymer is related to the intrinsic viscosity

of its dilute solution (Yamakawa, 1971). In 1949, Flory introduced an important concept, called

excluded volume (Flory, 1953). This effect arises from the fact that two segments in a chain

cannot occupy the same space at the same time. He also introduced a state, called the "θ-state",

where the excluded volume effect vanishes and the polymer chain behaves like an ideal random

1

flight chain. These concepts laid the foundation for the development of dilute polymer solution theories.

Many theoretical attempts have been made to establish the effect of excluded volume on various solution properties. The main part of the theory developed is the so-called two parameter theory (Yamakawa, 1971). In the two parameter theory, the dilute solution properties are expressed in terms of two basic parameters; one is the mean square radius of gyration of a chain in the θ-state ($<S_0^2>^{1/2}$) and the other is the excluded volume parameter, z, which is proportional to the effective volume excluded for a pair of chain elements and also to the square root of the number of elements in the chain. However, the validity of this theory is confined to the range of small z, i.e., near the θ-point, because the excluded volume perturbation series converges very slowly. Various approaches have been used to derive an approximate closed expression for the excluded volume perturbation series, which can be used for large z (Yamakawa, 1971). Recently, it has become possible to overcome this limitation by applying the renormalization group approach which enables the resummation of the excluded volume perturbation series to obtain closed-form expressions that can be used over a wide range of excluded volume interactions (Oono et al, 1983, Douglas et al, 1984).

Renormalization group theory predicts that, in the non-draining self-avoiding limit, dilute solution properties exhibit power scaling laws against molecular weight (M) given by (Oono et al, 1983)

$$R_G \sim M^\nu, \quad A_z \sim M^{\nu d-2}, \quad D_0 \sim M^{-(d-2)\nu}, \quad [\eta] \sim M^{\nu d-1} \qquad (1.1.1)$$

where ν is the characteristic exponent for the radius of gyration and d is the dimension.

Flory (1949, 1953) calculated the scaling of the radius of gyration with molecular weight for a single chain in a good solvent in three dimensions using mean-field theory. His method can also be used for other dimensions, d, than three(de Gennes, 1979, Freed, 1987):

$$<R_G^2>^{1/2} \sim M^v, \quad v = 3/(d+2) \tag{1.1.2}$$

The above formula gives the correct value for d = 1 and d = 4 (de Gennes, 1979). It seems to be correct in two dimensions (Nienhuis, 1982). In three dimensions, v = 0.6 and this value is consistent with some Monte-Carlo calculations (Alexandrowicz, 1983, Havlin et al, 1983). A more rigorous treatment by renormalization group theory predicts a slightly smaller value than 0.6, namely 0.588 (Le Guillou et al, 1980). A similar value, 0.5875, is obtained by careful extrapolation of exact enumerations (Majid et al, 1983). Recent Monte-Carlo calculations by de Forcrand et al (1987) and Madras et al (1988) also give similar values, 0.5745 and 0.592, respectively. The Flory value 0.6 for three dimensions can be considered exact for most practical applications (de Gennes, 1979). Hence the scaling expression for the dilute solution properties in the non-draining self-avoiding limits for three dimensions are, approximately,

$$R_G \sim M^{0.6}, \quad A_z \sim M^{-0.2}, \quad D_0 \sim M^{-0.6}, \quad [\eta] \sim M^{0.8} \tag{1.1.3}$$

The hydrodynamic radius (R_H) can be calculated from D_0 and Stokes-Einstein equation

$$D_0 = kT/6\pi\eta_0 R_H$$

where k is the Boltzmann constant, T the absolute temperature, η_0 the solvent viscosity and R_H the hydrodynamic radius. Because D_0 is proportional to $M^{-0.6}$, R_H should be proportional to $M^{0.6}$. Below the asymptotic limit, where the molecular weight is not large enough or the solvent is

3

not a good solvent, the ν value is expected to be smaller than 0.6, but larger than 0.5, which is the ν value in the θ-state (Yamakawa, 1971).

Experimental results of ν from the polystyrene-benzene system show that the exponent for the radius of gyration R_G, a "static" property, is close to the predicted value, 0.6, while the exponent for R_H, representing a "dynamic" property, is smaller than the predicted value (Miyaki et al,1978, Yamamoto et al, 1971, Adam et al, 1977). Similar results are also obtained for the polystyrene-toluene and polystyrene-ethylbenzene systems (Appelt et al, 1980, Bhatt et al, 1988). Weil et al (1979) suggest that the reason for this discrepancy is the much faster approach of R_G to the limiting behavior than R_H. However, Nemoto et al (1984) point out that it is difficult to conceive that the asymptotic range is not reached for R_H even at a molecular weight of 1.34 x 10^7, the highest molecular weight used in their work.

In addition to the scaling law expression, renormalization group theory also predicts, in the non-draining self-avoiding limit, the universal ratios between the dilute solution properties, which are independent of the chemical details of the polymer chain. These ratios are

$$U_{\eta s} = \frac{M\,[\eta]}{N_A\,R_G^3} = 4.078 \tag{1.1.4}$$

$$U_{A\eta} = \frac{(A_2 M)}{[\eta]} = 1.196 \tag{1.1.5}$$

$$U_{f s} = \frac{f}{\eta_0\,R_G} = 12.067 \tag{1.1.6}$$

$$U_{\eta f} = \left(\frac{M\,[\eta]}{N_A}\right)^{\frac{1}{3}} \frac{\eta_0}{f} = 0.1297 \tag{1.1.7}$$

In equations above, f is the friction coefficient defined as $6\pi\eta_0 R_H$ where η_0 is the viscosity of the solvent and N_A the Avogardro's number. $U_{\eta S}$ is the ratio containing $[\eta]$ and R_G. $U_{A\eta}$, U_{fs} and $U_{\eta f}$ are the ratios containing corresponding properties denoted by the subscripts. The universal nature of these ratios can be seen by the same molecular weight dependency of the numerator and the denominator in the asymptotic range.

These universal ratios are frequently represented in terms of the ratios between equivalent solid sphere sizes. Einstein's equation for the viscosity of a dilute suspension of hard spheres yields (Yamakawa, 1971)

$$[\eta] = 2.5\, N_A V_\eta / M \tag{1.1.8}$$

where N_A is the Avogardro's number and V_η is the equivalent volume of the sphere with radius R_V. By replacing $[\eta]$ in Eq. 1.1.4 with $2.5\, N_A \cdot (4/3\pi R_V^3)/M$, the universal ratio between R_V and R_G, 0.73, can be obtained. The second virial coefficient for hard spheres in dilute solution is given by (Yamakawa, 1971)

$$A_2 = 4 N_A \cdot V_A / M^2 \tag{1.1.9}$$

where V_A is the equivalent volume of the hard sphere with radius R_T. By the subsitution of A_2 in Eq. 1.1.5 with $4 N_A \cdot (4/3\pi R_T^3)/M^2$, the universal ratio between R_T/R_V, 0.91, can be obtained. R_H/R_G and R_V/R_H values can be calculated from Eq. 1.1.6 and Eq. 1.1.7, respectively in combination with the Stokes-Einstein equation. The ratios of these radii may be written as $R_G:R_V:R_T:R_H = 1.56:1.12:1.02:1.00$. Experimental results from various systems show good agreement with these theoretically predicted values (Oono et al, 1983, Davidson et al, 1987).

1.2 Scope of the Thesis

Until now, most of the experimental measurements of dilute solution properties for the comparison with theory have used homopolymers such as polystyrene and poly(α-methylstyrene) because these samples are available in nearly monodisperse form for a wide range of molecular weights. Polyisoprene has been studied recently (Davidson et al, 1987). These polymers were studied in aromatic solvents such as benzene (Nemoto et al, 1984, Miyaki et al, 1978, Appelt et al, 1980), toluene (Roover et al, 1980, Huber et al, 1985) and ethylbenzene (Venkataswamy, 1986) and the results showed good agreements with theoretical predictions by Oono (1983). Copolymers are rarely used for comparison with theory. Recently, alternating copolymers of ethylene and tetrafluoroethylene have been studied (Wang et al, 1990, Chu et al, 1989). The exponents obtained from the molecular weight dependence of dilute solution properties showed good agreement with the theoretically predicted values.

In the present thesis work, we studied the dilute solution properties of a copolymer composed of two monomers with very different polarities. These properties are expressed in terms of power of molecular weight and are compared with each other in terms of equivalent size, in order to provide tests of dilute solution theories. The copolymer employed in this work is the random copolymer of methylmethacrylate and acrylamide. The structures of the monomers used in this work are shown in Fig 1.1.

$$CH_2 = CH$$
$$|$$
$$C = O$$
$$|$$
$$NH_2$$

$$CH_3$$
$$|$$
$$CH_2 = C$$
$$|$$
$$C = O$$
$$|$$
$$OCH_3$$

Acrylamide (AA)   Methylmethacrylate (MMA)
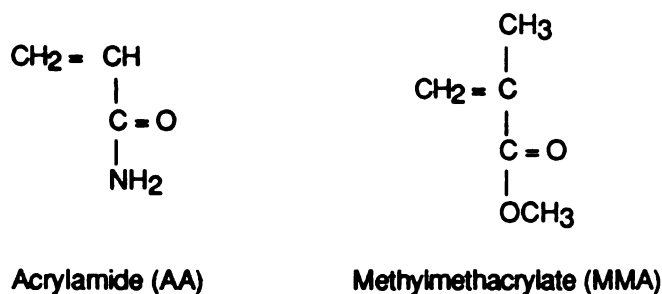
Fig. 1.1   Structure of two monomers used in this work

Acrylamide is a very hydrophilic monomer which is freely miscible with water. On the other hand, methylmethacrylate is a hydrophobic monomer which is insoluble to water. The structure of the copolymer is shown in Fig. 1.2, where the m and n subscripts denote the relative molar contents of acrylamide and methylmethacrylate.

$$
\begin{array}{ccc}
& & CH_3 \\
& & | \\
\underline{\quad} CH_2\text{-}CH \underline{\quad\quad} CH_2 \underline{\quad} C \underline{\quad\quad} \\
& | & | \\
& C=O & C=O \\
& | & | \\
& NH_2 & OCH_3 \\
& m & n
\end{array}
$$
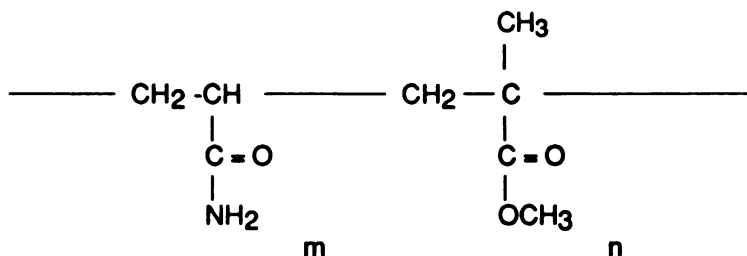
Fig. 1.2 Structure of the copolymer used in this work

The dilute solution properties of this copolymer are studied in an amphiphilic solvent, N-methylformamide.

The preparation of monomers, intitiator and solvent is described in Chapter 2, along with the synthesis and purification of the copolymer.

The characterization of the copolymer is provided in Chapter 3. Reactivity ratios for each monomer are determined and used in the analysis of the microstructure of the copolymer molecules. Compositional distribution due to the change of the feed composition is minimized by stopping the polymerization reaction at very low conversion. Fractionation by molecular weight is carried out and the molecular weight and second virial coefficient of each fraction are determined by static light scattering.

In Chapter 4, intrinsic viscosity and the diffusion coefficient of each fraction are measured. The results and the second virial coefficient are described using power scaling laws against

7

molecular weight and are analysed in terms of equivalent sizes. It will be shown that the data are in good agreement with theoretical predictions.

Conclusions and suggestions for future work are discussed in Chapter 5.

References

M. Adam and M. Delsanti, Macromolecules, 10, 1229, 1977

Z. Alexandrowicz, Phys. Rev. Lett. 50, 736, 1983

B. Appelt and G. Meyerhoff, Macromolecules, 13, 657, 1980

B. J. Bauer, L. J. Fetters, W. W. Graessley, N. Hadjichristidis and G. F. Quack, Macromolecules, 22, 2337, 1989

M. Bhatt and A. M. Jamieson, Macromolecules, 19, 124, 1986

N. S. Davidson, L. J. Fetters, W. G. Funk, N. Hadjichristidis and W. W. Graessley, Macromolecules, 20, 2614, 1987

Ph. de Forcrand, F. Koukiou and D. J. Petritis, J. Stat. Phys., 49, 223, 1987

P. G. de Gennes, Scaling Concepts in Polymer Physics, Cornell University Press, Ithaca, New York, 1979

J. F. Douglas and K. F. Freed, Macromolecules, 17, 2354, 1984

J. F. Douglas and K. F. Freed, Macromolecules, 17, 2334, 1984

J. F. Douglas, J. Roovers and K. F. Freed, Macromolecules, 23, 4168, 1990

P. J. Flory, J. Chem. Phys., 17, 303, 1949

P. J. Flory, Principles of Polymer Chemistry, Cornell University Press, Ithaca, 1953

K. F. Freed, Renormalization Group Theory of Macromolecules, John Wiley & Sons, New York, 1987

S. Havlin and D. Ben-Avraham, Phys. Rev., A27, 2759, 1983

W. R. Krigbaum and T. Tanaka, Macromolecules, 21, 743, 1988

J. C. Le Guillou and J. Zinn-Justin, J. Phys. Rev. B. 21, 3976, 1980

N. Madras and A. D. Sokal, J. Stat. Phys., 50, 109, 1988

I. Majid, Z. V. Djordevic and H. E. Stanley, Phys. Rev. Lett., 51, 1282, 1983

Y. Miyaki, Y. Einaga and H. Fujita, Macromolecules, 11, 1180, 1978

H. Murakami, T. Norisuye and H. Fujita, Macromolecules, 13, 345, 1980

N. Nemoto, Y. Makita, Y. Tsunashima and M. Kurata, Macromolecules, 17, 425, 1984

B. Nienhuis, Phys. Rev. Lett., 49, 1062, 1982

Y. Oono and M. Kohmoto, J. Chem. Phys., 78, 520, 1983

Y. Oono and M. Kohmoto, J. Chem. Phys., 79, 4629, 1983

A. Rey, J. J. Freire and J. G. de la Torre, Macromolecules, 20, 342, 1987

H. Staudinger, Kolloid Z., 51, 71, 1930

G. Weil and J. des Cloizeaux, J. Phys. (Orsay, Fr.), 40, 99, 1979

H. Yamakawa, Modern Theory of Polymer Solutions, Harper and Row, New York, 1971

A. Yamamoto, M. Fujii, G. Tanaka and H. Yamakawa, Polym. J., 2, 799, 1971

Chapter 2   POLYMER PREPARATION

2.1   Introduction

The purity of commercially available monomers is usually not high enough for their use, without treatment, in well-controlled polymerization reactions (Collins et al,1973). So, monomers must be further purified and their purity checked before they are used. The same criteria also apply to the purity of solvents used in a polymerization reaction. In addition polymerization, it is especially important to exclude water to ensure good control of polymerization. Air also should be excluded before starting the polymerization. The purpose of this chapter is to describe the methods and apparatus used to prepare the monomers, initiator, solvent and poly (methyl methacrylate-co-acrylamide).

2.2   Materials and Apparatus

All chemicals and reagents have been used as received unless otherwise indicated. Methyl methacrylate (MMA) and the free radical initiator Azobisisobutyronitrile (AIBN) were obtained from Polysciences, Inc. Acrylamide(AA) (99+%, electrophoresis grade) was purchased from Aldrich Chemical Company, Inc. Absolute ethanol was obtained from Gold Shield Chemical Co. For the dehydration of ethanol, a Distillation Apparatus for Solvent Repurification (Kotes Glass Co.) was used. Doubly distilled and deionized water (Barnstead Nanopure System) was used to prepare the aqueous NaOH (MallincKrodt) solution. Anhydrous methyl alcohol (99+%), calcium hydride (95+%), N,N-dimethyl formamide (99+%, A.C.S. Reagent) and N-methyl formamide were purchased from Aldrich Chemical Company Inc. and were used as received. Ethyl ether (anhydrous, A.C.S. Reagent) and acetone (certified A.C.S.) were obtained from Fisher Scientific and were used as received. Mineral oil (Aldrich) was used for the oil bath. For

constant temperature control, a Lauda model MS Immersion Circulator (Fisher Scientific) was used. A Thomas Hoover melting point apparatus was used for the measurement of melting point.

2.3   Monomer Purification

2.3.1 Recrystallization of Acrylamide

AA is received from Aldrich in the form of white solid granules. It must be recrystallized from methanol/ethyl ether before use. After recrystallization, the melting point is measured to check the purity.

a. Procedure

1) A solution of AA in methanol (1.53g/ml) is prepared in a water bath at 35°C with stirring.

2) The solution is allowed to cool to room temperature for 3 hours. Crystallization occurs slowly.

3) The same volume of ethyl ether is added to the solution.

4) The solution is cooled in an ice bath overnight.

5) Crystals are recovered by filtering on a fritted glass filter followed by washing with ice-cooled ethyl ether.

6) Crystals are dried in vacuum overnight at room temperature.

7) Dried AA is stored in a tightly sealed bottle wrapped with Parafilm in dessicator. The dessicator was stored in dark place.

Recrystallized AA consists of white needles. Usually the recrystallization yield is 65-75%.

b. Melting Point Measurement

Melting point is measured by the capillary-tube method (Pasto & Johnson,1979). A portion of finely ground recrystallized AA is introduced into a fine glass capillary, 1mm by 100mm, sealed at one end. Enough sample is placed in the capillary-tube and firmly packed by tapping against the bench until a column of sample 2 to 3 mm is obtained. After insertion of the capillary tube into the melting point apparatus, heating of the capillary tube begins at a rate of 1.5^O C/min. The melting point range obtained was 83.5-84.8^{O}C, which is in good agreement with the literature value, 84-85°C (Handbook Chem. Phys.,68th Ed.).

2.3.2 Distillation of Methylmethacrylate

Monomers for radical polymerization usually contain inhibitors when received, which prevent polymerization during shipment and storage. For example, the MMA from Polysciences contains the inhibitor hydroquinone (1,4-dihydroxybenzene, HQ) at levels of 10-2000 ppm (Catalog, Polyscience). These can be extracted by washing the monomer with dilute acid or base, depending on the type of inhibitor. After removing the inhibitor, monomer of high purity can be obtained by distillation.

a. Removal of Inhibitor

1) Roughly equal parts of 10% aqueous NaOH and MMA are placed in a separatory funnel and mixed by tumbling (1-2 minutes).

2) After clear separation of two phases, the heavier aqueous phase is drained off.

3) The procedure is repeated twice.

13

4) The MMA is then washed with distilled water.

5) As a drying agent, anhydrous sodium sulphate (Na_2SO_4) is added to the monomer (100g/l).

6) After 30 minutes with stirring, MMA is gravity filtered through a Whatman Qualitative filter.

b. Distillation

MMA is liquid at room temperature and is purified by vacuum distillation. The apparatus used in this procedure is shown in Figure 2.3. 1. Because the boiling point of water is very close to that of MMA, CaH_2 (2% W/V) was used to remove remaining water during distillation (Gordon & Ford,1972). The boiling point of MMA is 100-101° C at 760 mm Hg (Handbook Chem. Phys.,68th Ed.).

Procedure:

1) MMA is placed in the distilling flask with a magnetic stirring bar. The distillation flask is filled to not more than 50% of capacity.

2) CaH_2 (2% W/V) is introduced into distillation flask very slowly.

3) The distillation flask is connected to the distillation head and then to the condenser and vacuum line as shown in Figure 2.3.1.

4) The temperature is raised slowly after the vacuum has been applied.

5) Collection of distilled MMA starts after the first distillate fraction (5-10 ml) is discarded.

6) Distillation is stopped by removing the heating mantle and then purging with argon gas. This is done before the distillation flask has gone to dryness.

14
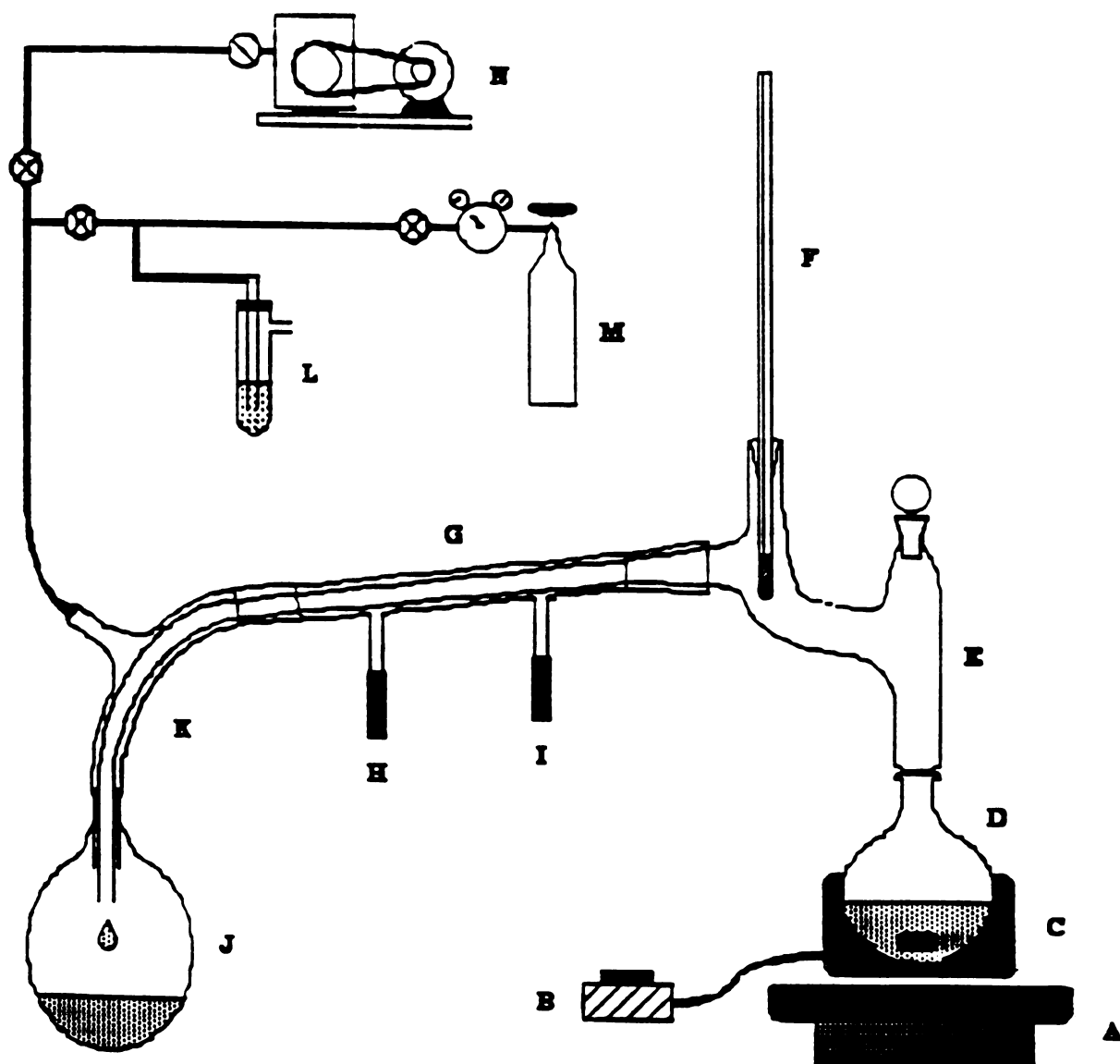
Figure 2.3.1 Apparatus for the vacuum distillation of MMA. A, magnetic stirrer; B, Variac voltage regulator; C, heating mantle; D, distillation flask; E, Claisen head; F, thermometer; G, condenser; H, water inlet; I, water outlet; J, receiving flask; K, vacuum adapter; L, bubbler; M, argon tank; N, vacuum pump (Firestone, 1989).

15

7) The collection flask is removed from the distillation setup and is capped with a serum stopper. The serum stopper is wrapped with Parafilm to avoid water. The collection flask is wrapped with aluminum foil to avoid light, and then stored in the freezer at -20° C.

The presence of polymer in distilled MMA was tested by adding a few drops of MMA into methanol. There was no turbidity developed, indicating that there is no polymer.

2.4   Initiator Purification

Commercial grade initiator AIBN from Polysciences is a white granular solid. It was purified by recrystallization from anhydrous methanol.

Procedure:

1) A solution of crude AIBN in anhydrous methanol (16g/100ml) is prepared in water bath at 40° C.

2) The solution is filtered by gravity through a Whatman Qualitative filter in oven at 40° C.

3) The filtrate is cooled at room temperature for about an hour. Crystals begin to form.

4) The filtrate is cooled in refrigerator at 4° C overnight.

5) The crystals are collected on a fritted glass filter and are washed with ice-cooled anhydrous methanol.

6) Crystals are air dried for 3 days in the dark place at room temperature and are then stored in a tightly sealed bottle wrapped with Parafilm in a light protected dessicator.

Recrystallized AIBN has the appearance of fine white needles. Yield was about 70%.

2.5 Dehydration of Ethanol

Pure ethanol is commercially available as "absolute" grade, which contains about 0.1 to 0.5% water plus (by law) anywhere from 0.5 to 10% of a denaturant (Gordon & Ford, 1972). Ethanol was purified by refluxing and distillation before use in the polymerization.

Procedure:

1) Commercial ethanol of "absolute" grade (50 ml) is introduced in the distillation flask with magnesium turnings (2.5g) and a few drops of chloroform as catalyst.

2) This mixture is refluxed for about 10 hours. A lot of bubbles (hydrogen gas) are generated.

3) 950 ml of "absolute" grade commercial ethanol is added to the mixture and distillation starts.

4) Distilled ethanol is used immediately.

Distilled ethanol was transfered strictly under argon gas.

2.6 Polymerization

The polymer was prepared by free radical polymerization in ethanol. The flask used in polymerization was washed and dried in an oven. When the flask was still warm, it was flushed with argon gas and capped with a serum stopper to avoid moisture from air.

Procedure:

1) AA, AIBN and magnetic stirring bar are placed in polymerization flask.

2) The mixture is degassed for 10 minutes by room vacuum and then flushed with argon gas.

3) Ethanol is introduced into the flask under argon gas pressure using a long transfer needle.

4) The mixture (solution) is degassed for 10 minutes by room vacuum with stirring and then filled with argon gas.

5) MMA is introduced into the flask by syringe.

6) Polymerization is carried out on 70° C constant temperature oil bath with stirring.

7) Polymerization is stopped by removing the flask from the oil bath and cooling quickly in ice.

8) Polymer remaining in solution is recovered by the addition of about 10 volumes of a nonsolvent.

9) Polymer already precipitated is dissolved in a suitable solvent and recovered by the addition of a nonsolvent as in step (8).

10) The precipitated polymer is collected by filtration using a fritted-glass filter.

11) The polymer is dried in a vacuum oven overnight at 60° C .

12) The dried polymer is weighed to calculate the percentage of monomer which is converted to polymer.

2.7   Purification of Polymer

Polymers are purified by repeating the cycle of dissolving, precipitation and washing.

Procedure:

1) The dried polymer is dissolved in a solvent(about 5% w/v).

2) Polymer solution is added dropwise to about 10 volumes of nonsolvent with vigorous stirring.

3) Precipitated polymer is recovered by filtering on fritted-glass filter.

4) Recovered polymer is washed in 10-20 volumes of nonsolvent on a fritted-glass filter.

5) Without drying the recovered polymer, steps (1) through (4) are repeated.

6) Finally, polymer is dried in a vacuum oven overnight at 60° C.

The purified polymer was stored in a dessicator in the dark place at room temperature.

References

Chemical and Supply Catalog, Polysciences, Inc., 1989-1990

E. A. Collins, J. Bares and F. W. Billmeyer, Jr., Experiments in Polymer Science, Chapter 3 & 4, John Wiley & Sons, New York,1973

B. A. Firestone, in Thesis, "Swelling and transport properties of hydrophobic polyelectrolyte gels", University of california, San Francisco, 1989

A. J. Gordon and R. A. Ford, The Chemist's Companion, John Wiley & Sons, New York, 1972

Handbook of Chemistry and Physics, 68th Ed., CRC press, 1987-1988

D. J. Pasto and C. R. Johnson, Laboratory Text for Organic Chemistry, Prentice-Hall, Inc., 1979

Chapter 3 POLYMER CHARACTERIZATION

3.1 Introduction

When a polymer is synthesized, it is heterogeneous in terms of molecular weight; that is, there is a molecular weight distribution (Flory,1953). In the case of copolymers, they have additional distributions of chemical composition (Stockmayer,1945) and sequence length (Allcock & Lampe,1981). Because many physical properties of a polymer are affected by these distributions, it is necessary to understand the nature of these distributions.

The purpose of this chapter is to describe three experiments, and the theories behind them, to characterize the copolymer, Poly(MMA-co-AA). Determination of the reactivity ratios provides information about the chemical composition distribution as well as sequential distribution of monomers, while fractionation and subsequent determination of molecular weight provide knowledge about the nature of molecular weight distribution.

3.2 Reactivity Ratio Determination

The composition of a copolymer in most instances is found to be different than that of the comonomer feed from which it is produced. This is because different monomers have differing tendencies (reactivities) to undergo copolymerization. When a copolymer is made from a feed of two kinds of monomers, the composition of each monomer is determined, in overall amount, by their relative concentration in the feed and by their reactivities (Flory,1953). Sequential distribution of each monomer in a copolymer molecule is also determined by the same factors (Alfrey et al,1944).

In this section, the copolymer composition equation is reviewed. This equation gives the composition of the copolymer being formed, at a given instant, in terms of the combination of the monomer feed composition and the relative reactivities of the two monomers. Experimental determination of relative reactivities is carried out. Sequential distribution of the comonomers in the copolymer molecule is considered. Finally, a Monte Carlo simulation of the actual generation of copolymer molecules is discussed.

3.2.1 Copolymer Composition Equation

When a copolymer is synthesized by free-radical polymerization from a reaction mixture of two monomers, M_1 and M_2, we can consider two types of propagating radicals - one with M_1 at the propagating end and the other with M_2 (Allcock & Lampe, 1981). These can be represented by $M_1 \cdot$ and $M_2 \cdot$ where the dot represents a radical. If it is assumed that the reactivity of a particular radical is independent of its size, and of the nature of the polymeric chain bound to the radical, and is dependent only on the monomer unit at the end of the chain, four propagation reactions are then possible

$$M_1 \cdot + M_1 \longrightarrow M_1 \cdot \qquad (3.2.1)$$

$$M_1 \cdot + M_2 \longrightarrow M_2 \cdot \qquad (3.2.2)$$

$$M_2 \cdot + M_1 \longrightarrow M_1 \cdot \qquad (3.2.3)$$

$$M_2 \cdot + M_2 \longrightarrow M_2 \cdot \qquad (3.2.4)$$

K_{11} is the rate constant for a propagating chain ending in M_1 adding to monomer M_1, and so on. The rates of monomer depletion, which are equal to their rates of incorporation into the copolymer, can be given by

$$- d[M_1]/dt = K_{11} [M_1 \cdot] [M_1] + K_{21} [M_2 \cdot] [M_1] \qquad (3.2.5)$$

22

$$- d[M_2]/dt = K_{12} [M_1 \cdot] [M_2] + K_{22} [M_2 \cdot] [M_2] \tag{3.2.6}$$

Dividing Eq. (3.2.5) by Eq. (3.2.6) yields

$$\frac{d[M_1]/dt}{d[M_2]/dt} = \frac{K_{11} [M_1 \cdot] [M_1] + K_{21} [M_2 \cdot] [M_1]}{K_{12} [M_1 \cdot] [M_2] + K_{22} [M_2 \cdot] [M_2]} \tag{3.2.7}$$

Free radicals undergo a mutual termination reaction very rapidly due to their high reactivity and are thus removed from the reaction system. If the initiation reaction is slow, an steady state is attained whereby the rate of formation of radicals is exactly balanced by their rate of disapperance. Under these circumstances a steady state concentration of free radicals will exist for any initiator concentration. As long as the initiator concentration is essentially unchanged, the equilibrium concentration of free radicals can be assumed to be constant. This is the so-called steady state assumption (North,1966). Applying this assumption to each of the radicals, we have

$$K_{21} [M_2 \cdot] [M_1] = K_{12} [M_1 \cdot] [M_2] \tag{3.2.8}$$

Eq. (3.2.7) is not directly usable because it has a term for the concentration of radicals. It is very difficult to measure the radical concentrations, because they are very low (10^{-8} M) (Odian,1984). The term for the concentration of radicals can be removed by combining Eq. (3.2.8) with Eq. (3.2.7):

$$d[M_1]/d[M_2] = [M_1]/[M_2] \{ (r_1[M_1] + [M_1]) / ([M_2] + r_2[M_2]) \} \tag{3.2.9}$$

where r_1 and r_2 are monomer reactivity ratios defined by

23

$$r_1 = K_{11}/K_{12} \text{ and } r_2 = K_{22}/K_{21} \qquad (3.2.10)$$

Thus r_1 represents the ratio of the rate constants for the reaction of M_1 radical with monomer M_1 and with monomer M_2, respectively. Similarly, the r_2 expresses the relative reactivity of an M_2 radical toward an M_2 compared with an M_1 monomer. The quantity $d[M_1]/d[M_2]$ given by Eq. (3.2.9) represents the ratio of the two comonomers in the increment of polymer formed when the ratio of unreacted monomer is $[M_1]/[M_2]$. Eq. (3.2.9) is known as the copolymer composition equation or the copolymerization equation. The copolymerization equation can also be expressed in terms of mole fractions instead of concentration. If F_1 and F_2 are the mole fractions of monomers M_1 and M_2 in the feed, and f_1 and f_2 are the mole fractions of M_1 and M_2 in the copolymer, then

$$F_1 = 1 - F_2 = [M_1]/([M_1] + [M_2]) \qquad (3.2.11)$$

$$f_1 = 1 - f_2 = d[M_1]/(d[M_1] + d[M_2]) \qquad (3.2.12)$$

Combining Eq. (3.2.11) and (3.2.12) with Eq. (3.2.9) yields

$$f_1 = (r_1 F_1^2 + F_1 F_2)/(r_1 F_1^2 + 2 F_1 F_2 + r_2 F_2^2) \qquad (3.2.13)$$

It should be noted that F_1, F_2, f_1 and f_2 can be defined only instantaneously because they change with time. Also the steady state assumption may hold only at a given instant. Thus, in order to get a meaningful result, the polymerization reaction should be stopped at an early stage.

3.2.2 Types of Copolymerization Behavior

Different types of copolymerization behavior are observed depending on the values of the monomer reactivity ratios. Three types of copolymerizations can be considered based on whether the product of the two monomer reactivity ratios $r_1 r_2$ is unity, less than unity, or greater than unity (Odian,1981).

The first type is called an ideal copolymerization, where the $r_1 r_2$ product is unity. This copolymerization occurs when the two types of propagating species $M_1 \cdot$ and $M_2 \cdot$ show the same preference for adding one or the others of the two monomers. Under these conditions

$$K_{11}/K_{12} = K_{21}/K_{22} \quad \text{or} \quad r_1 = 1/r_2 \tag{3.2.14}$$

and the relative rates of incorporation of the two monomers into the copolymer are independent of the identity of the unit at the end of the propagating species. That is to say, the likelihood of occurrence of an M_1 unit immediately following an M_2 unit is the same as for an M_1 to follow an M_1 unit. The probability of either unit at any place in the chain is always equal to its mole fraction. So, it is apparent that the sequence of monomer units in an ideal copolymer must necessarily be random.

The second type is alternating copolymerization, where r_1 and r_2 are very small. In this case a copolymer is obtained in which the monomers alternate with near perfect regularity along the chain.

The third type is block copolymerization, where $r_1 r_2$ is larger than unity. Here there is a tendency to form a copolymer in which there are blocks of each monomers in the chains. In the extreme case of both r_1 and r_2 being much larger than unity, simultaneous and independent homopolymerizations of the two monomers occur.

25

3.2.3 Experimental Evaluation of Monomer Reactivity Ratios

3.2.3.1   Graphical Methods

Experimental data are usually analyzed graphically using, for example, the Fineman-Ross (Fineman & Ross,1950) and the Kelen-Tudos methods (Kelen-Tudos,1975).

In the Fineman-Ross method, the copolymer composition Eq. (3.2.9) is rewritten as:

$$f = F(r_1F + 1)/(r_2 + F) \qquad\qquad (3.2.15)$$

where $f = d[M_1]/d[M_2]$ and $F = [M_1]/[M_2]$. By rearranging, one obtains

$$F/f\,(f\text{-}1) = r_1F^2/f - r_2 \qquad\qquad (3.2.16)$$

A plot of $F(f\text{-}1)/f$ versus F^2/f gives r_1 as the slope and r_2 as the intercept. Eq. (3.2.16) can also be rearranged to

$$(f\text{-}1)/F = -r_2f/F^2 + r_1 \qquad\qquad (3.2.17)$$

In this case, the slope is minus r_2 and the intercept is r_1. f values can be obtained from experimental measurements of the molar ratios of the monomers in the copolymer that is formed from reactant mixtures of known initial monomer concentration ratios (F values).

A disadvantage of the Fineman-Ross method is that the experimental data are unequally weighted and the data obtained under extreme experimental conditions [in Eq. (3.2.16) at rather low M_2 and in Eq. (3.2.17) at very low M_1 comonomer concentrations] have the greatest influence

26

on the slope of the line. More uniform weights of the experimental data can be achieved with the Kelen-Tudos method. In this method, Eq.(3.2.9) is rewritten as

$$G/(\alpha + H) = (r_1 + r_2/\alpha)H/(\alpha + H) - r_2/\alpha \qquad (3.2.18)$$

where α denotes an arbitrary constant ($\alpha > 0$), and

$$G = F(f-1)/f \quad \text{and} \quad H = F^2/f \qquad (3.2.19)$$

$H/(\alpha+H)$ can take only those values in the interval (0,1). By plotting $G/(\alpha+H)$ as a function of $H/(\alpha+H)$, r_1 and r_2 values can be obtained.

Uniform distribution of the experimental data in the interval (0,1) can be attained by proper choice of the α value. Kelen & Tudos suggest $\alpha = 1$ when the reactivity ratios are nearly identical: in the case of markedly different reactivity ratios, or if the choice of $\alpha = 1$ involves rather asymmetric data distribution along the interval (0,1), they suggest $\alpha = (H_M H_m)^{1/2}$ where H_M stands for the highest of the calculated H values and H_m for the lowest value.

3.2.3.2 Experiments and Results

Copolymers from feeds of five different comonomer concentrations were prepared by the procedure described in Chapter 2. Polymerization was stopped before 10% of the monomers were incorporated into the polymer in order to minimize the errors arising from changes in the monomer feed composition. The total concentration of monomers was held constant at 0.8 mole/L of ethanol. The initiator was used at a concentration of 2 g/L of ethanol. Polymerization results are given in Table 3.2.1. The composition of the copolymers was determined by elemental analysis and the results are summarized in Table 3.2.2.

27

The reactivity ratios were calculated by both the Fineman-Ross (Figure 3.2.1) and the Kelen-Tudos Method (Figure 3.2.2). The results are given in Table 3.2.3.

Table 3.2.1   Polymerization time and conversion for feeds of different comonomer concentrations, along with the solvent and nonsolvent for the copolymers made

AA mole fraction in feed	Polymerization time (min)	Conversion (%)	Solvent	Nonsolvent
0.3	34.5	7.95	tetrahydrofuran	ethyl ether
0.5	30	10.5	methanol	ethyl ether
0.6	25	6.69	methanol	ethyl ether
0.7	26	6.05	methanol	ethyl ether
0.9	9	5.62	water	acetone

Both methods agree satisfactorily, so we may be quite confident of the r_1 and r_2 values. The results indicate that a random copolymer is made, because the $r_1 r_2$ product is close to unity. The copolymerization diagrams are given in Figure 3.2.3, where the open circles are the experimental points and the line are fits based on the indicated r_1 and r_2 values.

Reactivity ratios were also studied by use of the copolymers prepared at a different monomer and initiator concentration (3.2 mole/L and 0.625 g/L, respectively). The solid squares and + in Figure 3.2.3 represents the copolymers prepared from these concentrations of total monomer and initiator, which agree well with the calculated composition. This indicates that the reactivity ratios are not affected by changing the total monomer and initiator concentration in the feed.

Table 3.2.2   Results of copolymerization of methylmethacrylate (MMA) and acrylamide (AA)

AA mole fraction in feed	Nitrogen % (wt %)	AA mole % in copolymer	MMA mole % in copolymer
0.3	1.74	11.94	88.06
0.5	3.52	23.62	76.38
0.6	4.88	32.67	67.33
0.7	6.40	41.12	58.88
0.9	12.96	74.43	25.57

Table 3.2.3   Reactivity ratios determined by Fineman-Ross and Kelen-Tudos methods for the copolymerization of MMA(r_1) and AA(r_2)

	Fineman-Ross	Kelen-Tudos
r_1	3.17 +/- 0.10	3.20 +/- 0.20
r_2	0.32 +/- 0.04	0.31 +/- 0.02
$r_1 r_2$	1.01	0.99
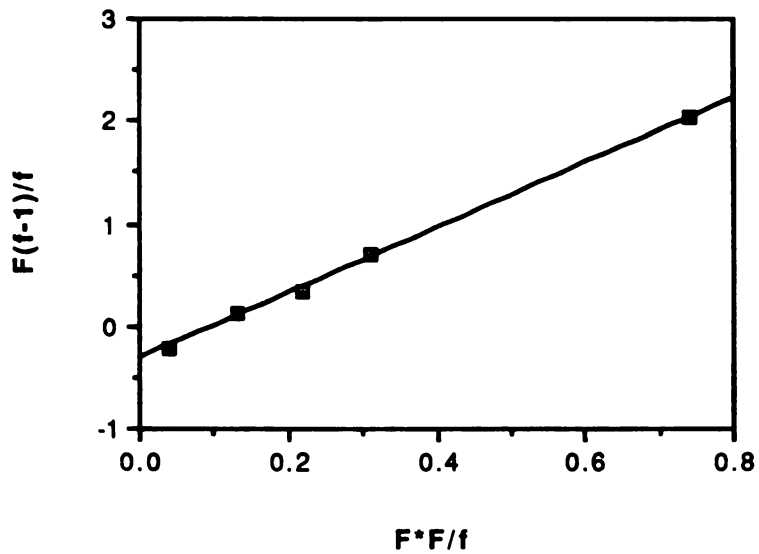
Figure 3.2.1 Fineman-Ross plot for the determination of reactivity ratios of MMA and AA. F is the ratio of $MMA(M_1)$ to $AA(M_2)$ mole concentrations in the feed and f is the ratio of MMA to AA mole fractions in the copolymer. The slope is $r_1(r_{MMA})$ and the intercept is $r_2(r_{AA})$.
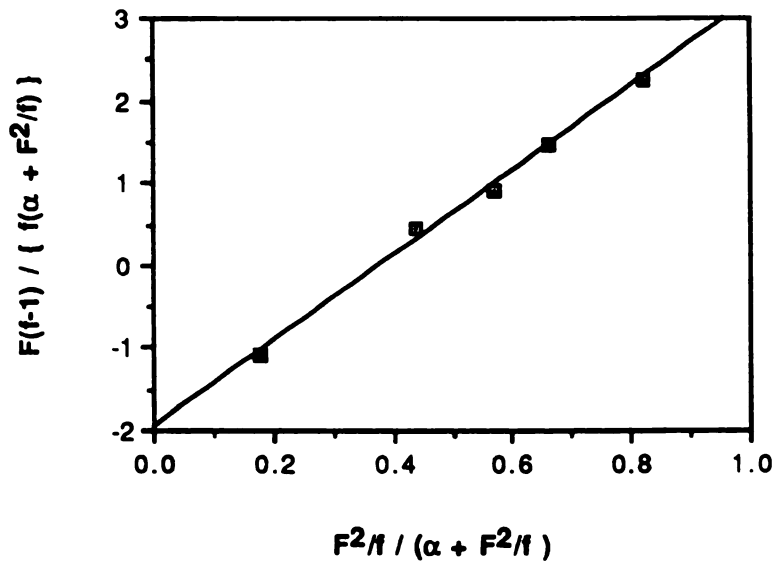
Figure 3.2.2   Kelen-Tudos plot for the determination of reactivity ratios of MMA and AA.   F is the ratio of MMA(M_1) to AA(M_2) mole concentrations in the feed and f is the ratio of MMA to AA mole fractions in the copolymer. α is $(H_M H_m)^{0.5}$ where H_M is the highest value of F^2/f and H_m is the lowest value of F^2/f.   The slope is $(r_1 + r_2/\alpha)$ and the intercept is $-r_2/\alpha$.
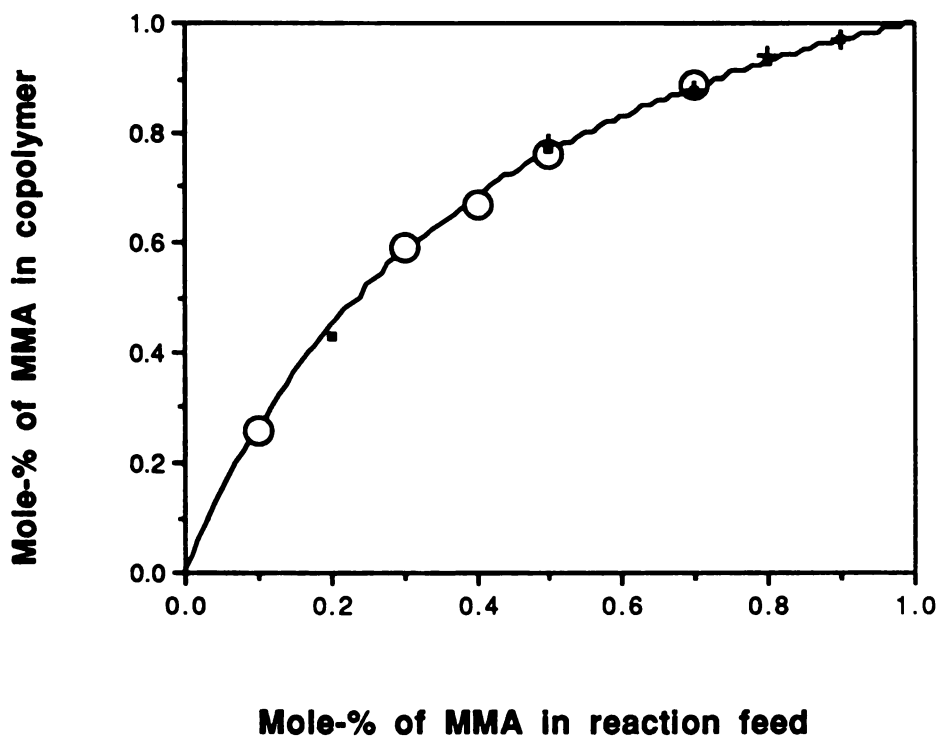
Figure 3.2.3 Monomer-copolymer composition curve for the MMA-AA system. Copolymers are made from feeds of (0.8 mole of monomer + 2g of initiator) / L of solvent (open circle) and (3.2 mole of monomer + 0.625g of initiator) / L of solvent (x and solid triangle). The line are fits based on the r_{MMA} and r_{AA} values calculated from the data of open circles.

Similar results are reported by Saini et al (1971). There is however a small difference in r

values between the values (r_1 =2.65, r_2 = 0.47) they reported and the values obtained in this

experiment. In Figure 3.2.4, composition curve, which is constructed on the basis of r values from

this thesis is compared with that from Saini et al. There is a small difference between these two

curves at high methyl methacrylate concentration in the feed. A maximum difference of about 8%

occurs when the MMA mole fraction in the feed is around 0.3. Although the reason for the

difference in r values is not clear, it may be due to the differences in copolymerization conditions

like pressure, temperature control and the purity of the monomers (Collins et al,1973).

3.2.4 Sequential Distribution Analysis

While the copolymerization equation describes the copolymer composition on a

macroscopic scale, it does not reveal the manner in which the monomer units are arranged within

the copolymer. Thus, the mole ratio of each monomer in the copolymer gives no information on

the distribution of the length of M_1 and M_2 sequences in a linear copolymer as illustrated by

$$-M_1 - M_1 - M_1 - M_2 - M_1 - M_2 - M_2 - M_2 - M_2 - M_1 -$$

This sequence length distribution can be calculated by probabilistic consideration of the chain

formation (Alfrey et al, 1944).

Let P_{11} be the probability that a growing radical chain $M_1\cdot$ will add to monomer M_1. To a

good approximation the only two possible fates of the growing chain $M_1\cdot$ are addition of M_1 or

addition of M_2. Hence, it is possible to write this probability as

3 3
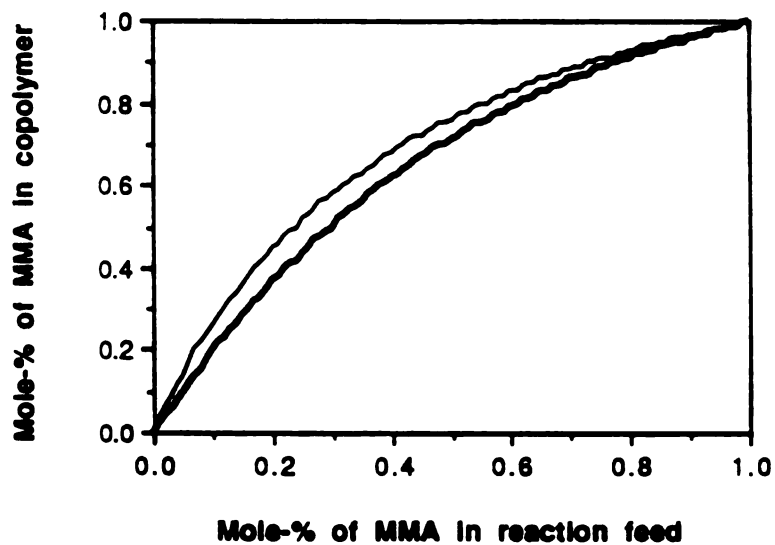
Figure 3.2.4 Comparison of monomer-copolymer composition curve from this work (—) with that of Saini et al (1971) (▬) for MMA-AA system

$$P_{11} = \frac{k_{11}[M_1\cdot][M_1]}{k_{11}[M_1\cdot][M_1] + k_{12}[M_1\cdot][M_2]} \quad \text{or} \quad P_{11} = \frac{r_1[M_1]}{r_1[M_1] + [M_2]} = 1 - P_{12} \qquad (3.2.20)$$

where P_{12} is the probability that $M_1\cdot$ will react with M_2. Given an initial radical site of type M_1 in the copolymer, the probability of forming a sequence of exactly m units of monomer M_1, $P_m(M_1)$ is

$$P_m(M_1) = P_{11}^{(m-1)} P_{12} \qquad (3.2.21)$$

P_{12} is multiplied by $P_{11}^{(m-1)}$, because in order to form a sequence of exactly m units the sequence must end with the M_2 monomer. Similarly, the probability that a sequence of m units of M_2 will be formed, given a radical site of type M_2, is given by

$$P_m(M_2) = P_{22}^{(m-1)} P_{21} \qquad (3.2.22)$$

where

$$P_{22} = r_2[M_2] /(r_2[M_2] + [M_1]) \qquad (3.2.23)$$

From Eqs. (3.2.21) and (3.2.22), the mole fractions or probabilities of different lengths of M_1 and M_2 can be calculated. Results of calculation with a monomer ratio, $[M_2]/[M_1] = 0.75/0.25 = 3$, are shown in Table 3.2.4 and Figure 3.2.5.

The most plentiful sequence is the monad, AA(M_2), at 52%. Other sequences such as diads and triads also exist in considerable amounts. Tetrad, pentad, hexad and heptad sequences also exist but only in a small amount. The distribution of M_1 sequences is almost the same as for M_2 sequences. Average sequence lengths, $m(M_1)$ and $m(M_2)$, can be calculated from Eqs. (3.2.21) and (3.2.22).

$$m(M_1) = \sum_{m=1}^{\infty} m P_m(M_1) / \sum_{m=1}^{\infty} P_m(M_1) = \sum_{m=1}^{\infty} m P_{11}^{(m-1)} / \sum_{m=1}^{\infty} P_{11}^{(m-1)} \qquad (3.2.24)$$

35

Table 3.2.4 Sequence length distribution of each monomer, $P_{11} = 0.52$, $P_{12} = 0.48$, $P_{21} = 0.52$, $P_{22} = 0.48$

m	MMA	AA
1	0.48	0.52
2	0.25	0.25
3	0.13	0.12
4	0.07	0.06
5	0.04	0.03
6	0.02	0.01
7	0.01	0.01
8	0.00	0.00
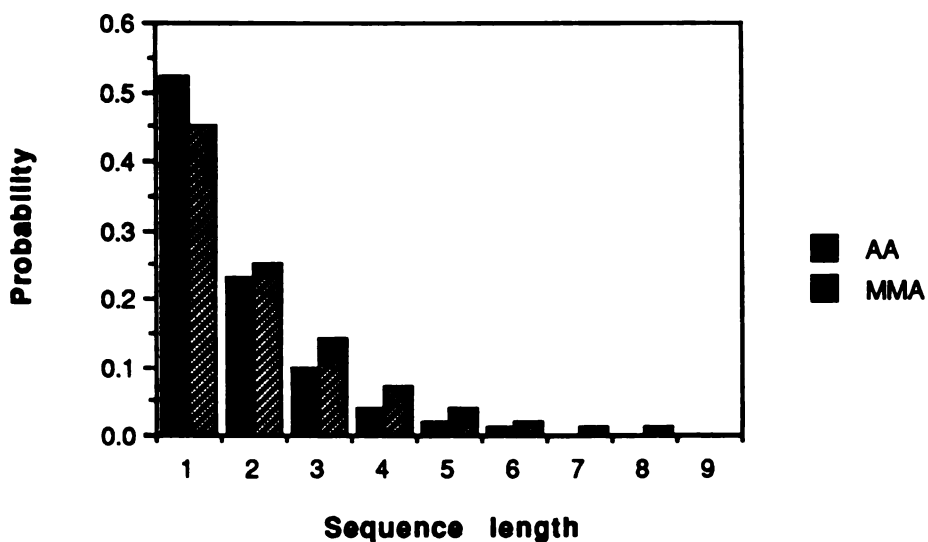
Figure 3.2.5   Sequence length distribution of MMA(M_1) and AA(M_2)

The numerator of the last expression is the MacLaurin's series expansion of $1/(1-P_{11})^2$ and the denominator is that of $1/(1-P_{11})$. Therefore Eq. (3.2.5) can be written as (Alfrey et al, 1944)

$$m(M_1) = 1/(1-P_{11}) = 1/P_{12} \qquad (3.2.25)$$

From Eqs. (3.2.19) and (3.2.24), $m(M_1)$ can be expressed as

$$m(M_1) = 1 + r_1[M_1]/[M_2] \qquad (3.2.26)$$

Similarly, the average sequence length of M_2 units is given by

$$m(M_2) = 1 + r_2[M_2]/[M_1] \qquad (3.2.27)$$

The average sequence lengths calculated with feed monomer ratio $[M_2]/[M_1] = 3$ are shown in Table 3.2.5.

The average sequence length discussed above is the number average sequence length. It might also be interesting to look at the weight average sequence length, $m_w(M_1)$, which can be defined in analogy to weight average molecular weight (Ring, 1963).

$$m_w(M_1) = \sum_{m=1}^{\infty} m^2 P_m(M_1) \left/ \sum_{m=1}^{\infty} m P_m(M_1) \right. \qquad (3.2.28)$$

This equation can be simplified to

$$m_w(M_1) = (1 + P_{11})/(1 - P_{11}) \qquad (3.2.29)$$

3 7

The weight average sequence lengths calculated with feed monomer ratio $[M_2]/[M_1] = 3$ are also shown in Table 3.2.5.

Table 3.2.5   Average sequence length of each monomer

	MMA	AA
number average	2.03	1.97
weight average	3.17	2.85

Another useful parameter that can be deduced from a knowledge of r_1, r_2, $[M_1]$, and $[M_2]$ is the run number R, which is defined as the average number of sequences of either type per 100 monomer units (Harwood & Ritchey, 1964). The rate of sequence formation, ds/dt, regardless of length, is simply the rate at which sequences are ended.

$$ds/dt = k_{12}[M_1 \cdot][M_2] + k_{21}[M_2 \cdot][M_1] \tag{3.2.30}$$

The total rate of polymerization $(dP_t/dt = -d([M1]+[M2])/dt)$ is given by

$$dP_t/dt = k_{11}[M_1 \cdot][M_1] + k_{12}[M_1 \cdot][M_2] + k_{21}[M_2 \cdot][M_1] + k_{22}[M_2 \cdot][M_2] \tag{3.2.31}$$

Dividing Eq. (3.2.30) by Eq. (3.2.31) gives the probability of sequence formation (or breaking) by a unit in the copolymer.

$$-ds/dP_t = 2/(2 + r_1[M_1]/[M_2] + r_2[M_2]/[M_1]) \tag{3.2.32}$$

From the definition of run number,

38

$$R = 200/(2 + r_1[M_1]/[M_2] + r_2[M_2]/[M_1]) = 200/(m(M_1) + m(M_2)) \qquad (3.2.33)$$

The run number calculated with a feed monomer ratio, $[M_2]/[M_1] = 3$, is 50 ($= 200/(1.93 + 2.07)$).

3.2.5 Monte-Carlo Generation of Poly(MMA-co-AA)

Further details of the microstructure of poly(MMA-co-AA) were examined by Monte-Carlo generation of the molecules. A basic program was written as shown in next two pages. In the program, the probabilities of an $M_1 \cdot$ radical reacting with M_1 and M_2 monomers are given by

$$k_{11}[M_1]/(k_{11}[M_1] + k_{12}[M_2]) \quad \text{and} \quad k_{12}[M_2]/(k_{11}[M_1] + k_{12}[M_2])$$

respectively. Similarly, the probabilities of an $M_2 \cdot$ radical reacting with M_2 and M_1 monomers are given by

$$k_{22}[M_2]/(k_{22}[M_2] + k_{21}[M_1]) \quad \text{and} \quad k_{21}[M_1]/(k_{22}[M_2] + k_{21}[M_1])$$

respectively. It is assumed that the feed is infinite and the probability that a monomer is the starting monomer of a chain is proportional to its composition in the feed.

Table 3.2.6 shows five molecules generated together with the average composition of each monomer and the standard deviation. As expected by the probabilistic nature of the reaction, the run number of each molecule produced is approximately 50. The average MMA composition of 5 molecules is 51.3%, which is close to the expected value, 52%, from the copolymer composition equation. Some molecules have rather large blocks or blocks

39

```
REM***This program calculates mean composition and  standard deviation of
REM***copolymers generated when reactivity ratio and feed composition are
REM***given. It also prints out each molecules produced.

INPUT "Enter # of molecules",Nmol
INPUT "Enter Chain length",Cnl
INPUT "Enter k11",k11
INPUT "Enter k12",k12
INPUT "Enter k22",k22
INPUT "Enter k21",k21
INPUT "Enter Feed Composition of M1",Com1
INPUT "Enter Feed Composition of M2",Com2


LPRINT"# of molecules=";Nmol
LPRINT"Chain length=";Cnl
LPRINT"k11=";k11,"k12=";k12,"k22=";k22,"k21=";k21
LPRINT"M1=";Com1," M2=";Com2


DIM Ntot1(Nmol),Ntot2(Nmol)
DIM Seg(Cnl)

Kcs1=k11*Com1 + k12*Com2
Kcs2=k22*Com2 + k21*Com1


FOR J=1 TO Nmol
  N1=0
  N2=0

  REM***Selection of first segment(assumed to be proportional to composition)
    RANDOMIZE TIMER
    Nmd=RND(2)
     IF Nmd<Com1 OR Nmd=Com1 THEN Seg(1)=1 ELSE Seg(1)=2
     IF Nmd<Com1 OR Nmd=Com1 THEN N1=1
     IF Nmd>Com1 THEN N2=1

     LPRINT"
     LPRINT Seg(1);
  FOR I=1 TO (Cnl-1)
    IF Seg(I)=1 THEN GOSUB Subr1
    IF Seg(I)=2 THEN GOSUB Subr2
      Checkpoint:
      LPRINT Seg(I+1);
  NEXT I
     LPRINT"


  Ntot1(J)=N1
  Ntot2(J)=N2

NEXT J

sm1=0
sm2=0
FOR K=1 TO Nmol
   sm1=sm1+Ntot1(K)
   sm2=sm2+Ntot2(K)
```

40

```
NEXT K

Av1=sm1/Nmol
Av2=sm2/Nmol

Ssu1=0
Ssu2=0
FOR L=1 TO Nmol
    Ssu1=Ssu1+(Ntot1(L)-Av1)*(Ntot1(L)-Av1)
    Ssu2=Ssu2+(Ntot2(L)-Av2)*(Ntot2(L)-Av2)
NEXT L

Stdv1=SQR(Ssu1/Nmol)
Stdv2=SQR(Ssu2/Nmol)

LPRINT"Avr com1=";Av1, "Avr com2=";Av2
LPRINT"Stdv1=";Stdv1,"Stdv2=";Stdv2
LPRINT""


END

Subr1:
   RANDOMIZE TIMER
   Nrnd=RND(2)
      IF Nrnd<(k11*Com1/Kcs1) OR  Nrnd=(k11*Com1/Kcs1) THEN  N1=N1+1 ELSE N2=N2
      IF Nrnd<(k11*Com1/Kcs1) OR  Nrnd=(k11*Com1/Kcs1) THEN  Seg(I+1)=1
      IF Nrnd>(k11*Com1/Kcs1) THEN N2=N2+1 ELSE N1=N1
      IF Nrnd>(k11*Com1/Kcs1) THEN Seg(I+1)=2

   GOTO Checkpoint
RETURN

Subr2:
   RANDOMIZE TIMER
   Nrnd=RND(2)
      IF Nrnd<(k22*Com2/Kcs2) OR Nrnd=(k22*Com2/Kcs2) THEN  N2=N2+1 ELSE N1=N1
      IF Nrnd<(k22*Com2/Kcs2) OR Nrnd=(k22*Com2/Kcs2) THEN Seg(I+1)=2
      IF Nrnd>(k22*Com2/Kcs2) THEN  N1=N1+1 ELSE N2=N2
      IF Nrnd>(k22*Com2/Kcs2) THEN Seg(I+1)=1

   GOTO Checkpoint
RETURN
```

constructed of one monomer. The first molecule has two blocks, octad and heptad, made of AA, while the third molecule has 3 blocks (octad, nonad and octad) made of MMA. The fifth molecule doesn't have any block larger than a pentad. These blocks may play important roles in the solution behavior of the molecules, such as inter- or intramolecular aggregation. Crystallinity is also influenced by the sequence length distribution (Ring,1963).

Table 3.2.6 Five copolymer molecules (chain length = 200) generated from an infinite feed of MMA and AA (0.25 and 0.75 in mole farction, respectively); MMA = 1, AA = 2

```
2 1 2 1 2 1 2 1 1 1 1 1 2 1 1 2 1 2 2 2 2 1 1 2 2 1 1 2 2 1 1 1 1 1 1 2 1 1 1 2 1 2 2 2 2 1 2 1 1 2 1 2 1 2
1 2 2 2 2 2 2 2 1 1 1 1 2 2 1 1 2 2 1 1 2 2 2 2 2 2 1 2 2 2 1 2 2 2 2 1 2 1 1 1 1 2 1 2 1 1 1 2 1 2
2 2 1 1 1 2 2 1 2 1 1 1 1 2 1 2 1 2 1 2 1 2 1 2 2 1 1 2 2 1 1 2 2 2 1 2 1 1 2 1 2 2 2 1 1 1 1 2 1 2 1 1 1 2
1 1 1 2 2 1 2 2 2 1 2 1 1 1 1 2 2 2 1 1 1 2 1 2 1 2 2 2 1 2 2 1 1 2 1 2 2 1      run number = 51

2 1 2 2 2 2 2 1 1 2 2 2 1 1 2 1 2 2 1 1 2 2 2 1 1 2 2 2 1 2 1 2 1 2 1 1 1 2 2 1 2 2 1 2 2 2 2 1 2 2 1 1 1 1
2 1 1 2 2 1 1 2 2 1 2 2 2 2 1 1 1 1 1 1 2 1 1 2 1 2 2 1 1 2 1 1 2 1 1 2 1 2 1 1 1 1 1 2 1 1 1 2 2 1 1 2 1 1
2 2 1 1 1 2 1 2 2 2 1 2 2 1 2 2 2 1 1 1 1 2 1 2 1 2 2 2 2 2 1 1 1 2 2 2 1 2 2 2 2 2 2 2 1 2 1 1 2 1 1 2 1
2 2 1 2 2 1 2 1 1 2 2 1 2 1 2 1 1 1 2 1 2 1 1 2 2 1 1 2 1 1 2 1 2 2 1 1 2 1      run number = 54

2 1 1 1 1 1 1 1 1 1 1 2 2 1 2 2 2 2 1 2 2 1 1 2 2 1 2 2 1 2 2 1 2 2 1 1 2 1 2 1 2 1 2 2 2 2 1 2 2 1 1 1 2 2 1 2 2
2 2 1 2 2 2 2 1 2 2 2 2 1 1 1 1 1 2 1 1 2 1 2 2 1 1 1 2 2 1 1 2 1 2 1 1 2 1 2 2 2 1 1 2 1 2 2 2 1 2 2 1 1 2
1 1 2 1 1 2 1 2 1 1 1 2 2 2 2 2 1 1 1 1 1 1 2 2 1 1 1 1 2 2 1 1 2 2 2 1 1 1 2 1 2 2 2 1 2 1 1 1 1 1 2 1 1 1
2 2 1 1 2 2 1 1 2 2 1 1 1 1 2 1 1 2 1 2 2 1 1 1 1 2 2 2 1 1 2 1 1 2 2 1 1 2      run number = 49

1 2 2 1 1 1 1 1 1 1 1 2 1 2 2 2 1 2 1 1 2 1 2 2 2 2 1 1 2 2 1 1 1 1 1 1 1 1 1 2 1 2 1 2 1 2 2 1 1 2 1 2 2 1 1
1 2 1 1 2 1 2 2 2 1 1 2 1 2 1 2 2 1 1 2 1 1 2 1 2 1 2 2 2 2 1 1 2 2 1 1 2 2 2 2 2 2 1 2 1 1 1 2 2 2 2 1 2 1 1 2
1 1 1 1 1 2 2 2 1 2 2 1 2 2 2 2 1 1 1 2 1 2 2 2 1 2 1 1 2 2 1 2 2 1 2 2 1 2 1 1 2 2 2 2 2 2 1 2 1 1 1 1 2 2
1 2 2 1 2 1 2 1 1 2 2 2 1 1 1 2 1 1 1 2 1 1 1 1 1 1 1 1 2 1 1 1 2 2 1 1 1 1      run number = 50

2 1 2 2 2 1 2 1 2 1 2 1 2 1 1 1 2 1 1 2 1 1 2 1 1 1 2 2 2 2 1 1 1 2 1 1 1 1 2 2 2 1 1 1 2 1 1 1 1 1 2 1 2 1
1 2 1 2 2 2 1 1 2 1 2 2 2 1 2 1 1 1 2 1 1 1 1 1 2 2 2 1 1 1 2 1 2 1 2 2 1 1 2 1 1 1 1 1 2 1 1 2 2 1 2 1 1 1
2 1 1 1 2 1 2 2 2 1 2 1 1 2 2 2 1 2 2 2 2 1 1 1 2 1 2 2 1 1 2 2 2 1 1 2 2 1 1 2 1 1 1 2 2 2 2 1 2 2 2 2 1 2
2 1 1 1 1 2 1 2 2 1 2 2 1 2 2 1 2 2 2 2 1 1 2 1 2 1 1 1 2 2 2 1 2 2 2 1 1 2      run number = 53
```

Average number of MMA per chain = 102.6 +/- 3.5

Average number of AA per chain = 97.4 +/- 3.5

4 2

3.3 Fractionation of Poly(MMA-co-AA)

3.3.1 Introduction

As already mentioned in 3.1, copolymer molecules can differ from each other not only in their molecular weight but also in the relative content of each type of monomer unit, i.e., in their chemical composition (Fuchs et al, 1966). The chemical composition distribution can arise from two sources; one source is the statistical nature of the formation of copolymers (statistical distribution), formulated by Stockmayer (1945), and the other is the change in the feed comonomer ratio at various stages of the copolymerization reaction.

The magnitude of the statistical distribution depends on the size of the copolymer molecules. At a high degree of polymerization, sections which are produced at consecutive instants, and which possibly differ in composition, merge into one final molecule. The composition of the molecule is the average of the sections included. For this reason, smaller variations in chemical composition are more likely in a large size molecule than a small size one.

Compositional distribution due to drift in the feed comonomer composition at low conversion (<10%) is usually negligible (Stejskal, 1978), but with increasing conversion it becomes more significant than the statistical distribution (Teramachi et al, 1971 & 1981). As an extreme example, the latermost stage of a copolymerization is essentially a homopolymerization, since usually one comonomer is used up first, unless extreme care is taken to rebalance the feed. Compositional drift can be minimized by stopping the polymerization reaction at low degrees of conversion.

Because many physical properties of polymers (viscosity, scattering of light, second virial coefficient, etc) are dependent on the molecular weight and chemical composition, it is necessary

43

to prepare homogeneous samples which have a narrow distribution in molecular weight and composition in order to study these properties. This can be accomplished by fractionation. The basic strategy for fractionation of copolymers is to fractionate first by molecular weight, and then to further fractionate each molecular weight fraction by composition, or vice versa (Reiss et al, 1977, Tung, 1985). Several methods such as fractional precipitation, Gel Permeation Chromatography (GPC) and Thin Layer Chromatography (TLC) are applicable for preparing such samples.

Fractional precipitation is the classical approach to the simultaneous determination of molecular weight distribution and composition distribution, and it has been widely used (Litmanovich et al, 1967 and Teramachi et al, 1974). In this method, two sets of solvent-precipitant systems are used, one for the fractionation by molecular weight and the other for the fractionation by chemical composition. A suitable solvent-precipitant system for fractional precipitation is usually selected empirically, using the determination of the cloud point of the constituent homopolymers. For the fractionation by molecular weight, a solvent-precipitant system which has identical or close cloud points for each homopolymer of the constituents of the copolymer is a proper choice (Juranicova et al, 1970). On the contrary, for the fractionation by chemical composition, a solvent-precipitant system which shows markedly different cloud points for the two homopolymers is suitable. Fractional precipitation is a very simple, but time consuming experiment.

Preparative Gel Permeation Chromatography (GPC) has been used to fractionate copolymer molecules by their molecular size, however GPC does not strictly guarantee fractionation by molecular weight, because the size is also affected by composition. Each GPC fraction thus obtained is further fractionated by composition using other methods (Hoffmann et al, 1977, van den Berg et al, 1984). Nakano and Goto (1981) used GPC for the analysis of molecular weight distribution after they had fractionated polyethylene by composition using crystallization.

Thin Layer Chromatography (TLC) has been used mainly for separation by composition (Inagake et al, 1968 and Belenkii, 1979), based on the finding that the adsorption of macromolecules on solid surfaces is essentially independent of molecular weight but depends strongly on chemical composition (Ellerstein et al, 1961). Application of TLC to fractionation has also been carried out by Bellce and Patel (1980) in two-dimensions. Recently, column adsorption chromatography has been applied to fractionation by chemical composition (Teramachi et al, 1981 and Sato et al, 1986).

Fractionation by both molecular weight and chemical composition can be more efficiently performed by combination of the methods discussed above.

As mentioned already, if we stop the polymerization reaction at very low conversion, compositional heterogeneity due to the change of the feed composition can be minimized, and we can assume that there is only statistical distribution of chemical composition. Stejskal and Kratochvil (1978) discussed the conditions under which random copolymers with infinite molecular weight, for which statistical heterogeneity is zero, may acquire compositional heterogeneities due to the feed drift high enough to be perceived or determined by fractionation or light scattering. They concluded that if copolymerization is carried out to low weight conversion (<10%) and the reactivity parameters of the comonomers lie within the interval 0.2 - 2.5, chemical heterogeneity due to the feed drift can be proved neither by light scattering nor by fractionation. They also concluded that, within the limits of experimental error of the methods used, such copolymers can be regarded as chemically homogeneous.

Chemical compositional heterogeneity has been studied experimentally by fractionation in both high conversion copolymers and low conversion copolymers (Teramachi et al, 1971 & 1981). A high conversion (92%) copolymer (M_n = 4.82 x 10^5) showed a very broad distribution ranging between 86 mole % and 44 mole %; however, a low conversion (14%) copolymer (M_n =

2.07×10^5) showed a very narrow distribution around the average value (49.7 mole %) ranging between 53.5 mole % and 46.7 mole %.

The dependence of the distribution breadth on the size of the molecules can be shown by the theoretical expression for the variance of chemical composition (Stejskal et al,1981), where σ^2 is expressed as $\sigma^2 = w_{av} (1 - w_{av})k/P_n$ [w_{av} is average composition, P_n number average chain length and $k = [1 - 4w_{av} (1-w_{av}) (1-r_1r_2)]^{1/2}$ where r_1 and r_2 are the reactivity ratios of each monomer]. For a random copolymer, $r_1r_2=1$ and this formula gives $\sigma^2 = w_{av} (1 - w_{av})/P_n$. The breadth of the distribution becomes smaller as P_n increases and it becomes zero for a copolymer with infinite molecular weight.

Fig 3.3.1 shows a normalized composition distribution curve around the mean of various molecules with different chain lengths. The copolymer with average composition 52% of a monomer(M1) is chosen, because this is the copolymer used in the present work. The standard deviations of these distributions are listed in Table 3.3.1. They are calculated assuming Gaussian distribution of composition. The standard error calculated from the Monte-Carlo generation of molecules using the reactivity ratios obtained experimentally is also shown in Table 3.3.1.

When the chain length is 100, the distribution is rather broad with normalized standard deviation 5%. As chain length increases, the distribution becomes narrower. When chain length is 500, 95% of molecules fall within +/-4.3% of the mean. A fractionation procedure with the accuracy to separate this level of compositional heterogeneity does not exist.

Based on the discussions above, we decided to prepare a poly(MMA-co-AA) with low conversion (minimizing the compositional heterogeneity due to the drift of feed comonomer concentration) and to carry out fractionation in a solvent-nonsolvent system by mlecular weight,

46
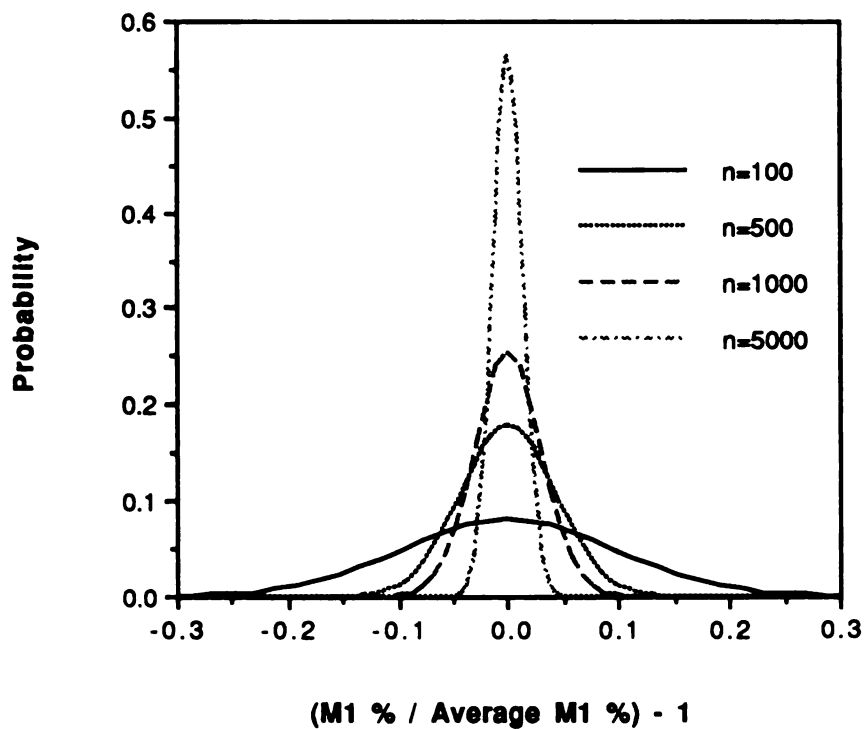
Figure 3.3.1 A normalized composition distribution curve around the mean for a random copolymer with the mole fraction of each monomer 0.52(M1) and 0.48(M2). n is the number of monomers in the copolymer (chain length). Gaussian distribution of composition is assumed.

assuming that compositional heterogeneity is negligible.

Table 3.3.1 Standard deviation of average composition for copolymers with various chain lengths

Chain length (n)	Average composition of M1	Standard deviation (SD)	SD/n	Standard error* (SE)	SE/n
100	52	5	0.050	5	0.049
500	260	11	0.020	11	0.022
1000	520	16	0.020	16	0.016
5000	2600	35	0.007	38	0.008

* calculated from the composition of molecules generated by Monte-Carlo method

3.3.2 Theoretical Background

We now present the theoretical background for fractionation by molecular weight. Fundamentally, fractionation is based on the effect of solvent power and molecular weight in polymer/solvent phase equilibria. The Flory-Huggins treatment of polymer solutions leads to an expression for the free energy of mixing of a solvent with a polymer (Flory, 1953):

$$\Delta F_M = RT \, [n_1 \ln v_1 + n_2 \ln v_2 + \chi n_1 v_2] \tag{3.3.1}$$

where k is Boltzman's constant, T the absolute temperature, n_1 and n_2 the numbers of moles of solvent and solute, respectively, and v_1 and v_2 the respective volume fractions. The interaction between polymer and solvent molecule is represented by the interaction parameter X, defined as

$$X = Z \, \Delta W_{12}/kT \tag{3.3.2}$$

where Z is the lattice coordination number and ΔW_{12} the free energy associated with pair contact between solvent and polymer segment (Flory, 1953). The parameter X is a measure of solvent power, with poorer solvents having larger values of X. The solvent chemical potential (μ_1) can be obtained by differentiating the free energy of mixing ΔF_M, with respect to n_1. Similarly, the solute chemical potential (μ_2) can be derived by differentiating ΔF_M with respect to n_2.

$$\mu_1 - \mu_1{}^0 = RT \left[\ln (1 - v_2) + (1 - 1/x)v_2 + X v_2{}^2 \right] \tag{3.3.3}$$

$$\mu_2 - \mu_2{}^0 = RT \left[\ln v_2 - (x - 1)(1 - v_2) + X x (1 - v_2)^2 \right] \tag{3.3.4}$$

In the above expressions, $\mu_1{}^0$ and $\mu_2{}^0$ represent the chemical potentials of pure liquid and pure liquid polymer, respectively, and x is the degree of polymerization. In a polydisperse system for which the number average value of x is x_n, the appropriate equations are (Flory, 1953)

$$(\mu_1 - \mu_1{}^0)/RT = \ln v_1 + (1 - 1/x_n) v_2 + X v_2{}^2 \tag{3.3.3'}$$

$$(\mu_x - \mu_x{}^0)/RT = \ln v_x - (x - 1) + x(1 - 1/x_n) v_2 + X x v_1{}^2 \tag{3.3.4'}$$

The phase equilibrium of a binary mixture can be understood by studying the free energy of mixing as a function of composition. A schematic representation of the free energy of mixing for both complete and partial miscibility is shown in Fig 3.3.2. The convexity or concavity of the

49
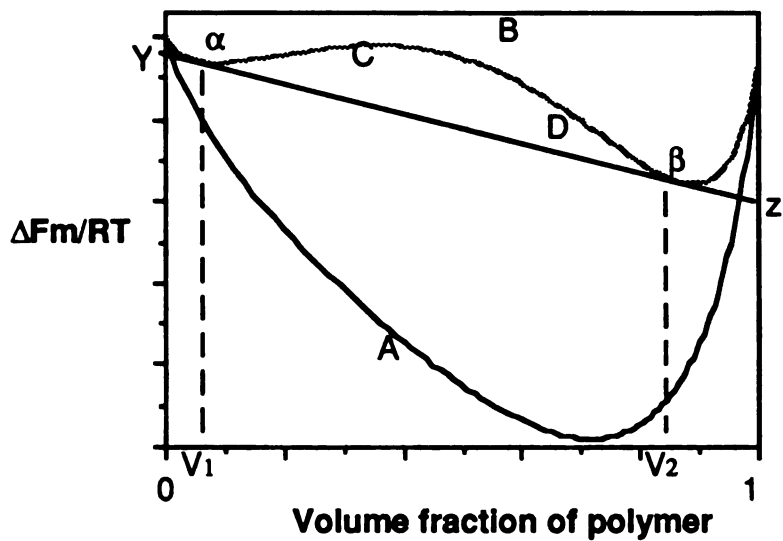
Figure 3.3.2   Free energy of mixing of a binary mixture for both complete (curve A) and partial miscibility (curve B). The free energy of mixing is calculated using Equation (3.3.1) with a polymer of chain length 2 (dimer). χ is 0.8 (curve A) and 2.0 (curve B). α and β represent dilute and concentrated phases with concentrations of v_1 and v_2, respectively. C and D are inflection points and YZ is the common tangent line of the two phases α and β.

free energy of mixing curve determines whether the system is miscible or not (Dill,1985). Curve A is everywhere concave upward and has no inflection point. If phase separation were to occur, then the system would always have a higher free energy and, hence, would be unstable with respect to the mixed system. Therefore, curve A represents the condition where the binary mixture is miscible in all proportions. The case of partial miscibility is shown in curve B. Between volume fractions v_1 and v_2, the curve is concave downward and has two inflection points (C & D). In this region, the system can lower its free energy by separating into two phases, represented by α (dilute phase) and β (concentrated phase). These two phases share a common tangent line, shown as line YZ, which specifies the composition of the two phases into which the system will separate. The two phases are in equilibrium and, hence, have the same chemical potential ($\mu_{1,\alpha}$ = $\mu_{1,\beta}$ and $\mu_{2,\alpha}$ = $\mu_{2,\beta}$). In the region below v_1 and above v_2, where ΔF_m concave is upward, a homogeneous phase is stable. Fulfillment of the condition, $\mu_{1,\alpha}$ = $\mu_{1,\beta}$, requires that μ_1 pass through a minimum and then a maximum as v_2 is increased from zero to unity (Fig 3.3.3). At both the maximum and minimum, $\partial \mu_i / \partial v_i$ = 0. Between the maximum and minimum, there is an inflection point, I, where $\partial^2 \mu_i / \partial v_i^2$ = 0.

Because μ_1 and μ_2 are derived by differentiating the same free energy function (ΔF_M), the Gibbs-Duhem relationship, $n_1 d\mu_1$ = $-n_2 d\mu_2$, predicts that any increase in μ_1 is mirrored by a decrease in μ_2. When μ_1 passes through a maximum, μ_2 should pass through a minimum. Hence it will suffice to consider either chemical potential. In the discussion below, only μ_1 is considered.

Fig 3.3.4 shows the transition from complete to partial miscibility. When X is small, solvent and solute are completely miscible. Partial miscibility begins to occur when X reaches its critical value X_c. Above X_c, ΔF_m curves have two minima; thus, the μ_1 curve exhibits a minimum, a maximum, and an inflection as shown in Fig 3.3.3. The curve c in Fig 3.3.4 is called the coexistence curve, which is the boundary between complete miscibility and partial miscibility. At

51
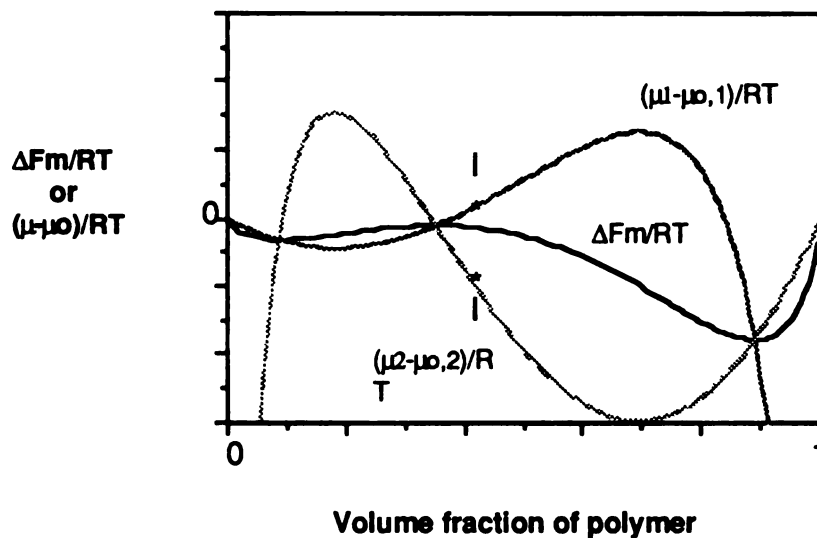
Figure 3.3.3 Comparison of free energy of mixing curve (curve A in Figure 3.3.2) with chemical potential curves for solvent(μ_1) and polymer(μ_2) calculated from Equations (3.3.2) and (3.3.3) with a polymer of chain length 2 (dimer). $\mu_{o,1}$ and $\mu_{o,2}$ are the chemical potentials of pure liquid and   pure liquid polymer, respectively.
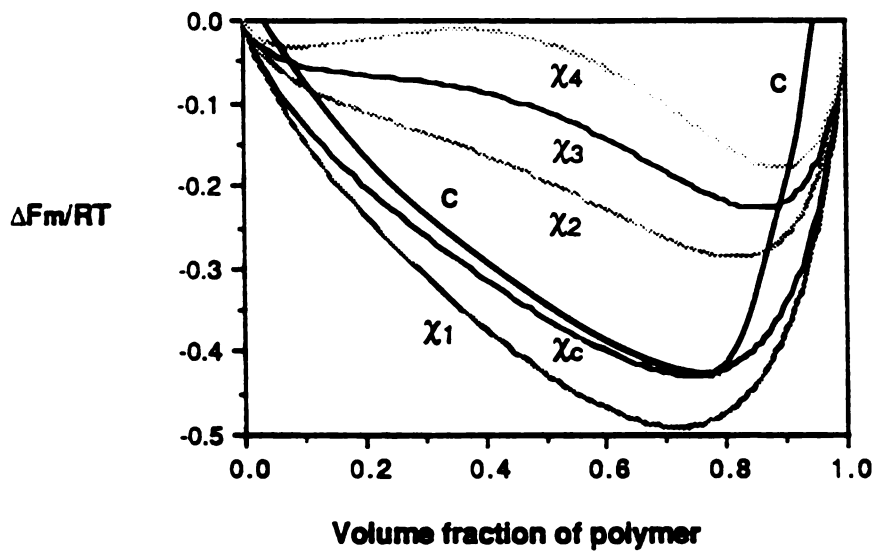
Figure 3.3.4 Transition from complete to partial miscibility. The free energy of mixing is calculated using Equation (3.3.1) with a polymer of chain length 2 (dimer). $\chi_1=0.8$, $\chi_c=1.0$, $\chi_2=1.5$, $\chi_3=1.75$, $\chi_4=2.0$.

χ_c, these features will occur simultaneously at the same concentration. Hence the conditions for incipient phase separation are

$$(\partial \mu_1/\partial v_2) = 0 \qquad\qquad (3.3.5)$$

$$(\partial^2 \mu_1/\partial v_2^2) = 0 \qquad\qquad (3.3.6)$$

Application of these conditions to equation (3.3.3) yields

$$1/(1 - v_2) - (1 - 1/x) - 2\chi v_2 = 0 \qquad\qquad (3.3.7)$$

and

$$1/(1 - v_2)^2 - 2\chi = 0 \qquad\qquad (3.3.8)$$

Eliminating χ, expression for the critical v_2, v_{2c}, can be obtained.

$$v_{2c} = 1/(1 + x^{1/2}) \qquad\qquad (3.3.9)$$

which for large x reduces to

$$v_{2c} = 1/x^{1/2} \qquad\qquad (3.3.10)$$

This latter equation predicts that the critical volume fraction at which phase separation first appears is very small for long chain polymers. For example, the critical volume fraction for a polymer having a molecular weight of a hundred thousand ($x \sim 10^3$) is only about 3%. As x gets larger, the critical volume fraction approaches zero. This prediction has been tested by use of three polyisobutylene fractions in diisobutyl ketone and the result is shown in Fig 3.3.5 (Schulz et al, 1952). The Y axis is temperature. According to the more general interpretation of χ, in which

54

ΔW_{12} is regarded as a free energy, χ can be expressed as a linear function of $1/T$. Hence the Y axis can be interpreted as a linear function of $1/\chi$. Although the critical points occur at higher volume fraction than the values predicted by Eq. (3.3.10), they occur at very low volume fraction as expected.

By substituting Eq. (3.3.10) in Eq. (3.3.7), χ_c can be expressed as

$$\chi_c = (1 + x^{1/2})^2/2x \approx 1/2 + 1/x^{1/2} \tag{3.3.11}$$

This equation predicts that the critical value of χ will exceed 1/2 by a small increment depending on the degree of polymerization, and at infinite molecular weight, it should be 1/2. This indicates that, when the solvent condition is changed by the gradual addition of nonsolvent into a polymer solution containing different molecular weight species, that of highest molecular weight will separate first. This prediction is verified by experiment (Fig 3.3.5).

The distribution of a polymer of degree of polymerization x between these two phases can be obtained by applying the equilibrium condition, $\mu_{x,\alpha} = \mu_{x,\beta}$ to Eq.(3.3.4)'. The result is: (Kwei,1979)

$$\ln (v_{x,\beta}/v_{x,\alpha}) = \sigma x \tag{3.3.12}$$

where

$$\sigma = [1 - (1/x_{n,\alpha})]v_{p,\alpha} - [1 - (1/x_{n,\beta})]v_{p,\beta} + \chi [v_{1,\alpha}^2 - v_{1,\beta}^2] \tag{3.3.13}$$
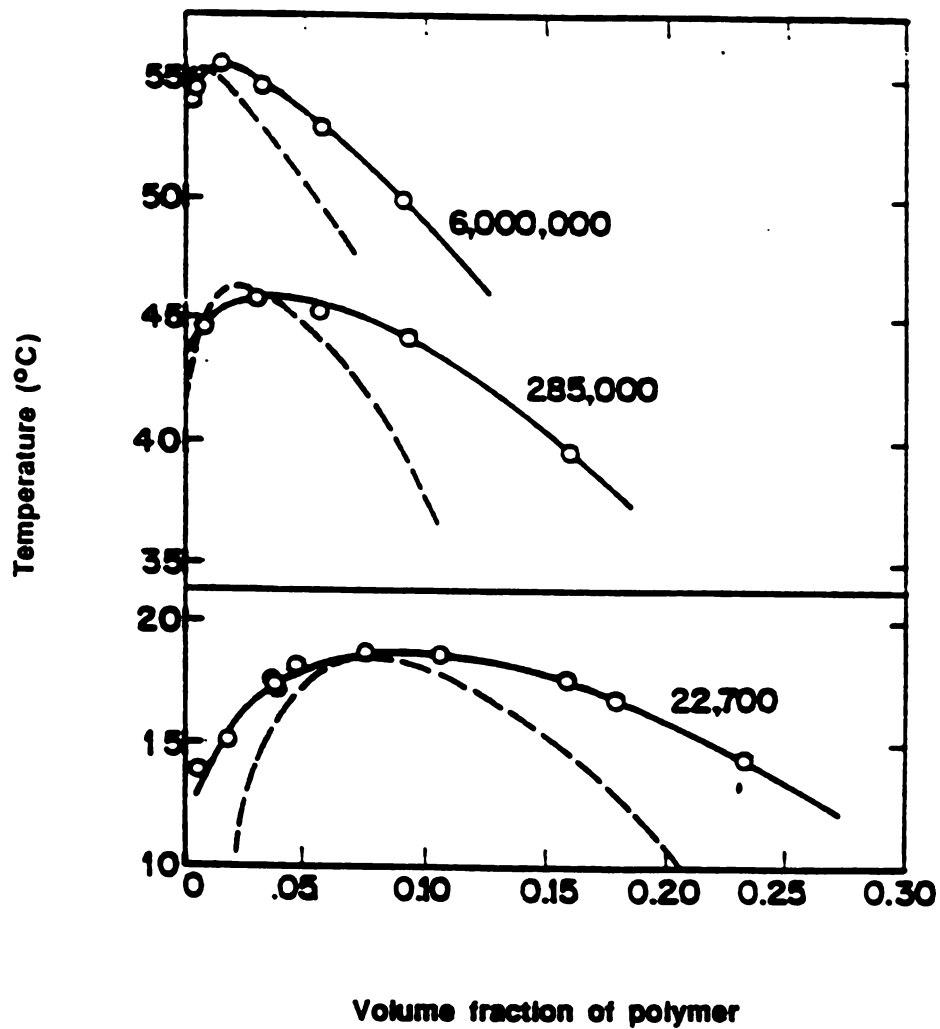
Figure 3.3.5 Phase diagram for three polyisobutylene fractions in diisobutyl ketone. Solid curves are drawn through the experimental points. The dashed curves have been calculated from theory (Schulz and Flory, 1952)

The terms $x_{n,\alpha}$ and $x_{n,\beta}$ are the number average degrees of polymerization in the dilute (denoted by a) and concentrated phases (denoted by b), respectively. The terms $v_{p,\alpha}$ and $v_{p,\beta}$ are the volume fractions of polymer and $v_{1,\alpha}$ and $v_{1,\beta}$ are those of solvent, in each phase. The quantity σ is a function of (a) the total polymer concentration, (b) the average degree of polymerization in both phases, and (c) the interaction parameter χ. However, it is independent of the particular degree of polymerization, x, and is always positive. σ can be considered as a constant for a given χ value.

According to Eq. (3.3.12), every polymer species is more concentrated in the precipitated phase. However, because the ratio $v_{x,\beta}/v_{x,\alpha}$ increases exponentially with x, there is a much stronger tendency for the higher molecular weight species to concentrate itself in the concentrated phase. The concentrated phase is usually a gel phase of precipitated molecules after settlement. This is the basis of fractionation by precipitation.

The volume of the dilute phase should be much greater than that of the concentrated phase for efficient fractionation, because most of the smaller molecules will be retained in the dilute phase due to the gain in entropy. The higher molecular weight species will be mostly in the concentrated phase, despite its small volume, because of the large exponential factor in the distribution (Equation 3.3.12). The volume ratio of each phase can be calculated by the "lever rule". A large volume ratio v_{α}/v_{β} can be obtained using a very dilute solution whose concentration is much less than that of the maximum in the plot of T_p against v_2 (Fig 3.3.5). Otherwise, the two phases will have a similar amount of polymer. If the initial concentration is larger than that at the maximum, the volume of the concentrated phase will even exceed that of the more dilute phase.

The foregoing discussion refers specifically to the fractionation of a binary solvent-polymer mixture by lowering temperature. If fractionation is carried out by adding nonsolvent to

the polymer solution at a constant temperature, equations for ternary systems should be used; however, the general considerations outlined above remain applicable.

Fig 3.3.6 shows the phase diagram calculated for the three component system consisting of nonsolvent (1), solvent (2) and polymer (3) with $x_1 = x_2 = 1$ and x_3 values of 10, 100 and ∞ (Tompa, 1949). It is assumed that the reduced free energy of interaction of the nonsolvent - solvent and the nonsolvent-polymer segment (X_{12} and X_{13}, respectively) is 1.5, while that for the the solvent-polymer segment (X_{23}) is zero. All critical points (o) are shown and tie lines are drawn for $x_3 = 100$ curve. An interesting point is that, for the two phases in equilibrium, the nonsolvent-solvent ratios differ markedly. The ratio is smaller in the concentrated phase than the dilute phase. This difference in nonsolvent-solvent ratio will effect the σ value, indicating that the concentration of polymer in the concentrated phase will be larger than that in the binary case. Hence, we may expect that more favorable fractionation conditions can be achieved by using solvent-nonsolvent mixtures.

There are two important methods of fractionation based on the discussions above. One is fractional precipitation, and the other is fractional dissolution.

In fractional precipitation, fractionation is carried out by adding small amounts of nonsolvent to a large volume of dilute polymer solution at a constant temperature until precipitation (indicated by turbidity) occurs. The precipitated phase, which contains the high molecular weight species, is allowed to settle into a gel layer. The gel layer is recovered as the first fraction and the supernatant layer is then further fractionated for the next fraction.

In fractional dissolution, the polymer is first deposited from solution onto a column of finely divided inert (for example, sand or glass)particles. By eluting a series of mixtures of solvents
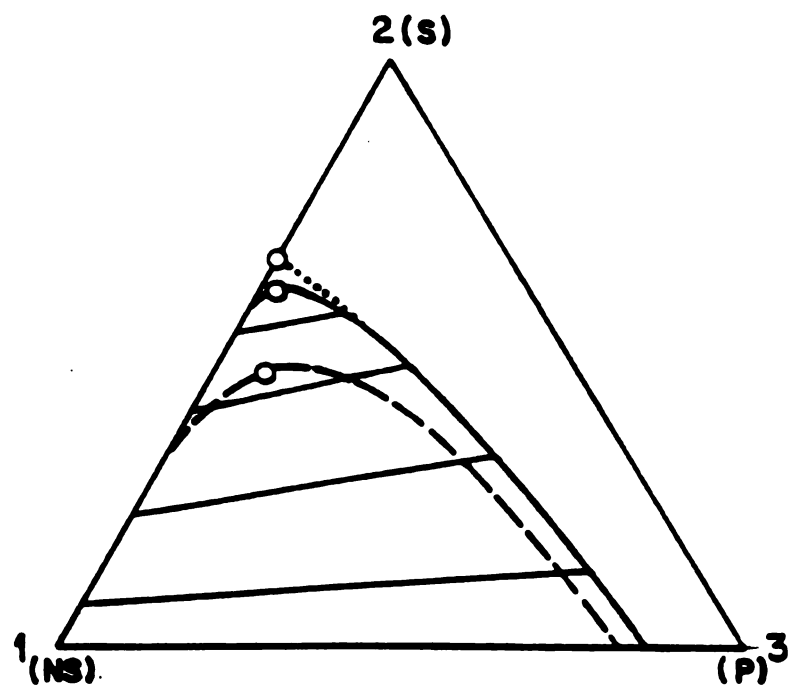
Figure 3.3.6   Phase diagram for three component system consisting of nonsolvent (1), solvent (2) and polymer (3): (---)x_3 = 10; (-)x_3 = 100; and (...) x_3 = ∞ (Tompa, 1949)

and nonsolvents of increasing solvent power, deposited polymer molecules can be recovered biginning with the lowest molecular weight species.

In the fractionation of poly (MMA-co-AA) (51:49) used in the present work, fractional precipitation is carried out in methyl formamide (solvent) - ethanol (nonsolvent) mixture.

3.3.3 Experimental

3.3.3.1 Experiments and Results

Copolymer with 51 mol % of MMA was prepared as described in Chapter 2. Total monomer concentration in the feed was 3.2 mole/L and initiator concentration was 3.8×10^{-4} mole/L. Polymerization was stopped at low conversion (8.8 wt %). Fractionation was performed in MFA (solvent) - ethanol (precipitant) mixture under argon gas. 8.1 g of polymer was dissolved in 2360 ml MFA (0.34 w/v %) in a round-bottomed flask. 1,500 ml of absolute ethanol was added to this solution with vigorous stirring. The solution remained clear. This flask was then immersed in a water bath maintained at 26 +/- 0.05° C. More ethanol was gradually added to the solution (2 ml/min) with stirring, until turbidity was apparent. The quantity added was slightly in excess of that required for incipient cloudiness. In order to assure the establishment of equilibrium between the two phases, the solution was warmed until it became clear, and was then allowed to precipitate during gradual cooling to 26° C. The magnetic bar was removed and the precipitate was allowed to settle at the bottom of the flask for 3-7 days. Polymer in the precipitated phase was separated by decanting the supernatant layer carefully. Separated polymer was redissolved in MFA and precipitated by acetone. This precipitate was recovered by filtering on a fritted glass filter and was then dried in vacuum oven at 60° C. The supernatant layer recovered was further titrated with absolute ethanol as before to obtain subsequent fractions. Polymer remaining in the supernatant

60

solution after the last fraction could not be recovered because there was no precipitate when a very large amount of nonsolvent was added. 10 fractions were obtained (Table 3.3.2).

Table 3.3.2   Results of fractionation from methylformamide solution by ethanol

fraction	weight(g)	ethanol / methylformamide
1st	0.9	0.97
2nd	0.5	1.07
3rd	0.41	1.14
4th	1.04	1.21
5th	0.46	1.26
6th	0.52	1.34
7th	0.50	1.42
8th	0.28	1.56
9th	0.34	1.85
10th	0.30	2.89
total	5.25	
recovery	65%	

3.3.3.2 Discussion

The copolymer dissolves in dipolar solvents such as N-methylformamide (MFA) and N, N-dimethylformamide (DMA). DMA was not used as solvent, because when the copolymer is dissolved in this solvent, the copolymer molecules form small aggregates instead of dispersing

themselves as single molecules. An interesting point concerning these aggregates is that they disappear when about 5 % (v/v) of water is added to the solution, indicated by the size (hydrodynamic radius) change from ~100 nm to ~17 nm determined by dynamic light scattering. It seems that the hydrogen bonds formed between the copolymer molecules through carbonyl or amide groups are broken by water molecules, dismantling the aggregates into single molecules. Association behavior like this is similar to that observed in the solutions of polyisoprenes with amine and zwitterion end groups (Davidson,1988). It was observed that the aggregates formed readily dissolve when small amounts of alcohol are added to the solution.

Ethanol was chosen as the nonsolvent for the fractionation. Ethanol is a nonsolvent for both polymethyl methacrylate (PMMA) and polyacrylamide (PAA). The solubility parameter of ethanol is 12.7 $(cal/cm^3)^{1/2}$, which is about the average of the values of PMMA (0) and PAA (23.4) in strongly hydrogen bonding solvents (Encyclopedia of Polymer Science, 1985). This helps the fractionation to be less discriminative in terms of composition. Other nonsolvents such as methanol can also be used, but the volume needed for the incipient turbidity is almost two times of that of ethanol. So, for large scale fractionation, methanol is inappropriate because it becomes necessary to handle very large volumes of solution.

Separation of the precipitates of the first fraction from the supernatant layer was very difficult because of their fluid-like gel consistency, due to the high swelling by the solvent. This fluidity of the precipitates decreased as fractionation proceeded to smaller molecular weights.

Fractionation was carried out in a very dilute solution (0.2 - 0.05 w/v %), despite the large volumes (5 - 9 L) involved, because fractionation is significantly more efficient in very dilute solutions. Separation efficiency increased as fractionation proceeded, because the sample concentration decreased continuously.
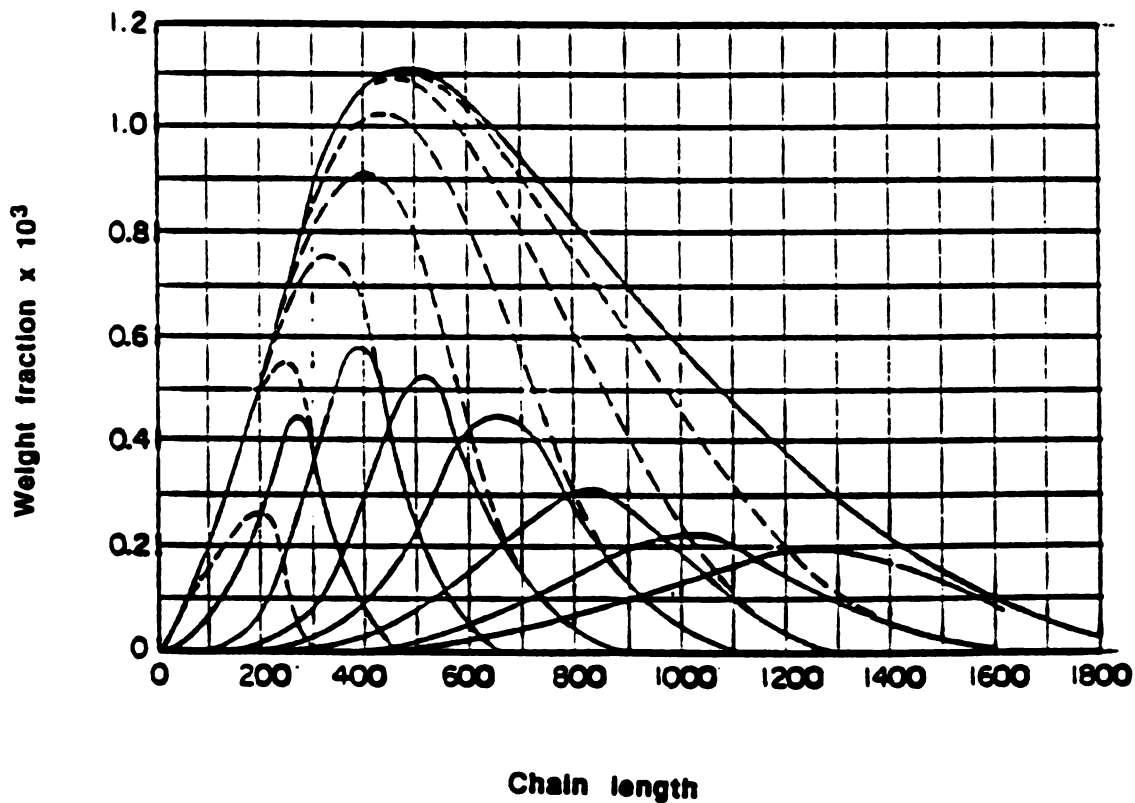
Figure 3.3.7   Calculated distribution for each of eight fractions separated from the initial distribution shown by the uppermost curve. Dotted lines represent distribution of polymer remaining in the dilute phase after each succesive precipitation with v_α/v_β = 1,000 in each case. The distribution for each fraction, obtained as the differences between successive dotted curves, is shown by a solid curve (Schulz, 1940)

Theoretical simulations of fractionation have been reported (Schulz, 1940, Tung. 1962). Fig. 3.3.7 shows one such attempt (Schulz, 1940). Even under the condition of high volume ratio $(V_\alpha/V_\beta = 1,000)$, the fractions are not sharp, and they overlap one another extensively. It should be noticed that the distribution curves become narrower at low molecular weight fractions.

The polydispersity (Mw/Mn) of each fraction was not determined because the amount of sample needed for the measurement of Mw and Mn is much more than the amount obtained in the above fractionation. In theory, the polydispersity of the polymer prepared by free radical polymerization at low conversion is between 1.5 and 2.0 (Billmeyer, 1984). In practice, polydispersities between 2.0 and 2.5 are obtained. Usually, polydispersity of 1.3, which is the average value of each fraction obtained in the theoretical simulation of fractionation (Tung,1962), is assumed for the fractionated sample (Mays et al, 1988).

Only 7 fractions, numbers 4 to 10, were used in further studies; they are denoted as S-1(4th fraction), S-2(5th fraction) etc. There are two reasons for excluding the first three fractions. The first is related to the very low intrinsic viscosity values of the first three fractions, compared to those of the others (Chapter 4). The intrinsic viscosities $[\eta]$ of the first, second and third fractions were 61ml/g,52ml/g, and 61ml/g,respectively. The intrinsic viscosity of the remaining fractions are 60, 53, 47, 42, 38, 29, 22 ml/g from fourth to tenth, respectively. The very low values seem to originat from impurities from the surface of the fritted glass filter, to which these fractions strongly adhered. These impurities could sometimes be seen at the bottom of the test tubes in which these fractions were dissolved. Hence the concentrations used in the calculation of intrinsic viscosity are higher than the actual concentrations, leading to the lower values of $[\eta]$ than expected.

The second reason is the higher polydispersity of the earliest fractions, as discussed in the theoretical simulation of fractionation (Tung, 1962). The polydispersity of a sample can be

roughly estimated from the cumulant analysis of the dynamic light scattering data, to be discussed in Chapter 4. The polydispersity value of the first fraction is much larger than all other fractions; that of the second fraction is rather larger than fractions 4, 5, 6 and 7, and similar to fractions 8, 9, and 10.

3.4 Molecular Weight Determination by Light Scattering

3.4.1 Theory

When a beam of radiation travels through a medium, the formercan be either absorbed or scattered (Billingham,1977). In absorption, energy is lost from the incident radiation to the molecules in the medium. This energy absorbed may be dissipated by various ways such as fluorescence, phosphorescence and photochemical reaction. In scattering, the incident radiation is deflected from its original path and is scattered in all directions.

Scattering occurs because the local electric field of the radiation beam induces polarization of the electrons of a molecule leading to an instantaneous dipole moment (Casassa,1975). This induced dipole oscillates in phase with the electric field and scatters radiation in all directions. The major portion of the scattered light has the same wavelength as the incident beam.

The scattering of light by an ideal gas of point scatterers was considered by Rayleigh (1871). He showed that the intensity of scattered polarized light is given by

$$I_\theta = (I_0 b/r^2) \times (16\pi^4\alpha^2\cos^2\theta/\lambda^4) \qquad (3.4.1)$$

In this expression, I_θ is the intensity of scattered light that is detected at angle θ to the incident beam and at distance r from the center of the medium, I_0 is the intensity of light of wavelength λ incident on the medium, b is the number of scattering centers, and α is the polarizability of the molecule in the medium. It is convenient to lump the intensities and geometry-dependent terms into a single expression, called the Rayleigh ratio, R_θ, which is given by (Billingham,1977)

66

$$R_\theta = I(\theta)r^2 / (I_0 V \cos^2\theta) = 16\pi^4\alpha^2 a / (V\lambda^4) \qquad (3.4.2)$$

where V is the volume in which the a scattering centers are contained.

The scattering of light from liquid was considered by Einstein (1910). He noted that a pure liquid would exhibit zero scattering if it were completely uniform, due to the destructive interference of the scattered light from uniformly distributed solvent molecules. He attributed the scattering that is observed in pure liquids to local fluctuations in the density due to the thermal motions of the molecules. These density fluctuations lead directly to local fluctuations in the refractive index and hence to the scattering of the incident light.

Debye (1944) extended this idea to solutions, assuming that the additional scattering over that of the pure solvent (excess scattering) arises from the local fluctuations in solute concentration. A solution can be viewed as a collection of a large number of identical volume elements, which fluctuate randomly with time. The instantaneous value of the polarizability of one of the elements can be expressed as $\alpha = \alpha_0 + \delta\alpha$, where α_0 is the average polarizability of the solution which is the same for all the elements. The intensity of light scattered at a given time by one of the elements will then be proportional to $\alpha^2 = \alpha_0^2 + 2\alpha_0\delta\alpha + (\delta\alpha)^2$. The first term vanishes because of destructive interference (i.e., this term is same for all elements). The second term also vanishes, because the average value of $\delta\alpha$ is zero. Only the $(\delta\alpha)^2$ term contributes to the average intensity scattered by a single element. Since these fluctuations are random there is no constant phase relation between the scattered light from different elements. At constant temperature and pressure, $\delta\alpha$ is given by

$$\delta\alpha = (d\alpha/dc)_{T,P}\, \delta c \qquad (3.4.3)$$

where c denotes concentration. Thus we may write

$$<(\delta\alpha)^2> = (d\alpha/dc)^2_{T,P} <(\delta c)^2> \qquad (3.4.4)$$

According to the fluctuation theory of Debye (1944), the mean square concentration fluctuation is

$$<(\delta c)^2> = c\, a\, /\, N_A\, [1/M + 2A_2 c + \cdots] \qquad (3.4.5)$$

where N_A is the Avogadro's number, M the molecular weight and A_2 the second virial coefficient. The polarizability, α, of a small volume element is related to the refractive index of the solution, n, by

$$n^2 - 1 = 4\pi\alpha a \qquad (3.4.6)$$

Differentiation of Eq. (3.4.6) with respect to the solute concentration yields

$$(d\alpha/dc) = n/2\pi a \times (dn/dc) = n_0/2\pi a \times (dn/dc) \qquad (3.4.7)$$

Then by replacing α^2 in Eq. (3.4.2) by Eqs. (3.4.4), (3.4.5) and (3.4.7), an expression for the excess Rayleigh ratio due to solute concentration fluctuation is given by

$$R_\theta = 2\pi^2 n_0^2 (dn/dc)^2 c\, /\, \lambda^4 N_A(1/M + 2A_2 c + ...) \qquad (3.4.8)$$

Eq. (3.4.8) can be rewritten as

$$Kc/R_\theta = 1/M + 2A_2 c + \ldots \ldots \qquad (3.4.9)$$

where $K = 2\pi^2 n_0 (dn/dc)^2 / \lambda^4 N_A$ and is a constant containing all the optical parameters. Hence, molecular weight can be determined from the intercept of a plot of K_c/R_θ vs c. The second virial coefficient, A_2, can be obtained from the slope of the plot.

If the solute is polydisperse, the total R_θ at infinite dilution can be expressed as a sum of the Rayleigh ratios for each of the i species, of molar mass M_i and concentration c_i. Thus

$$R_\theta = \Sigma R_\theta \,(i) = K\Sigma c_i/M_i = K \Sigma W_i M_i/V \qquad (3.4.10)$$

where W_i is the weight of i'th species and V the total volume of the solution. K_c/R_θ then becomes

$$K_c/R_\theta = (K\Sigma W_i/V) / (K\Sigma W_i M_i/V) = \Sigma W_i / \Sigma W_i M_i = 1/M_w \qquad (3.4.11)$$

Hence, the molecular weight determined by light scattering is the weight average molecular weight (M_w).

Eq. (3.4.4) is valid when the size of the molecule is less than $\lambda/20$, because the molecule then behaves as a point scatterer. When the molecule is larger than $\lambda/20$, scattered light from two different parts of the molecule can differ sufficiently in phase to interfere destructively at the point of detection. This effect is termed internal interference; its consequence is that the Rayleigh ratio R_θ is a decreasing function of θ. In this case K_c/R_θ can be expressed in the form (Billingham,1977)

$$K_c/R_\theta = [1/M_w + 2A_2 C + ...] [1 + 16\pi^2 <S^2> \sin^2(\theta/2) / 3\lambda^2] \qquad (3.4.12)$$

where $<S^2>$ is the mean square radius of gyration of the polymer. M_W and A_2 can be obtained by extrapolating Kc/R_θ to zero angle for each concentration. $<S^2>$ can also be obtained by extrapolating to zero concentration for each angle. This double extrapolation is usually performed with the aid of a so-called Zimm plot (Zimm, 1948).

The light scattering of copolymers is somewhat different from that of homopolymers, because (dn/dc) for every molecule is not constant in case of copolymer (Yamakawa, 1971). This is due to the compositional heterogeneity. Hence, the molecular weight obtained by the methods discussed above is an apparent weight average molecular weight (M*), not the true weight average molecular weight. M* is related to the true weight average molecular weight (M_W) by (Benoit and Froelich, 1969)

$$M^* = M_W + 2PN + QN^2 \qquad (3.4.13)$$

where N is a constant of the order of unity which is related to the refractive index increment of homopolymers of monomers that constitute the copolymer, and P and Q are parameters characteristic of the distribution of composition in the copolymer. It has been shown that for random copolymers ($r_1 r_2 = 1$), P=0 and Q=0, and M* is the same as Mw (Benoit and Froelich,1969).

.

3.4.2   Experiments and Results

3.4.2.1   Introduction

Intensity measurements of scattered light from the copolymer solutions was done by a BI-200SM motorized goniometer and detection system of Brookhaven Instrument Corporation. Alignment of the goniometer was checked prior to any measurements of the samples and

calibration solvent. The measured intensity was corrected for various electronic (dark counts, dead time) and optical (reflection, refraction, scattering volume) effects (Brookhaven Goniometer manual). Light scattering from a solution of polystyrene with known molecular weight was measured and the molecular weight was determined, in order to check whether the system is reliable or not.

3.4.2.2 Light Scattering System

Fig. 3.4.1 is the schematic diagram of the system used in the experiment. A Lexel Model 95-2 argon ion laser was the light source. The vertically polarized 488nm blue line was used. Extraneous vibrations that might cause changes in the alignment were isolated by installing the laser and goniometer on a vibration isolation table. The goniometer consists of a specimen cell assembly plus a turntable with stepping motor and detector (photomultiplier). There are in/out ports for refractive index matching fluid (toluene) and temperature control fluid (water) in the specimen cell assembly. Inside the specimen cell assembly is a vat filled with toluene. The sample cell is located in this vat for measurement. Filtration/circulation of the index matching fluid was activated by a peristaltic pump and membrane filters (0.22μm). Temperature was controlled by circulating water through copper coils surrounding and below the cell holder. A Lauda model number RM6 circulator was used. The temperature in the sample cell (25°C) was controlled to within +/-0.05°C. In front of the detector, a narrow-band optical interference filter (488 nm) and a pinhole turret with various pinhole sizes for selecting coherence area and adjusting intensity are located. The photomultiplier(PMT) tube is the BI-DS type. A potential of 1.21kV is supplied to the PMT tube by high voltage supplier. The signal from the PMT tube is passed to the BI-2030 Digital Correlator (136 channels) to collect the intensity autocorrelation function in real time and to store the data. The average scattered intensity was obtained by use of the ZP-30 program provided by the Brookhaven Instrument Co.
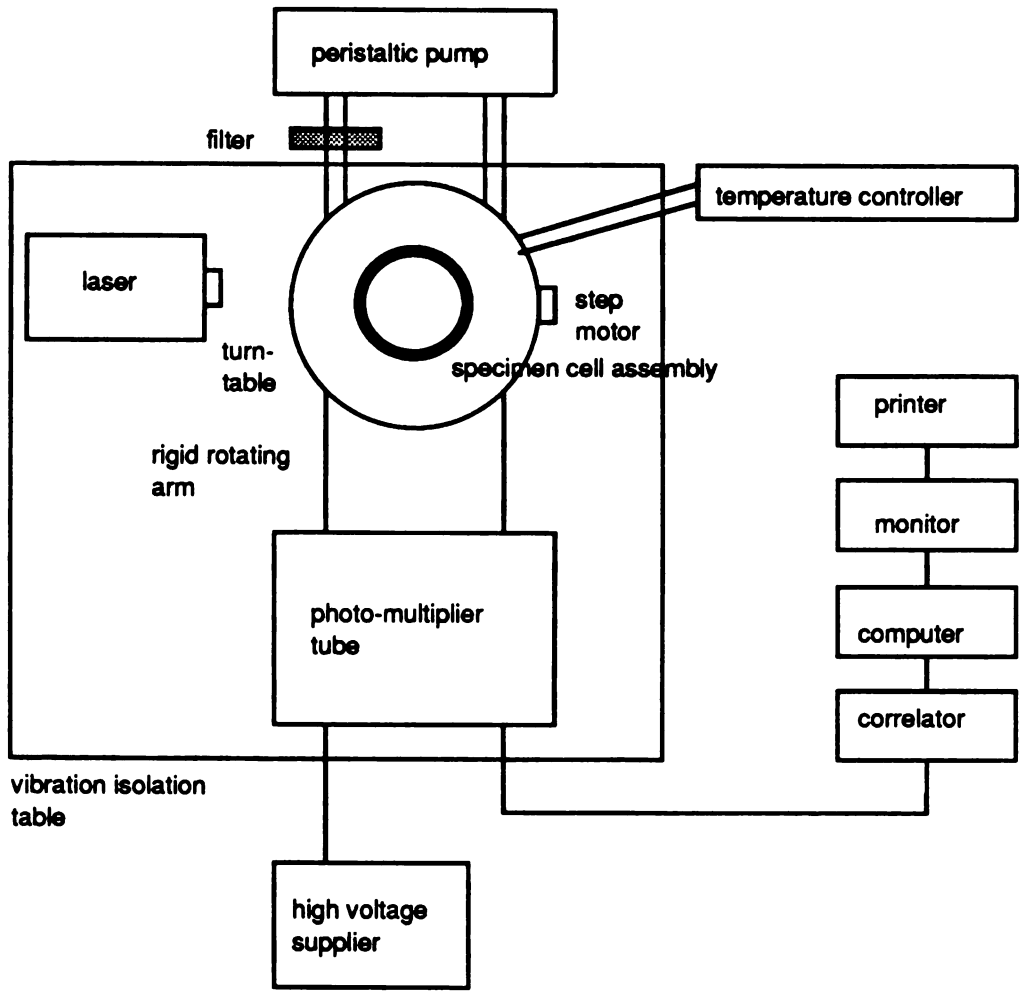
Figure 3.4.1   Schematic diagram of the light scattering system

3.4.2.3   Sample Preparation

Solutions used for light scattering measurements should be absolutely free of dust (Tabor, 1972). Dust was removed by filtration of the solution directly into the cell . The filters used were Millipore membrane filters (Fluoropore, 0.22μm) . They are made of poly-tetrafluoroethylene, which is compatible with most chemicals. The cylindrical glass cell was cleaned by soaking in concentrated sulfuric acid for a day, followed by washing with water which is filtered through a Nanopure filter system (Barnstead Co.). The cell was washed again 10 times with acetone that was filtered through a Fluoropore membrane filter (0.22μm) directly into the cell, and dried in the air by standing upside down on an aluminium foil for 1 or 2 hours. Cell stoppers were also cleaned by washing with filtered acetone 10 times. During the cleaning procedures, cells were handled with caution in order to prevent scratching and were always held at the top all the time.

3.4.2.4   Dark Count Correction

Even in the absence of light, counts will be registered by the PMT. These dark counts are due to a number of effects (e.g. shot noise) taking place in the photomultiplier tube. The dark count must be subtracted from the count measured. The dark count was measured by turning the pinhole turret midway between two click stops. Fourteen measurements were carried out. The average count rate (count / sec) was 1,657 with a standard deviation of 53.

3.4.2.5   Dead Time Correction

Every photon counting system has a dead time, T_d, during which photons arriving immediately after a recorded photon are not recorded. The dead time in a correlator system is normally equal to the shortest sample time, which is 100nsec for the correlator used in the

73

experiment. Only one pulse every 100nsec can be recorded. As a result the true count rate, I_t, is higher than the measured count rate, I_m. Correction for this effect can be made using the following equation (Brookhaven Goniometer Manual, 1984).

$$I_t = I_m / (1 - I_m T_d)$$

The percent error in neglecting the dead-time correction is then given by

$$E_d = 100 \, I_m T_d$$

The magnitude of this error for $T_d = 100nsec$ is completely negligible for $I_m = 10^3$, but it becomes significant as the count rate increases. When $I_m = 10^6$, $E_d = 10\%$ and the correction can no longer be trusted to reduce the systematic error below 1%. Therefore, in the measurement of the scattered intensity of copolymer solutions, the count rate was kept below 10^6 all the times.

3.4.2.6   Checking of Alignment

For a Rayleigh point scatterer excited by polarized light, the count rate should be independent of angle provided the detector views the same scattering volume. However, the scattering volume viewed by the detector increases on either side of 90 deg. Multiplying the count rate (corrected for dead time and dark count) by $\sin\theta$ corrects for this volume effect, and $I \sin\theta$ should be constant (Leite et al, 1965).

Before taking measurements, the laser was allowed to warm up for approximately 2 hours. The index matching fluid was filtered for 5 minutes after a new sample was placed in the bath, and every once in a while (~hourly) thereafter. The outside of the sample cell was washed with filtered acetone and dried in the air before placing in the bath. After introducing the sample into the bath,

about ten minutes were allowed for the sample to reach equilibrium. During the measurement, the room light was off. In all experiments, problems due to dust were minimal.

The count rate from benzene was measured for one second 5 times at each of the following angles: 40, 50, 60, 70, 80, 90, 100, 110, 120, 130 and 140. After count rates were corrected for dead time and dark count, I sinθ was calculated.

Fig. 3.4.2 is the plot of I sinθ vs θ. The count rates at various angles are constant within +/- 1%, indicating that the goniometer was well-aligned.

3.4.2.7   Reflection   Correction

Reflection occurs at any interface between 2 dielectrics with different indices of refraction. In our experiment, reflection correction was negligible because the refractive indices of all components of the light path were close to each other; vat (1.473), index matching fluid (toluene, 1.4903), calibration solvent (benzene, 1.4941), sample cell (1.514), and solvent (MFA, 1.4309). Back reflection of the incident beam by the air/glass interface was avoided by the beam stop in the vat.

3.4.2.8   Refraction   Correction

The volume of scattering viewed by the detector depends on the refractive index of the solvent. This can be corrected by multiplying the measured intensity by (n_0/n_c), where n_0 and n_c are the refractive indices of solvent and the calibration solvent, respectively.
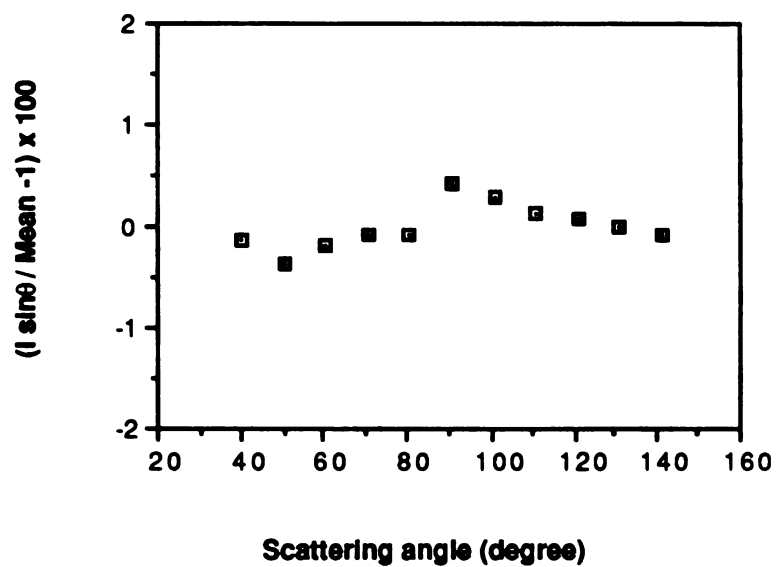
Figure 3.4.2   Plot of (Isinθ / Mean - 1) x 100 as a function of angle from benzene. I is the scattering intensity, θ is the angle of measurement, and Mean is the average value of Isinθ.

3.4.2.9 Refractive Index Increment Measurement

In order to determine the optical K value of Eq. (3.4.4), dn/dc should be evaluated first by experiment. A Milton Roy Differential Refractometer was used in this work. Both sample and reference cell were filled with solvent (N-methylformamide) initially, and then the sample cell was charged with each of 0.002g/ml and 0.004g/ml solution. Table 3.4.1 shows the results of these measurements.

Table 3.4.1   Refractive index increment of poly (MMA-co-AA) solution

	0.002 g/ml $(\times 10^{+4})$	0.004 g/ml $(\times 10^{+4})$
	1.704	3.360
	1.706	3.373
	1.705	3.388
		3.372
average	1.705	3.373

The average value of $1.705 \times 10^{-4}/0.002$ and $3.373 \times 10^{-4}/0.004$,0.0848, was used as dn/dc value in the calculation of the optical constant K.

3.4.2.10 Rayleigh Ratio Calculation

The calibration of the instrument was carried out using benzene (Utiyama, 1972). The Rayleigh ratio for the solute (ΔR_θ) was determined from the followingexpression (Tomimatsu et al, 1968, Evans, 1972)

$$\Delta R_\theta = (R_c/I_c) \, \Delta I_\theta \sin\theta \times (n_o/n_c)^2$$

where R_c is the Rayleigh ratio for benzene $= 38 \times 10^{-6}$ cm-^{1} (Goniometer Instruction Manual); I_c is the count rate of benzene; and ΔI_θ is the difference in count rate between solution and solvent. R_c/I_c is the instrumental calibration constant for the system used in this work.

3.4.2.11 Test Measurement of Polystyrene

In order to check the validity of the system for molecular weight determination, the molecular weight of polystyrene (from Polyscience) of known molecular weight ($M_w = 104,000$, $M_w/M_n = 1.05$) was determined. Five samples of different concentration were prepared. The count rate was measured at each of the following angles: 40, 50, 60, 70, 80, 90, 100, 110, 120, 130 and 140. The highest and the lowest count rates of 5 measurements were eliminated. Because the (count rate) x sinθ value was constant as shown in Fig. 3.4.2 irrespective of angles, no angular extrapolation was necessary. The count rate measured at 90 deg was used for the calculation of R_θ. The count rate from benzene was also measured and was subtracted from the count rate of solution. The value of (dn/dc) was obtained from the literature (Ikada et al, 1965).

Table 3.4.2 lists the scattering data (corrected for dead time and dark count) and the value of parameters used. Fig. 3.4.3 shows the plot of K_c/R_θ vs concentration. The slope and intercept are obtained by least-squares regression. The molecular weight determined from the intercept was 101,700, which is very close to the expected value.
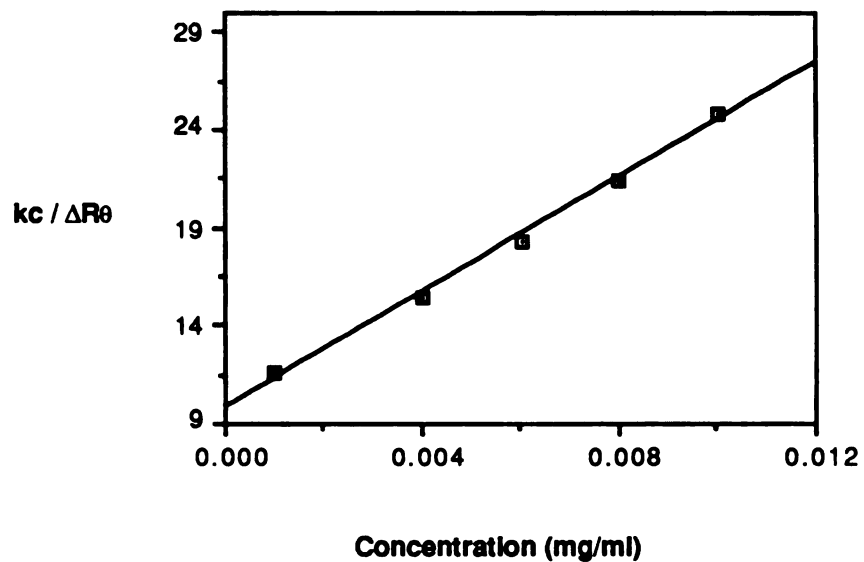
Figure 3.4.3 Plot of Kc/ΔRθ as a function of concentration for polystyrene. Each point represents the mean of triplicate measurements; the standard error bars are smaller than symbol. K is the optical constant, c the concentration and ΔRθ is the Rayleigh ratio for the solute.

Table 3.4.2 The scattering data from polystyrene-benzene solution and the value of parameters used

Concentration (g/ml)	Count Rate	Standard Error(%)	$Kc/\Delta R_\theta$
0.001	119,559	0.13	24.85
0.004	211,701	0.27	21.42
0.006	246,918	0.10	18.34
0.008	271,041	0.21	15.40
0.01	285,987	0.09	11.65
benzene	71,797	0.001	

$dn/dc = 0.106 \, cm^3/g$ $n_0 = 1.4941$ $\lambda = 4.88 \times 10^{-5} \, cm$

$R_c = 38 \times 10^{-6} \, cm^{-1}$

$K = [4\pi^2 n_0^2 \, (dn/dc)^2] / (\lambda^4 \, N_A) = 2.899 \times 10^{-7} \, cm^2/g^2$

3.4.2.12 Molecular Weight Determination of Copolymer Fractions

For each copolymer fraction, 4 to 6 solutions of different concentration were prepared from a stock solution of N-methylformamide. The count rate was measured five to ten times.The highest and the lowest values were discarded. Measurements were made at each of the following angles: 40, 50, 60, 70, 80, 90, 100, 110, 120, 130 and 140. Fig. 3.4.4 shows the (count rate) x sinθ vs angle plot of S-1, which is the largest molecular weight sample. Because the values of (count rate) x sinθ were independent of angle, we could conclude that there is no internal interference (as in the case of polystyrene solution). Hence, for subsequent measurements, only concentration extrapolations were carried out. The data measured at 90 deg were used for the calculation of molecular weight. The count rate of MFA was also measured.
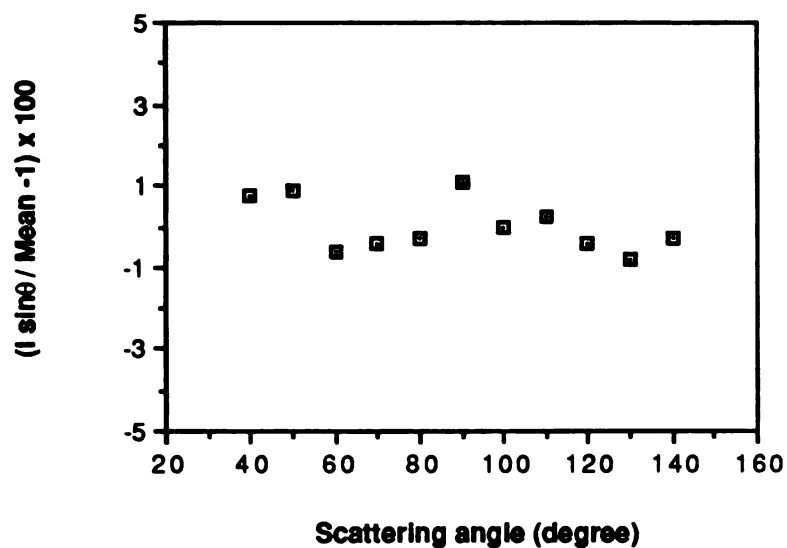
Figure 3.4.4   Plot of (Isinθ / Mean -1) x 100 as a function of angle from a solution of sample S-1 (concentration = 1 mg/ml). I is the scattering intensity, θ is the angle of measurements, and Mean is the average value of Isinθ.

Table 3.4.3 lists the scattering data (corrected for dead time and dark count) of S-1 and the value of parameters used for the calculation of K and R_θ. Fig. 3.4.5 shows the plot of $Kc/\Delta R_\theta$ vs concentration. The intercept and slope of the plot are obtained by least-squares linear regression. The molecular weights calculated from the intercepts are listed in Table 3.4.4, together with the second virial coefficients obtained from the slopes of the plots.

Table 3.4.3   The scattering data from the solutions of S - I and the values of parameters used

Concentration (g/ml)	Count Rate	Standard Error (%)	$Kc/\Delta R_\theta$
0.008	246,306	0.17	12.66
0.007	233,029	0.09	11.82
0.006	218,633	0.26	10.92
0.004	178,066	0.09	9.34
0.002	120,661	0.23	7.76
0.001	83,820	0.31	6.76
MFA	34,496	0.003	

$dn/dc = 0.0848$ cm^3/g, $\quad n_0 = 1.4309 \quad\quad \lambda = 4.88 \times 10^{-5}$ cm

$R_c = 38 \times 10^{-6}$ cm^{-1}

$K = 1.702 \times 10^{-7}$ cm^2/g^2

3.4.3   Discussion

The molecular weight determined in this work is an apparent weight average molecular weight. But, because the copolymer used in this work is a random copolymer whose $r_1 r_2$ value is very close to 1, the apparent molecular weight determined should be very close to the true weight
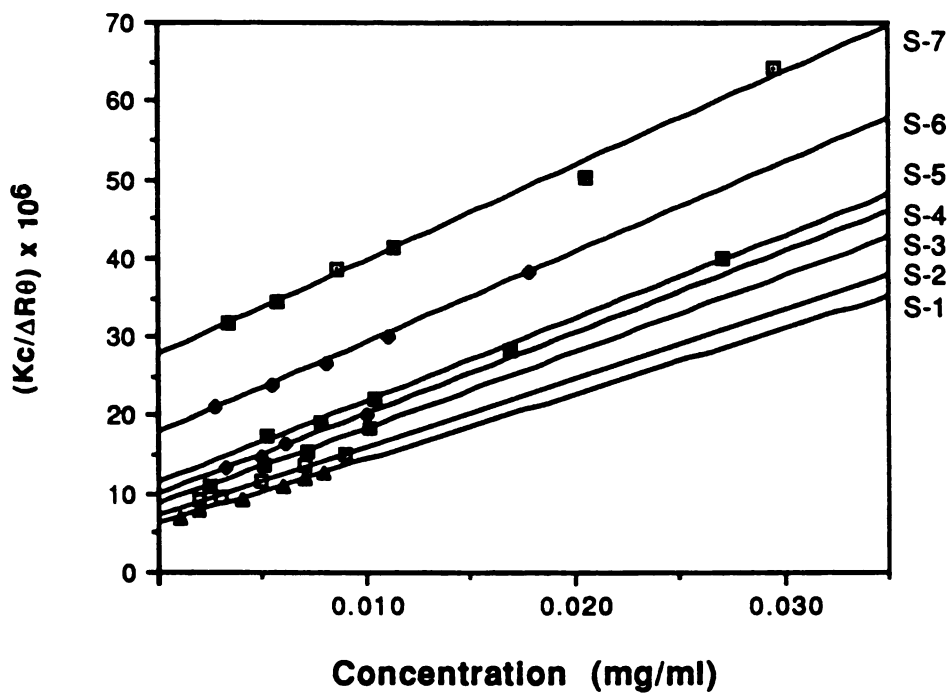
Figure 3.4.5   Plot of Kc/ΔRθ as a function of concentration for all samples (S-1 to S-7) measured in this work. Each symbol represents the mean of 3 to 6 measurements and the standard error bars are smaller than symbol. K is the optical constant, c is the concentration and ΔRθ is the Rayleigh ratio.

Table 3.4.4 Molecular weights and second virial coefficients (A$_2$) of the copolymer samples

sample	molecular weight +/- s.e. (g/mole)	A$_2$ +/- s.e. x10^4, (ml/g)
S-1	166500 +/- 1600	4.15 +/- 0.06
S-2	138600 +/- 4500	4.37 +/- 0.21
S-3	116700 +/- 1300	4.84 +/- 0.07
S-4	101600 +/- 4600	5.14 +/- 0.35
S-5	88800 +/- 3500	5.23 +/- 0.15
S-6	56200 +/- 1100	5.69 +/- 0.17
S-7	36400 +/- 1200	6.22 +/- 0.30

average molecular weight.

The reliability of the light scattering system used in this work was checked using a polystyrene sample of known molecular weight. The value obtained shows good agreement within experimental error with the expected value. The molecular weights and second virial coeffcients obtained for each sample are listed in Table 3.4.4. The standard errors are relatively small (<5%) except for S-4, which shows about 5% standard error for molecular weight and 7% for second virial coefficient.

Double extrapolation by a Zimm-plot was not conducted because no angular dependence of the scattered light was observed. The constancy of (count rate) x sinθ at various angles is shown in Fig. 3.4.4. The reason for this constancy will be clearer when the hydrodynamic size measurements are described in next chapter. In brief, it was found that the

84

measured size of the largest molecular weight sample,S-1, (22.6 nm in diameter) is less than $\lambda/20$ (24.4nm). Hence there is no internal interference of the scattered light.

The R_C (Rayleigh ratio for pure benzene) value used in the calibration is a value estimated by interpolation of data between 546 and 436 nm (Coumou et al, 1960, 1964); the values at 488 and 514.5 nm are not as well known. Coumou and his coworkers have performed very precise measurements for use in calibration. The relative error in the R_C value used was estimated to be +/-5% (Goniometer Instruction Manual).

The samples used in this work are not monodisperse. Hence, the second virial coefficients include some contributions due to the polydispersity of the samples. The effect of polydispersity on the second virial coeficient has been considered by Casassa (1962). He showed that the second virial coeficient increases as polydispersity increases, and the increase is larger for the osmotic second virial coeficient than light-scattering second virial coeficient, reflecting the different type of averages resulting from the two measurements. For example, when the polydispersity is 1.7, the osmotic second virial coeficient is about 24% larger than that of a monodisperse sample with molecular weight equal to the number average molecular weight of the polydisperse sample. On the other hand, for the same polydisperse sample, the light-scattering second virial coeficient is about 9% larger than that of the corresponding monodisperse sample. The second virial coeficient determined in this work was light-scattering second virial coeficient. The polydispersity of the samples used was about 1.3. The estimated effect with this polydispersity is about 3% and this suggests that the data may be analysed by using the theory for monodisperse polymers, considering an experimental error in determination of second virial coeficient (Yamakawa, 1971).

References

T. Alfrey, Jr. and G. Goldfinger, J. Chem. Phys., 12, 205, 1944

H. R. Allcock and F. W. Lampe, Contemporary polymer chemistry, Prentice-Hall, 1981

S. T. Balke and R. D. Patel, J. Polym. Sci., Polym. Lett. Ed. 18, 453, 1980

B. G. Belenkii, Pure & Appl. Chem., 51, 1519, 1979

H. Benoit and D. Froelich, in Light Scattering from Polymer Solutions, M.B. Hugglin (Ed.), Academic Press, New York, 1969

N. C. Billingham, Molar Mass Measurement in Polymer Science, Wiley, New York, 1977

F. W. Billmeyer, Jr., Textbook of Polymer Science, 3rd Ed., 68, 1984

E. A. Collins, J. Bares and F. W. Billmeyer, Jr., Experiments in Polymer Science, Chapter 3 & 4, J. Wiley & Sons, 1973

D. J. Coumou, J. Colloid Sci., 15, 408, 1960

D. J. Coumou and E. L. Macker, Trans Faraday Soc., 60, 1726, 1964

M. Danielewicz and M. Kubin, J. Appl. Polym. Sci., 26, 951, 1981

N. S. Davidson, L. J. Fetters, W. G. Funk, W. W. Graessley, N. Hadjichristidis, Macromolecules, 21, 112, 1988

P. Debye, J. Appl. Phys., 15, 338, 1944

K. A. Dill, Lecture note of Physical cemistry course (1985), University of California, San Francisco

A. Einstein, Ann. Physik., 33, 1275, 1910

S. Ellerstein and R. Uhlman, J. Polym. Sci., 55, 123, 1961

J. M. Evans, in Light Scattering from Polymer Solutions, M. B. Huglin (Ed.), Academic Press, New York, 1972, Chapter 5

M. Fineman and S. D. Ross, J. Polym. Sci., 5, 259, 1950

P. J. Flory, Principles of polymer chemistry, Cornell University Press, Ithaca, N.Y., 1953

O. Fuchs and W. Schmieder, in M. J. R. Cantow, ed., Polymer Fractionation, Academic Press, Inc., New York, 1966

Goniometer Instruction Manual, Brookhaven Instrument Co.,Chapter VI, 1984

H. J. Harwood and W. M. Ritchey, Polym. Lett., 2, 601, 1964

M. Hoffmann and H. Urban, Makromol. Chem., 178, 2683, 1977

Y. Ikada and W. Schnabel, Macromol. Chem., 86, 20-32, 1965

H. Inagaki, H. Matsuda and F. Kamyiama, Macromolecules, 1, 520, 1968

V. Juranicova, S. Florian and D. Berek, Eur. Polym. J., 6, 57, 1970

T. Kelen and F. Tudos, J. Macromol. Sci. - Chem., A9(1), 1, 1975

R. C. C. Leite, R. S. Moore, S. P. S. Porto and J. E. Ripper, Physical Review Letters, 14, 7, 1965

A. D. Litmanovich and V. Ya. Shtern, J. Polym. Sci. Part C, 16, 1375, 1967

F. R. Mayo and F. M. Lewis, J. Amer. Chem. Soc., 66, 1594, 1944

J. W. Mays and N. Hadjichristidis, Rev. Mocromol. Chem. Phys., C28 (3 & 4), 371, 1988

S. Nakano and Y. Goto, J. Appl. Polym. Sci., 26, 4217, 1981

A. M. North, The Kinetics of free radical polymerization, Pergamon Press, N. Y., 1966

G. Odian, Priciples of polymerization, John Wiley & Sons, New York, 1984

T. Ogawa and M. Sakai, J. Polym. Sci., Polym. Phys. Ed., 19, 1377, 1981

W. Ring, Polym. Lett., 1, 323, 1963

G. Saini, A. Leoni and S. Franco, Makromol. Chem., 144, 235, 1971

H. Sato, H. Takeuchi and Y. Tanaka, Macromolecules, 19, 2613, 1986

G. V. Schulz, Z. physik. Chem., B46, 137, 1940, J. Polym. Sci., 2. 90, 1947

J. Stejskal and P. Kratochvil, J. Appl. Pol. Sci., 22, 2925, 1978

J. Stejskal, P. Kratochvil and S. Strakova, Macromolecules, 14, 150, 1981

W. H. Stockmayer, J. Chem. Phys., 13, 199, 1945

J. W. Strutt (Lord Rayleigh), Phil. Mag., 41, 107, 274, 447, 1871

B. E. Tabor, in Light Scattering from Polymer Solutions, M. B. Huglin (Ed.), Academic Press, New York, 1972, Chapter 1,

S. Teramachi, A. Hasegawa, S. Hasegawa and I. Ishibe, Polym. J., 13, 319, 1981

S. Teramachi, A. Hasegawa, Y. Shima, M. Akatsuka and M. Nakajima, Macromolecules, 12, 992, 1979

S. Teramachi and Y. Kato, Macromolecules, 4, 54, 1971

Y. Tomimatsu, L. Vitello and K. Fong, J. Colloid Interface Sci., 21, 298, 1966

L. J. Tung, in Encyclopedia of Polymer Science, Vol. 7, 1985

L. H. Tung, J. Polym. Sci. 61, 449, 1962

H. Utiyama, in Light Scattering from Polymer Solutions, OD. Cit., Chapter 4

J. H. M. van den Berg, N. L. J. Meijerink, T. G. Scholte and R. Koningsveld, Macromolecules, 17, 962, 1984

H. Yamakawa, Modern Theory of Polymer Solutions, Chapter V, 1971

Chapter 4   DIMENSIONAL STUDY IN DILUTE SOLUTION

4.1   Introduction

Several methods are available for determining the size of polymer molecules in dilute solution. Angular dependency of light scattering intensity provides the radius of gyration (R_G). Diffusion and sedimentation coefficients provide the hydrodynamic radius (R_H), while intrinsic viscosity provides the viscometric radius (R_V). The second virial coefficient in a good solvent provides the thermodynamic or excluded volume radius (R_T). Such data are used extensively to test dilute solution theories predicting the influence of chain length, chain architecture, and polymer-solvent thermodynamic interactions.

In this chapter, measurements of intrinsic viscosity (by viscometry) and diffusion coefficient (by dynamic light scattering) are described. R_V and R_H are calculated from these measurements. R_T is calculated from the second virial coefficient determined as described in Chapter 3. In the analysis of the data, these radii are expressed in terms of power of molecular weight. The ratios between different radii are also calculated and compared with theoretical predictions.

4.2   Viscosity Measurement

4.2.1   Theory

According to Newton's law of viscous flow, the frictional force, F, that resists the flow of any two adjacent layers of liquid is given by (Allcock et al, 1981)

$$F = \eta A. \, dv/dx \qquad\qquad (4.2.1)$$

where A is the area of contact of the layers, dv/dx the velocity gradient between them, and the proportionality constant, η, is called the viscosity. The rate of laminar Newtonian flow of a liquid through a capillary tube is given by Poiseuille's law,

$$dv/dt = \pi R^4 \Delta P / 8\eta L \qquad (4.2.2)$$

where dv/dt is the volume of liquid that flows through the tube per unit time; R and L are the radius and length of the tube, respectively; and ΔP is the difference in external pressure between the ends of the tube. Because the viscometric measurements are usually carried out in viscometer tubes in which the capillary is in a vertical position, ΔP can be expressed as

$$\Delta P = \rho g h \qquad (4.2.3)$$

where ρ is the density, g the gravitational acceleration and h the average height of the liquid during measurement. Substitution of (4.2.3) into (4.2.2), along with the assumption of a constant flow rate, yields

$$\eta = (\pi R^4 gh/8LV)\rho t = A\rho t \qquad (4.2.4)$$

where A is a constant for a particular viscometer and V is the total volume that flows during time t. The time t must be sufficiently long to render negligible inertial effects that occur when the fluid is set in motion. The relative viscosity (η_r), which is defined by the ratio of solution viscosity (η) to solvent viscosity (η_0), is given by

$$\eta_r = \eta/\eta_0 = (t/t_0) \times (\rho/\rho_0) \qquad (4.2.5)$$

where the flow time and density of a solution are denoted as t and ρ respectively, and the corresponding values for the pure solvent are t_0 and ρ_0. For the very dilute solutions used in polymer studies, the densities of solution and solvent can usually be equated without significant error, so that $\eta_r = t / t_0$ (Collins et al, 1973). Since η_r has a limiting value of 1, it is often more convenient to define the specific viscosity (η_{sp}) which is defined

$$\eta_{sp} = \eta_r - 1 = (t - t_0)/t_0 \qquad (4.2.6)$$

The specific viscosity is the fractional increase in viscosity which results from the presence of polymer in the solution. The ratio η_{sp}/c, where c is the weight concentration (g/cm^3) of polymer in the solution, is termed the reduced viscosity of the solution. Reduced viscosity is a measure of the ability of the polymer to increase the viscosity.

A linear dependence of the reduced viscosity on polymer concentration is usually found when $\eta_r < 2$. The linear dependence is described well by the Huggins equation (Allcock et al, 1981)

$$\eta_{sp}/c = [\eta] + k'[\eta]^2 c \qquad (4.2.7)$$

where k' is the so-called Huggins constant and $[\eta]$ is the intrinsic viscosity, defined by

$$[\eta] = \lim_{c \to 0} (\eta_{sp} / c) \qquad (4.2.8)$$

Hence, intrinsic viscosity can be obtained from the intercept of the plot of η_{sp}/c against c, while the Huggins constant can be obtained from the slope. The Huggins constant is related to the intermolecular interactions between the polymer molecules in the solution.

91

Intrinsic viscosity is a measure of the ability of the polymer molecule to increase the viscosity of the solvent in the absence of any intermolecular effects. It is related to the molecular weight by the semi-empirical Mark-Houwink Equation.(Flory, 1953)

$$[\eta] = KM^v$$

Where K and v are constants, which are dependent on the solvent used and the temperature. The exponent v is usually lies between 0.5 and 0.8 (Flory, 1953).

4.2.2 Experiment

Viscosities were measured in methylformamide solution in a 25°C bath using an Ostwald viscometer (Fig. 4.2.1). The bath temperature was maintained within +/-0.05°C with a Lauda Immersion circulator (Model MS). Concentrations were chosen to obtain relative viscosities in the range 1.1 to 1.5. Stock solution for each sample was prepared by dissolving a known quantity of the copolymer in N-methylformamide. The stock solution was filtered through a Millipore filter (Fluoropore, 0.22μm) before preparing solutions of various concentrations.

Procedure:

1. 3ml of solution is transfered to chamber B of the viscometer (Fig. 4.2.1) with a syringe.

2. The viscometer is clamped vertically in the bath.

3. After 10 minutes for temperature equilibration, the solution is brought to chamber A above the line m_1.

4. The solution is allowed to drain down the capillary.

5. The flow time is measured by starting the timer as the meniscus passes the upper graduation mark (m_1) and by stopping as the meniscus passes the lower mark (m_2)
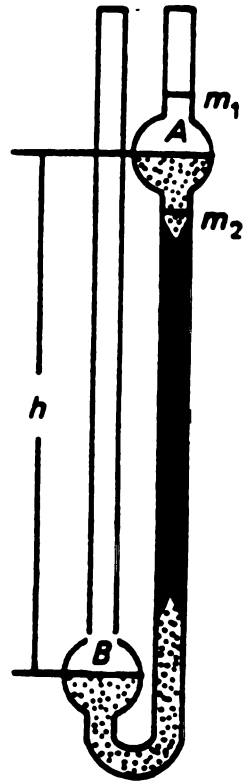
Figure 4.2.1   An Ostwald capillary viscometer

For each sample, three to five measurements were made. After each measurement, the viscometer was rinsed several times with MFA and acetone. The viscometer was dried by blowing a stream of argon gas into the lumen.

4.2.3 Results

Table 4.2.1 shows the data for solutions of S-1, and the various calculated viscosities. The standard error of the reduced viscosity is also given.

Table 4.2.1   Viscosity data from the measurement of the solution of S-1

c, g/dl	t, sec	η_r	η_{sp}	η_{red} (dl/g) +/- s.e.
0.761	183.83	1.541	0.541	0.710 +/- 0.005
0.609	169.68	1.422	0.422	0.693 +/- 0.005
0.457	156.83	1.308	0.308	0.673 +/- 0.005
0.305	142.49	1.194	0.194	0.638 +/- 0.002
0	119.32			

Intrinsic viscosity was obtained from the intercepts of plots of η_{red} against concentration (Fig. 4.2.2). The Huggins constant was obtained from the slope. These values are listed in Table 4.2.2.
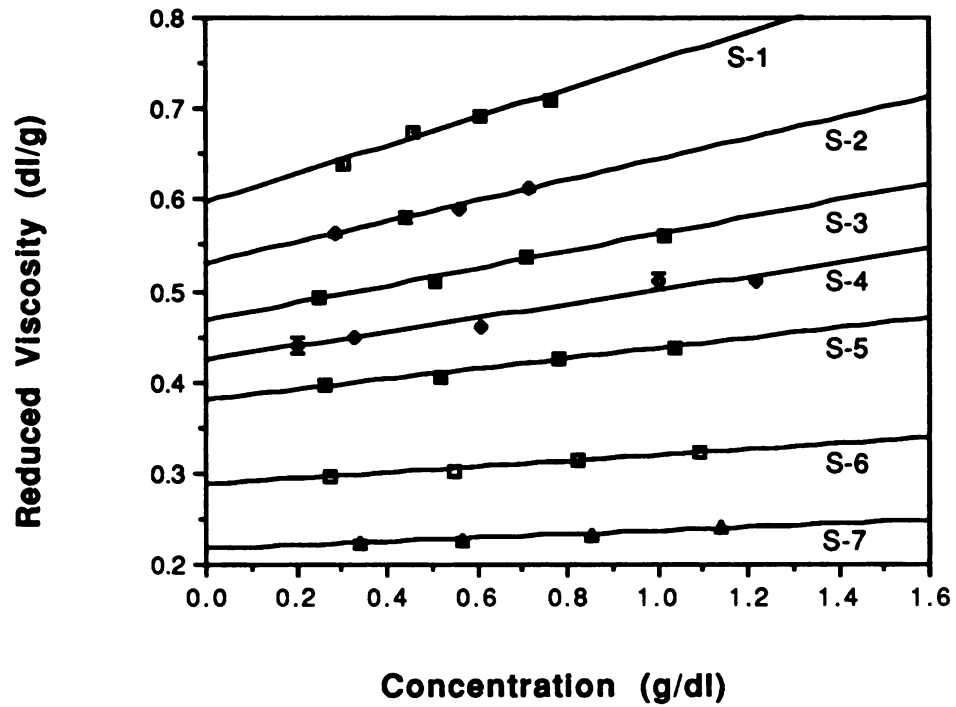
Figure 4.2.2   Plot of reduced viscosity as a function of concentration for each sample. Each data point represents the mean of 3 to 5 measurements and the standard error is shown as bar.

Table 4.2.2   Intrinsic viscosity and Huggins constant of each sample

Sample	MW (g/mole)	[η] (ml/g) +/- s.e.	k'
S-1	166,500	59.6 +/- 1.1	0.44
S-2	138,600	52.9 +/- 0.4	0.41
S-3	116,700	46.7 +/- 0.5	0.42
S-4	101,600	42.3 +/- 0.1	0.42
S-5	88,800	37.9 +/- 0.4	0.40
S-6	56,200	28.7 +/- 0.2	0.38
S-7	36,400	21.6 +/- 0.3	0.43

4.2.4 Discussion

The use of a capillary viscometer is based on the application of Poiseuille's equation (Eq. 4.2.2) to the flow of solution through the capillary. In deriving this equation it is assumed that the potential energy of the liquid above the capillary is used entirely to overcome viscous forces within the capillary and that the liquid emerges from the capillary with essentially zero velocity, i.e. with zero kinetic energy. This is not true because part of the potential energy of the liquid column appears as the kinetic energy of efflux. The error associated with ignoring this kinetic energy can be minimized by reducing the capillary radius and the capillary length (i.e., by increasing the flow time). In commonly used viscometers, the error due to the kinetic energy effect is less than 0.5 % (Billingham, 1977).

The Huggins constant k', for flexibly coiled polymers in good solvents, usually has a value between 0.3 and 0.5 and is approximately constant for any given polymer-solvent combination. The values obtained in this work, with an average of 0.41, lie well within this range.

4.3   Measurement of Hydrodynamic Radius by Dynamic Light Scattering

4.3.1 Background

The scattering intensity discussed in Chapter 3 is a time-averaged intensity. However the actual scattering intensity fluctuates around this averaged value. The time varying total scattering intensity, $I_S(t)$, can be expressed (Ford Jr., 1985)

$$\bar{I}_S(t) = \bar{I}_S(1) [N + 2 \sum_{i=1}^{N} \sum_{j=i+1}^{N} \cos(\phi_i - \phi_j)]$$

(4.3.1)

where $\bar{I}_s$ (1) is the time averaged intensity of light scattered by one molecule, N the total number of molecules in the volume being observed, ϕ_i the phase of the electric field scattered by i'th molecule and ϕ_j that of jth molecule. The first term of Eq. (4.3.1) is the static term which corresponds to the time-averaged intensity. The second term is the fluctuation term whose instantaneous value is not zero, but ranges from -N to +N, due to the random change in phase arising from the diffusion of the molecules. The time-averaged value of this second term is zero with excursions in both positive and negative directions.

The time required for the fluctuation to take place is the most important characteristic of the signal because that time contains information about the diffusion coefficients and hence the sizes of the solute molecules; a large molecule shows a slower fluctuation than a small molecule, because the phase change is slow for a large molecule, having a smaller translational diffusion coefficient. This diffusion coefficient can therefore be obtained by analysing the fluctuation data using correlation techniques.

98

In digital correlation experiments, the quantity usually determined is the intensity autocorrelation function defined as (Berne and Pecora, 1976)

$$G^2(\tau) = < I(0) \; I(\tau) > \tag{4.3.2}$$

where the angular brackets denote the time average of the product of two intensities separared by a delay time , τ. The measured intensity autocorrelation function has the form (Berne et al, 1976)

$$G^2(\tau) = B(1 + b \; |g^1(\tau)|^2) \tag{4.3.3}$$

where $g^1(\tau)$ is the scattered electric field autocorrelation function, B the baseline of the intensity autocorrelation function which can be obtained either from the delay channels (measured baseline) or from calculating the average intensity (calculated baseline), and b is a constant that is a function of detecting electronics and accounts for the nonideal point detector. The value of b is not known and it is used as a parameter in the fitting procedure. For a dilute solution of relatively small monodisperse particles undergoing Brownian motion, the electric field autocorrelation function is (Berne et al, 1976)

$$g^1(\tau) = \exp(-Dq^2\tau) \tag{4.3.4}$$

where D is the translational diffusion coefficient and q is the magnitude of scattering vector given by

$$q = (4\pi n_0 / \lambda_0) \sin\left(\frac{\theta}{2}\right) \tag{4.3.5}$$

with n_0 being the refractive index of the solvent, λ the wavelength of the incident light in vacuum and θ the scattering angle. For a monodisperse polymer solution, the measured $G^2(\tau)$ can be transformed into $\ln g^1(\tau)$ using Eq. (4.3.3)

$$\ln g^1(\tau) = 1/2 \ln(1/b) + 1/2 \ln\{G^2(\tau)/B - 1\} \tag{4.3.6}$$

Eq. (4.3.6) combined with Eq. (4.3.4) allows the diffusion coefficient to be obtained. The hydrodynamic radius can then be calculated from the Stokes-Einstein equation

$$D = kT / 6\pi\eta_0 R_H \tag{4.3.7}$$

where D is the translational diffusion coefficient, k the Boltzmann constant, T the absolute temperature and η_0 the viscosity of the solvent.

For a polydisperse solution, in the absence of internal motions, the electric field autocorrelation function consists of a sum or distribution of single exponentials (Koppel,1972)

$$g^1(\tau) = \int_0^\infty G(\Gamma) \exp(-\Gamma\tau) \, d\Gamma \tag{4.3.8}$$

where $G(\Gamma)$ is the normalized distribution function of the decay rates and $\Gamma = Dq^2$. $G(\Gamma)d\Gamma$ is the fraction of the total (normalized) intensity scattered by molecules for which $\Gamma \leq Dq^2 \leq \Gamma + d\Gamma$. In principle, $G(\Gamma)$ can be calculated by Laplace inversion of $g^1(\tau)$ in Eq. (4.3.8). However, in practice, the experimentally obtained $G^2(\tau)$ contains noise and Laplace inversion becomes an ill-posed problem, in which the number of available $g^1(\tau)$ data is always less than that needed to describe $G(\Gamma)$ uniquely (Provencher[1], 1982). To address this problem, various data interpretation

methods have been developed (Stock et al, 1985). Two methods, known as cumulant and constrained regularization, are discussed below and are used in the data analysis here.

In the method of cumulants (Koppel, 1972, Brown 1975), the evaluation of $G(\Gamma)$ is based on the formalism of the statistical cumulant generating function. With a simple fit of the experimental estimates of $\ln g^1(\tau)$ to a polynomial, $G(\Gamma)$ can be characterized by its moments or cumulants. The correlation function of the light scattered by polydisperse solutions lends itself naturally to an analysis in terms of moments or cumulants. Consider the exact formal correspondence between the form of the correlation function (Eq. 4.3.8) and the moment generating function (Cantrell, 1970, Schaefer et al, 1971),

$$M(-\tau;\Gamma) \equiv <\exp(-\Gamma\tau)> = g^1(\tau) \tag{4.3.9}$$

where < > signifies an average over Γ, weighted by the distribution function $G(\Gamma)$. The moments of the distribution are related to the derivatives of $M(-\tau;\Gamma)$ with respect to $(-\tau)$:

$$\mu_m(\Gamma) \equiv <\Gamma^m> = [d^m/d(-\tau)^m] \, M \, (-\tau;\Gamma)|_{-\tau=0} \tag{4.3.10}$$

Similarly, the cumulant generating function $K(-\tau;\Gamma)$ can be obtained as the natural logarithm of the moment generating function;

$$K(-\tau;\Gamma) \equiv \ln M(-\tau;\Gamma) = \ln |g^1(\tau)| \tag{4.3.11}$$

where

$$K(-\tau;\Gamma) = \sum_{m=1}^{\infty} K_m(\Gamma) \frac{(-\tau)^m}{m!} \tag{4.3.12}$$

The mth cumulant of Γ, K_m (Γ), is the coefficient of $(-\tau)^m/m!$ in this MacLaurin expansion of $K(-\tau;\Gamma)$:

$$K_m (\Gamma) = [d^m/d(-\tau)^m] K(-\tau;\Gamma)|_{-\tau=0} \tag{4.3.13}$$

It can be shown that the cumulants may be written in terms of moments about the mean (Cantrell, 1970):

$$K_1 = \Gamma_{ave} = \int_0^\infty \Gamma G(\Gamma) d\Gamma$$

$$K_2 = \mu_2, K_3 = \mu_3 \tag{4.3.14}$$

$$K_4 = \mu_4 - 3 (\mu_2)^2, \ - - - - - -$$

where the mth central moment of $G(\Gamma)$ is defined as

$$\mu_m = \int_0^\infty G(\Gamma) \ (\Gamma - \Gamma_{ave})^m \ d\Gamma \tag{4.3.15}$$

The second cumulant, K_2, normalized by K_1^2, is a measure of the width of the distribution, while K_3 and K_4 are measures of the skewness (asymmetry) or the kurtosis (flatness) of the distribution, respectively.

In the analysis of data, the measured intensity correlation function is transformed to the natural logarithm of the field correlation function $(y_m(\tau))$ given by Eq. (4.3.6)

$$y_m(\tau) = \ln g^{(1)}(\tau) = 1/2 \ln(1/b) + 1/2 \ln\{G^2(\tau)/B - 1\} \tag{4.3.16}$$

The exponential term in the righthand side of Eq. (4.3.8) can be expanded about the mean value of Γ_{ave} (Brown et al, 1975)

$$\exp(-\Gamma\tau) = \exp(-\Gamma_{ave}\tau)\exp[-(\Gamma-\Gamma_{ave})\tau]$$

$$= \exp(-\Gamma_{ave}\tau)\,[\,1- (\Gamma-\Gamma_{ave})\tau + (\Gamma-\Gamma_{ave})^2\tau^2/2! - (\Gamma-\Gamma_{ave})^3\tau^3/3! + \cdots \cdots] \qquad (4.3.17)$$

Substituting Eq. (4.3.17) into Eq.(4.3.8), $g(1)(\tau)$ may be written as

$$|g^{(1)}(\tau)| = \exp(-\Gamma_{ave}\tau)(\,1 + \mu_2\tau^2/2! - \mu_3\tau^3/3! + \cdots \cdots) \qquad (4.3.18)$$

The natural logarithm of $b|g^{(1)}(\tau)|$ ($=y^*(\tau)$) can be expanded and expressed as

$$y^*(\tau) = \ln [\, b^{1/2} |g^{(1)}(\tau)| \,]$$

$$= 1/2\ln b - \Gamma_{ave}\tau + 1/2!\,(\mu_2/\Gamma_{ave}^2)(\Gamma_{ave}\tau)^2 - 1/3!(\mu_3/\Gamma_{ave}^3)(\Gamma_{ave}\tau)^3 + \cdots \cdots \qquad (4.3.19)$$

Equation (4.3.19) represents the polynomial in sample time with cumulants as parameters to be fitted, usually by a weighted least squares technique. The function to be minimized is the sum of the residuals (the square of the difference between the log values of the calculated and measured field autocorrelation function) weighted by the standard deviation, $\sigma(\tau)$:

$$\chi^2 = \sum_{i=1}^{N} \left[\frac{y_m(\tau_i) - y^*(\tau_i)}{\sigma(\tau_i)} \right]^2 \qquad (4.3.20)$$

by varing the values of the cumulants ($\Gamma_{ave}, \mu_2, \mu_3, \ldots$). Because, in practice, it is difficult to extract moments higher than μ_2 and the contribution of the second moment term is small (<5% of

103

the first moment term for fractionated polymer samples), cumulant fit to the second moment is usually used (Chu, 1983).

If the intensity of light scattered by macromolecular species i is proportional to the molecular weight m_i, multiplied by the weight concentration c_i, then $G(\Gamma)$ may be written as (Brown et al,1975)

$$G(\Gamma) = c_i\, m_i / \sum_i c_i\, m_i = N_i m_i^2 / \sum_i N_i m_i^2 \qquad (4.3.21)$$

where N_i is the number of molecules in the scattering volume. Therefore Γ_{ave} can be calculated using

$$\Gamma_{ave} = \sum_i \Gamma_i\, G(\Gamma_i) = \sum_i N_i m_i^2\, \Gamma_i / \sum_i N_i m_i^2 = \sum_i N_i m_i^2 D_i\, q^2 / \sum_i N_i m_i^2 = \bar{D}_z q^2 \qquad (4.3.22)$$

Thus the diffusion coefficient obtained from dynamic light scattering is the so-called z-average diffusion coefficient since it is weighted by $N_i M_i^2$.

The second method for analyzing the intensity correlation function is the constrained regularization method developed by Provencher (1978, 1984). This method uses a Fortran program, called CONTIN. CONTIN analyses data that can be represented by a set of linear equations;

$$y_k = \sum_{j=1}^{m} A_{kj} x_j + \Delta, \qquad K = 1, \ldots, n \qquad (4.3.23)$$

where the data y_k generally contain experimental noise, the A_{kj} are known, the x_j are to be estimated, and Δ is a constant term. Solving this equation is generally an ill-posed problem. This

means that, even for arbitrarily small (but nonzero) noise levels in the y_k, there still exists a large (typically infinite) set of solutions $G(\Gamma)$ that all fit the y_k in Eq. (4.3.23) to within the noise level. Even worse, solutions in this set can differ from each other by arbitrarily large amounts.

In CONTIN, the quadrature of Eq. (4.3.8) is made to obtain a set of linear algebraic equations(Provencher, 1979);

$$y = Ax \tag{4.3.24}$$

where y is the n x 1 data vector, x is the m x 1 vector of unknown values of $G(\Gamma)$ at the m points of the quadrature grid, A is the n x m matrix whose elements are the products of the exponential term and the weights of the quadrature formula (Phillips, 1962). The ordinary weighted least square solution of above equation (4.3.24), x_o, that minimizes the weighted sum of the squared residuals, R_o, is

$$R_O = (y - Ax_o)'\, W(y - Ax_o) = minimum \tag{4.3.25}$$

where the W is the n x n least squares weights matrix and prime denotes matrix transposition. However there is no reason to prefer this solution over any other number of solutions. In fact, it is extremely unlikely that this solution (or any other randomly chosen one) will be close to the true solution; on the contrary, in view of the large variation among the solution sets, it is very likely that this solution will be a very poor estimate.

CONTIN computes a unique regularized solution, X_α, that minimizes the objective function R_α defined as

$$R_\alpha = (y - AX_\alpha)'W(y - AX_\alpha) + \alpha(DX_\alpha)'(DX_\alpha) \tag{4.3.26}$$

subject to the constraint that all elements of X_α are nonnegative. D is the matrix of the second difference operator (Twomey, 1963).

The second term in the right hand side of Eq. (4.3.26) is called the regularizor. The effect of which is to increase the ordinary least squares term (first term of Eq (4.3.26)) by α times the sum of the squares of the finite difference approximations to the second derivatives of the solution at the grid points. Hence, the regularizor penalizes a solution for its deviation from smooth behavior, and it eliminates wild oscillations. The optimum amount of smoothing is large enough to smooth out supurious oscillations without distorting the true features of the solution. CONTIN calculates several solutions by increasing the regularizing parameter (α) from a value initially close to zero. A comparison of these solutions reveals the sensitivity of the results to the amount of smoothing. CONTIN software includes a statistical method to automatically choose the amount of smoothing based on a Fisher test. A "Probability one to reject" is calculated for each solution by comparing its variance with that of the unsmoothed solution, with values increasing monotonically (from zero to 1) with increased smoothing parameter. Provencher (1976) suggests choosing the solution with a "Probability one to reject" closest to 0.5, so that the increase in the objective function of the smoothed solution, compared to that of the unsmoothed solution, could be attributed 50% of the time to experimental noise and 50% to oversmoothing.

4.3.2 Experiments and Results

The same light scattering system used in the determination of molecular weight was used for the measurement of intensity autocorrelation functions in real time. The procedure for cell cleaning and sample preparation was the same as described in section 3.4.2.3. The concentration of the solutions measured was in the range $0.05c^*$ to $0.25c^*$, where c^* is the polymer coil overlap concentration, estimated as $[\eta]^{-1}$ (Davidson et al,1987, de Gennes, 1979).

106

Between three and seven measurements were made for every sample at 25°C. The measurements were carried out at a single angle θ=90°, because of the molecules of the samples are small and there is no intramolecular interference in the scattered light (Berne et al,1976). The best sampling time (τ) was estimated using the formula given in the Goniometer Instruction Manual (1984), $\Delta t = 2/m\Gamma$, where m is the total number of data channels and Γ is given by the initial measurement with a roughly estimated sampling time. The sampling times used were 0.75 - 2 microseconds and the measurement durations were 600-3,600 seconds. The viscosity of MFA used for the calculation of hydrodynamic size was 0.0165 poise (Gordon, 1972). Fig. 4.3.1 shows a typical intensity autocorrelation function.

The experimental autocorrelation function was fitted, by weighted least squares to a second-order cumulant expansion (Eq. 4.3.19), using the BI-30 software provided by Brookhaven Instrument Co. BI-30 determines both the measured and calculated baseline (flat and uncorrelated portion of the autocorrelation curve). The measured baseline is determined by the average of the values of the 8 delay channels (1024τ - 1031τ), and the calculated baseline is determined by squaring the average of the total count measured during each sample time. These two baselines should agree with each other. Typical differences between the two baselines obtained in this experiment were 0.05% or less, showing that the results were not sensitive to the choice of baseline. To be consistent, though, the measured baseline was used in all calculations reported. Table 4.3.1 shows the results of cumulant analysis and the polydispersity index [K_2 / K_1^2]. The error is the standard error of the mean.

The experimental autocorrelation function was also analysed by CONTIN (version 2DP). In this analysis, the first data channel was ignored in all samples for which the sampling time was 1microsecond or larger (S-1 through S-6) , because of the afterpulsing and dead time effect (Ford Jr.,1985). In sample S-7, the first two data channels were ignored because the sampling time was less than 1 microsecond.
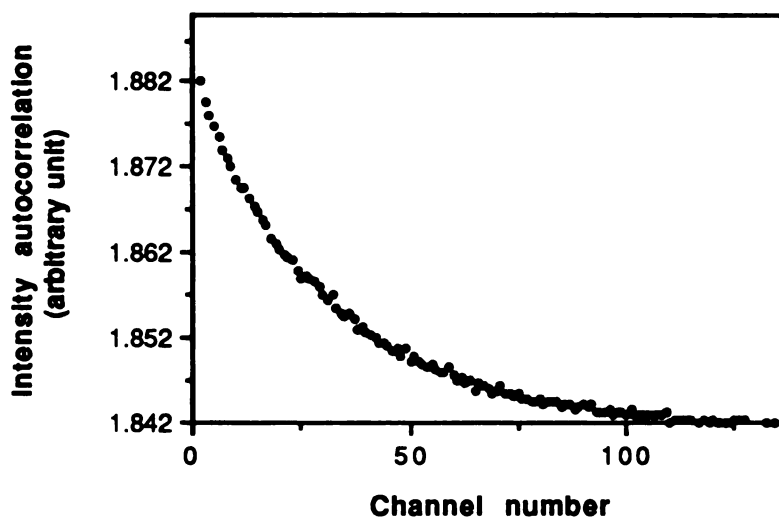
Figure 4.3.1   Plot of an intensity autocorrelation function. The sample measured is S-1 and the concentration is 1mg/ml.

Table 4.3.1 Hydrodynamic radius (R_H) and diffusion coefficient (D) of each sample at several concentrations. The data were analysed by the cumulant method.

Sample	Concentration (mg/ml)	Size (R_H) (nm)	Diffusion coefficient (D) ($\times 10^{+7}$, cm^2/sec)	$K_2/K_1{}^2$
S-1	1.0	10.8	1.219 +/- 0.002	0.17 +/- 0.00
	2.0	10.3	1.282 +/- 0.016	0.09 +/- 0.04
	3.0	10.1	1.313 +/- 0.016	0.10 +/- 0.03
	4.0	9.6	1.375 +/- 0.003	0.08 +/- 0.05
S-2	2.0	9.5	1.391 +/- 0.017	0.13 +/- 0.03
	3.4	9.5	1.396 +/- 0.016	0.12 +/- 0.01
	5.1	9.3	1.421 +/- 0.005	0.13 +/- 0.02
	6.4	9.3	1.433 +/- 0.010	0.16 +/- 0.02
S-3	2.5	8.1	1.635 +/- 0.021	0.10 +/- 0.03
	5.1	8.0	1.654 +/- 0.075	0.08 +/- 0.02
	7.1	7.6	1.733 +/- 0.005	0.08 +/- 0.03
	10.1	7.7	1.716 +/- 0.047	0.08 +/- 0.03
S-4	2.0	6.9	1.924 +/- 0.093	0.17 +/- 0.02
	3.3	6.8	1.942 +/- 0.010	0.12 +/- 0.02
	5.0	6.8	1.941 +/- 0.017	0.10 +/- 0.01
	10	6.7	1.964 +/- 0.004	0.09 +/- 0.01
S-5	2.6	6.8	1.945 +/- 0.014	0.24 +/- 0.02
S-6	2.7	5.3	2.496 +/- 0.055	0.17 +/- 0.05
S-7	11.4	4.3	3.089 +/- 0.007	0.19 +/- 0.01

Figure 4.3.2 shows an output file of the CONTIN anlysis. At the top of the file, residuals in

each channel are shown with the maximum and minimum values. The residuals are the differences

between the experimental correlation values and those corresponding to the chosen CONTIN fit.

Typical magnitudes of the maximum and minimum residual values obtained in all samples were

between 10^{-3}'s and 10^{-5}'s. The statistical tests on the number of runs (PRUNS) and the

autocorrelation with lags 1,2,3,4,5 (PUNCOR) in the residuals of the fit to the data

(Provencher,1976) are also shown together with the residual plot. PRUNS and PUNCOR give

information on how uncorrelated the residuals are (Provencher[2],1982), i.e. to what extent the

residuals represent random error or systematic error. They can have values between 0 and 1, and

the larger value indicates better residuals. Values greater than 0.1 indicate well scattered

residuals. Typical values obtained in the present experiment were between 0.1 and 0.9.

Below the residual plot, the chosen solution having the closest PROB1 TO REJECT

value to 0.5 shown. The ORDINATE column contains unnormalized point intensities of the

particles with hydrodynamic radii given by the corresponding ABSCISSA value. The range of the

grid points is 1 - 200 nm. The radii are given in cm. The ERROR column lists the error bar values

shown on the graph as dotted lines. The LINEAR COEFFICIENT gives the dust term

(Provencher[2], 1982). A dust term greater than 10^{-2} is of concern (R. Pecora, Stanford, personal

communication). In most of the samples measured in this experiment, this term was zero.

Nonzero values were obtained in a small fraction of samples, but the magnitudes were on the

order of 10^{-3} or less.

Below the size distribution graph, information about each individual peak and the whole

distribution are listed. M(0) gives the unnormalized area under the peak (The ratio of the area

under one peak to the total area gives the intensity fraction of that particular peak). The average

hydrodynamic size of the peak is given by the M(0)/M(-1) value (Flamberg et al, 1984). Frequently

Figure 4.3.2   A CONTIN output file. The range of the grid points is 1 - 200 nm.
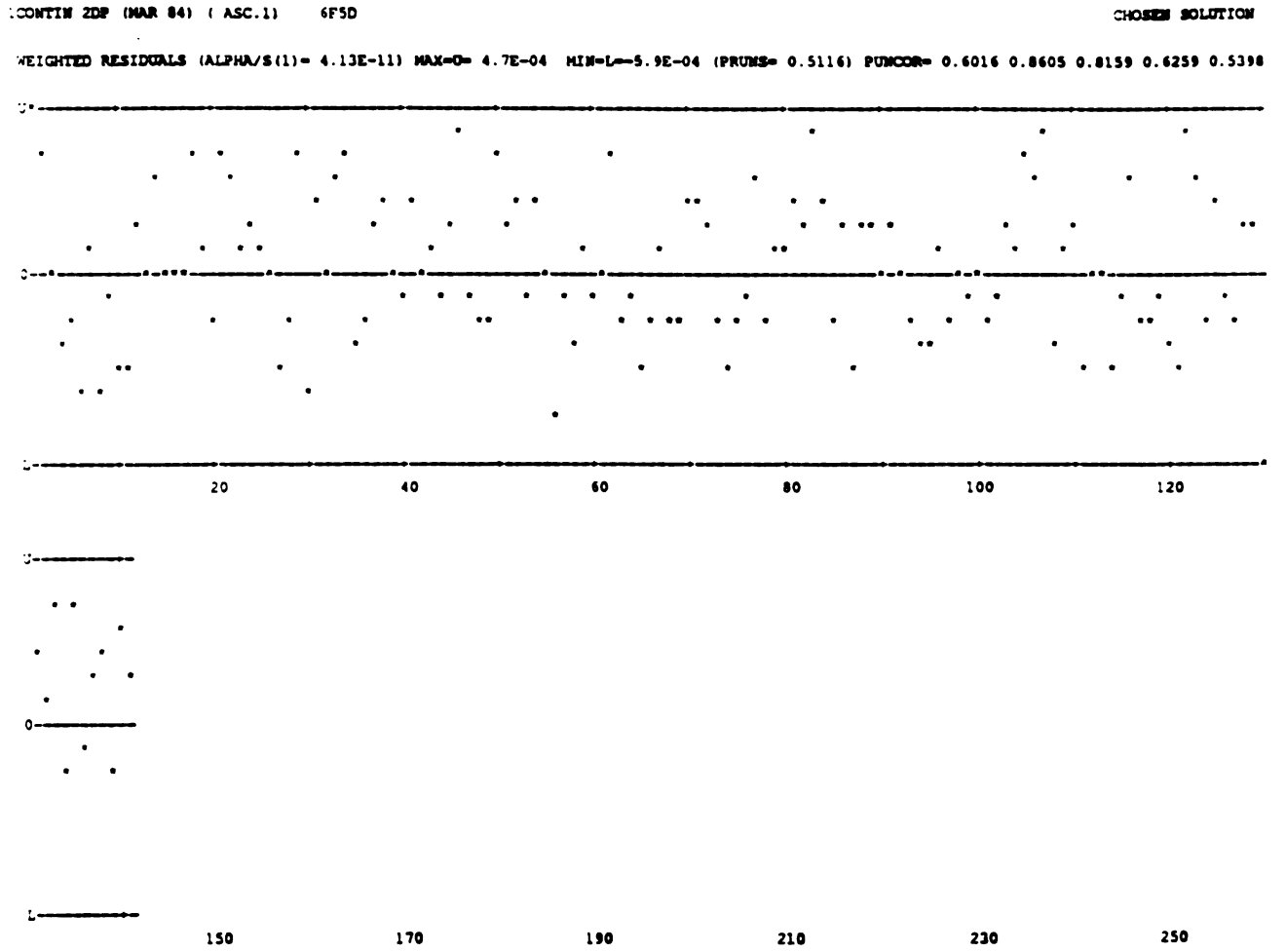
WEIGHTED RESIDUALS (ALPHA/S(1)= 4.13E-11) MAX=O= 4.7E-04 MIN=L=-5.9E-04 (PRUNS= 0.5116) PUNCOR= 0.6016 0.8605 0.8159 0.6259 0.5398

6FSD

ALPHA	ALPHA/S(1)	OBJ. FCTN.	VARIANCE	STD. DEV.	DEG FREEDOM	PROB1 TO REJECT	PROB2 TO REJECT
8.76E-06	4.13E-11	6.25173E-06	6.16947E-06	2.116E-04	3.172	0.498	0.947

ORDINATE	ERROR	ABSCISSA	
7.878E+04	2.2D+04	1.00E-07	....X....
1.175E+05	3.1D+04	1.17E-07	......X......
6.690E+04	2.1D+04	1.37E-07	....X....
4.197E+03	1.9D+04	1.60E-07X....
0.000E+00	8.6D-12	1.87E-07X
0.000E+00	1.8D-11	2.18E-07X
0.000E+00	1.1D-11	2.55E-07X
0.000E+00	1.8D-11	2.98E-07X
9.694E+04	2.6D+04	3.48E-07	......X.....
2.660E+05	2.8D+04	4.07E-07	......X.....
4.350E+05	1.4D+04	4.75E-07	...X..
5.177E+05	3.1D+04	5.55E-07	X
4.561E+05	2.3D+04	6.49E-07	.....X....
2.902E+05	9.3D+03	7.58E-07	..X.
1.051E+05	2.0D+04	8.86E-07	....X....
0.000E+00	3.8D-11	1.04E-06X
0.000E+00	3.5D-11	1.21E-06X

111

```
0.000E+00  6.3D-11  1.41E-06X
0.000E+00  2.8D-11  1.65E-06X
0.000E+00  2.8D-11  1.93E-06X
0.000E+00  4.9D-11  2.26E-06X
0.000E+00  3.0D-11  2.64E-06X
0.000E+00  3.7D-11  3.08E-06X
0.000E+00  3.4D-11  3.60E-06X
0.000E+00  9.7D-12  4.21E-06X
0.000E+00  4.0D-11  4.92E-06X
0.000E+00  5.8D-11  5.75E-06X
0.000E+00  7.9D-11  6.72E-06X
0.000E+00  7.1D-11  7.85E-06X
0.000E+00  7.5D-12  9.18E-06X
0.000E+00  6.4D-11  1.07E-05X
0.000E+00  2.0D-11  1.25E-05X
0.000E+00  3.1D-11  1.46E-05X
0.000E+00  1.1D-11  1.71E-05X
0.000E+00  1.8D-11  2.00E-05X
```

LINEAR COEFFICIENTS = 0.0000E+00 +- 6.7D-18

	J	MOMENT(J)	PERCENT ERROR	M(J)/M(J-1)	PERCENT ERROR	J
PEAK 1 GOES FROM 1.000E-07 TO 2.977E-07	-1	3.6323 X (10** 4)	2.7E+01			
	0	4.3500 X (10** -3)	2.9E+01	1.1976E-07	5.6E+01	0
	1	5.2611 X (10** -10)	3.2E+01	1.2094E-07	6.1E+01	1
(STD. DEV.)/MEAN = 1.0E-01	2	6.4296 X (10** -17)	3.6E+01	1.2221E-07	6.8E+01	2
	3	7.9452 X (10** -24)	4.2E+01	1.2357E-07	7.8E+01	3
PEAK 2 GOES FROM 3.479E-07 TO 2.000E-05	-1	3.3672 X (10** 5)	1.2E+00			
	0	1.9331 X (10** -1)	5.1E-01	5.7411E-07	1.7E+00	0
	1	1.1690 X (10** -7)	3.0E-01	6.0474E-07	8.1E-01	1
(STD. DEV.)/MEAN = 2.2E-01	2	7.4221 X (10** -14)	1.0E+00	6.3489E-07	1.3E+00	2
	3	4.9242 X (10** -20)	2.0E+00	6.6345E-07	3.0E+00	3
MOMENTS OF ENTIRE SOLUTION	-1	3.7304 X (10** 5)	2.9E+00			
	0	1.9766 X (10** -1)	8.1E-01	5.2987E-07	3.7E+00	0
	1	1.1743 X (10** -7)	3.3E-01	5.9409E-07	1.1E+00	1
(STD. DEV.)/MEAN = 2.5E-01	2	7.4285 X (10** -14)	1.0E+00	6.3259E-07	1.4E+00	2
	3	4.9250 X (10** -20)	2.0E+00	6.6298E-07	3.0E+00	3

a small peak is observed at the lower end of the size distribution with a very large percent error value, as shown in Fig. 4.3.2. This peak usually represents about 0.1% to 3 % of the total intensity. This small peak has been also observed by other researchers who have used CONTIN to analyse both experimental data and simulated data with added noise (Sorlie et al,1988). The peak was never observed when analysing simulated data without added noise. It was also noted that, in the analysis of simulated data with noise, the presence of the small peak did not appreciably alter the positions of the other peaks. In this work, the size of the main peak was used as the size of the sample molecules. Table 4.3.2 shows the result of CONTIN analysis of the same data previously analysed by the cumulant method.

Because the diffusion coefficient measured at a finite concentration (D_c) contains the effects of intermolecular interactions, the true diffusion coefficient (D_0) should be determined at zero concentration. The concentration dependence of the translational diffusion can be expressed (Yamakawa, 1962)

$$D_c = D_0 (1 + k_d c) \qquad (4.3.27)$$

where D_0 is the diffusion coefficient at zero concentration and k_d represents the first order concentration dependence of diffusion coefficient. D_0 values were determined for samples S-1,S-2,S-3 and S-4 from the intercepts of D_c versus concentration plots (Fig. 4.3.3). The k_d values for these samples were determined from the slope. CONTIN results were used for this plot. D_0 values for samples S-5,S-6 and S-7 were also calculated from theoretically estimatied k_d values and a D_c measured at a single concentration. The coefficient k_d was estimated from (Yamakawa, 1962)

$$k_d = 0.8 A_2 M - [\eta]/2.5 - v_2 \qquad (4.3.28)$$

Table 4.3.2   Hydrodynamic radius (R_H) and diffusion coefficient (D) of each sample at several concentrations. The data were analysed by CONTIN.

Sample	Concentration (mg/ml)	Size (R_H) (nm)	Diffusion coefficient (D) ($x\ 10^{+7}$, cm^2/sec) +/- SE
S-1	1.0	10.9	1.210+/- 0.003
	2.0	10.5	1.254 +/- 0.016
	3.0	10.2	1.298 +/- 0.042
	4.0	9.9	1.331 +/- 0.000
S-2	2.0	9.8	1.349 +/- 0.048
	3.4	9.5	1.398 +/- 0.035
	5.1	9.2	1.445 +/- 0.023
	6.4	9.0	1.475 +/- 0.016
S-3	2.5	8.5	1.551 +/- 0.024
	5.1	8.0	1.652 +/- 0.050
	7.1	7.7	1.722 +/- 0.054
	10.1	7.3	1.793+/- 0.059
S-4	2.0	7.7	1.710 +/- 0.037
	3.3	7.4	1.787 +/- 0.007
	5.0	7.1	1.859 +/- 0.021
	10	7.1	1.865 +/- 0.008
S-5	2.6	7.0	1.909 +/- 0.190
S-6	2.7	5.6	2.347 +/- 0.178
S-7	11.4	4.2	3.114 +/- 0.022
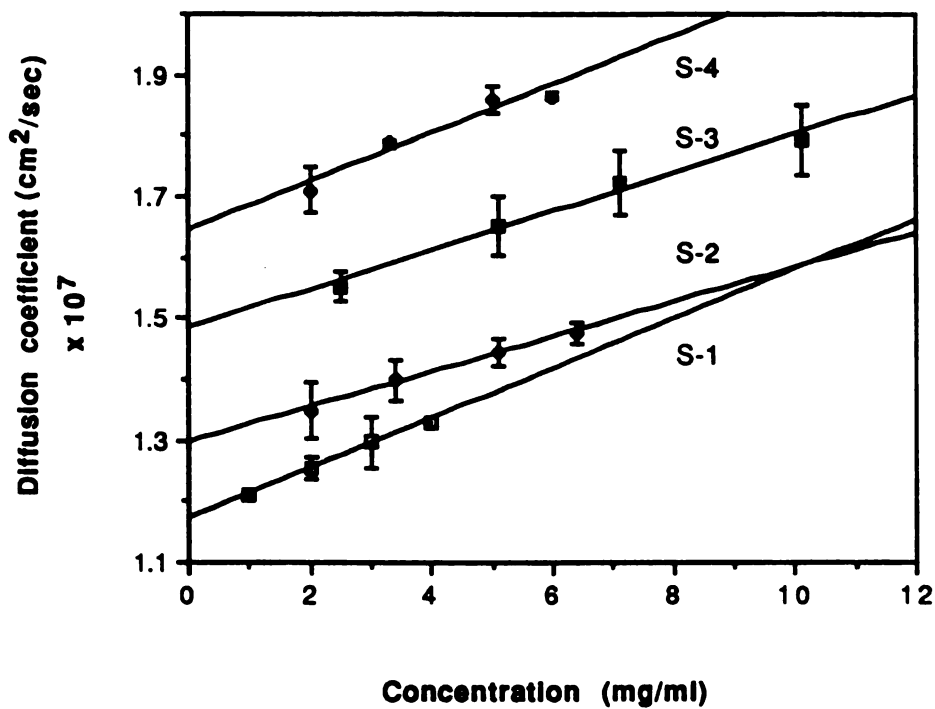
Figure 4.3.3 Plot of the concentration dependence of diffusion coefficient for samples S-1,S-2,S-3 and S-4. Each data point represents the mean of three to seven measurements. Standard error bars are shown for each data point.

where A_2 is the second virial coefficient, M the molecular weight and v_2 the partial specific volume of the polymer. The partial specific volume v_2 is about 1ml/g or less and can be neglected (Van Krevelen, 1976). Table 4.3.3 shows the calculated k_d values for each sample. Measured k_d values and standard errors are shown in parentheses. Table 4.3.4 shows D_0 (+/- standard error) and the hydrodynamic radius at zero concentration for each sample.

4.3.3   Discussion

Figure 4.3.2 shows a typical output file from CONTIN analysis. On top of the file, a plot of the residuals is shown. The residuals are quite randomly distributed as shown by the large values of PUNCOR, the probability that the residuals are uncorrelated. There are two peaks in the distribution curve shown in the lower part of the figure. The small peak around 1.0×10^{-7} cm (1 nm) is thought to be spurious, as discussed above. To verify this hypothesis, the data was reanalysed using CONTIN by changing the range of grid points from 1 - 200nm to 0.1 - 1,000nm. The result is shown in Fig. 4.3.4. The position, and the average size of the main peak is not changed, while the position of the small peak is moved to the lower end and the size is also changed from 1.2nm to 0.2nm. This result indicates that the small peak is an artifact. Other samples where this small peak appeared were also checked and same behavior was observed.

Tables 4.3.1 and 4.3.2 show the results of data analyses by the cumulant and CONTIN methods, respectively. In general, the hydrodynamic radii obtained by each method are in good agreement, although the sizes obtained by CONTIN method are slightly larger than those calculated by cumulant method. The difference is usually within 5% except for the S-4 samples at low concentrations, which show differences of 8 - 10%. Cumulant results show a weaker concentration dependence of the diffusion coefficient compared to the CONTIN results.

116

Table 4.3.3   Calculated values of the first order concentration dependence of diffusion coefficient (k_d) by Eq. (4.3.28)

Sample	MW (g)	$A_2 \times 10^4$ (ml/g)	$[\eta]$ (ml/g)	k_d (ml/g)
S-1	166,500	4.15	60	31.3 (34.7 +/- 1.7)
S-2	138,600	4.37	53	27.3 (22.0 +/- 1.5)
S-3	116,700	4.84	47	26.4 (21.5 +/- 2.0)
S-4	101,600	5.14	42	25.0 (24.2 +/- 4.3)
S-5	88,800	5.23	38	22.0
S-6	56,200	5.69	29	14.0
S-7	36,400	6.22	22	9.3

Table 4.3.4   Hydrodynamic radius (R_H) and diffusion coefficient at zero concentration (D_0)

Sample	MW(g)	Size (R_H), nm	$D_0 \times 10^7$, (cm2/sec)
S-1	166,500	11.3	1.171 +/- 0.005
S-2	138,600	10.2	1.296 +/- 0.008
S-3	116,700	8.9	1.482 +/- 0.019
S-4	101,600	8.0	1.643 +/- 0.030
S-5	88,800	7.4	1.797
S-6	56,200	5.8	2.262
S-7	36,400	4.7	2.825

Figure 4.3.4 A CONTIN output file. The range of grid points is 0.1 - 1,000 nm.

Figure 4.3.4 A CONTIN output file. The range of grid points is 0.1 - 1,000 nm.

.CONTIN 2DP (MAR 84) (ASC.1)   6F5D   CHOSEN SOLUTION

WEIGHTED RESIDUALS (ALPHA/S(1)= 7.56E-12) MAX=U= 4.4E-04 MIN=L=-5.8E-04 (PRUNS= 0.7508) PUNCOR= 0.7428 0.8371 0.8676 0.5993 0.6615

```
U---------+---------+---------+---------+---------+---------+---------+---------+---------+---------+---------+---------+---------+
                .    .   .         .   .              .                  .                       .      ..      .       .
                   .        .         .                 .            .
           .   .     .    .       .   .     .    .   .           ...          .   ..                    .                   . .
0*---------+---------+---------+---------+---------+---------+---------+---------+---------+---------+---------+---------+---------+
    . .            .    .        .                   .    ..                 .   .               . .    .              ...     .
              .        .             .    .    .               .  ..  . ..  .          .                   ..
          .   . .       .        .        .             .            .   .   .             .                   .  .   .
                 .                                         .             .                  .
                .                          .

L---------+---------+---------+---------+---------+---------+---------+---------+---------+---------+---------+---------+---------+
         20            40            60            80           100           120
```

```
U--------+-
      .
        .
      . .
    .   .
        .
0-*--------
      .
    .   .
```

```
L--------+-
       150           170           190           210           230           250
```
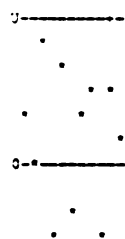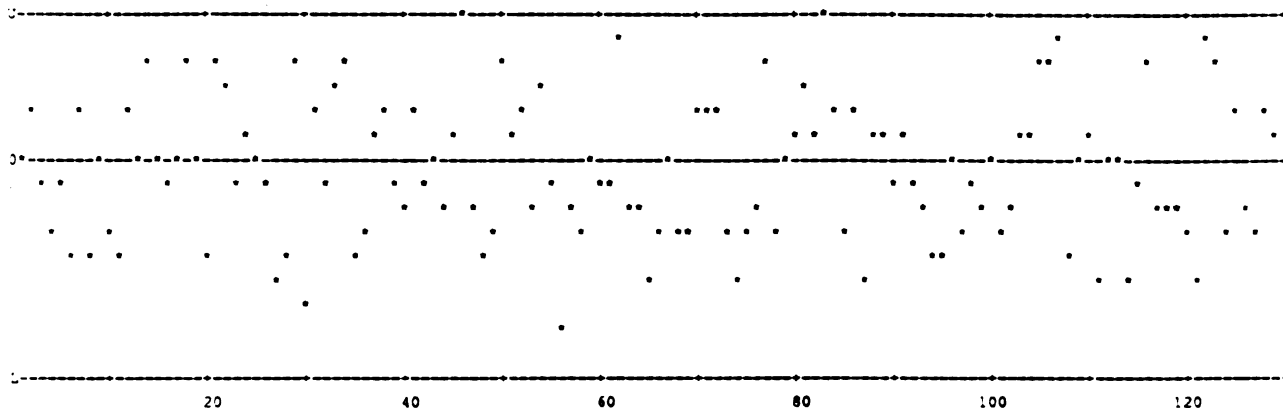
:CONTIN VERSION 2DP (MAR 1984) (ASC.1 PACKAGE) ++++++++++++++++++++++++++++++++ CHOSEN SOLUTION +++++++++++++++++++++++++++++++++

       6F5D

ALPHA	ALPHA/S(1)	OBJ. FCTN.	VARIANCE	STD. DEV.	DEG FREEDOM	PROB1 TO REJECT	PROB2 TO REJECT
1.60E-06	7.56E-12	5.79989E-06	5.59545E-06	2.020E-04	3.845	0.314	0.902

```
ORDINATE   ERROR   ABSCISSA
1.085E+05  3.1D+04  1.00E-08          ......X.......
2.391E+05  6.4D+04  1.31E-08                       ..............X............
3.114E+05  7.4D+04  1.72E-08                                ................X...............
2.910E+05  6.2D+04  2.25E-08                          ..............X............
1.789E+05  4.4D+04  2.96E-08              ..........X.........
5.183E+04  3.2D+04  3.87E-08    ......X.......
0.000E+00  2.9D-12  5.08E-08X
0.000E+00  7.7D-12  6.66E-08X
0.000E+00  7.1D-12  8.73E-08X
0.000E+00  1.0D-11  1.15E-07X
0.000E+00  2.3D-11  1.50E-07X
0.000E+00  2.2D-11  1.97E-07X
0.000E+00  3.3D-11  2.58E-07X
1.264E+05  3.0D+04  3.38E-07              ......X......
3.686E+05  6.4D+03  4.44E-07                                              ..X.
4.769E+05  2.9D+04  5.82E-07                                                          ......X
2.917E+05  1.7D+04  7.63E-07                              ....X...
```

118

```
2.856E+04  1.3D+04  1.00E-06   ..X...
0.000E+00  1.3D-10  1.31E-06X
0.000E+00  2.7D-11  1.72E-06X
0.000E+00  7.2D-11  2.25E-06X
0.000E+00  6.7D-11  2.96E-06X
0.000E+00  8.0D-11  3.87E-06X
0.000E+00  7.8D-11  5.08E-06X
0.000E+00  7.5D-11  6.66E-06X
0.000E+00  9.7D-11  8.73E-06X
0.000E+00  1.3D-10  1.15E-05X
0.000E+00  7.5D-11  1.50E-05X
0.000E+00  3.9D-11  1.97E-05X
0.000E+00  6.7D-11  2.58E-05X
0.000E+00  2.9D-11  3.38E-05X
0.000E+00  3.6D-11  4.44E-05X
0.000E+00  2.5D-11  5.82E-05X
0.000E+00  1.4D-11  7.63E-05X
0.000E+00  1.2D-11  1.00E-04X
```

LINEAR COEFFICIENTS = 0.0000E+00 +- 7.8D-17

PEAK 1 GOES FROM 1.000E-08 TO 2.581E-07	J	MOMENT(J)	PERCENT ERROR	M(J)/M(J-1)	PERCENT ERROR	J
	-1	3.0854 X (10** 5)	2.2E+01			
	0	6.2461 X (10** -3)	2.2E+01	2.0244E-08	4.3E+01	0
	1	1.4216 X (10** -10)	2.4E+01	2.2759E-08	4.5E+01	1
(STD. DEV.)/MEAN = 3.4E-01	2	3.6163 X (10** -18)	2.8E+01	2.5439E-08	5.1E+01	2
	3	1.0152 X (10** -25)	3.3E+01	2.8073E-08	6.1E+01	3

PEAK 2 GOES FROM 3.384E-07 TO 1.000E-04	J	MOMENT(J)	PERCENT ERROR	M(J)/M(J-1)	PERCENT ERROR	J
	-1	3.4749 X (10** 5)	9.4E-01			
	0	1.9569 X (10** -1)	2.0E-01	5.6314E-07	1.1E+00	0
	1	1.1758 X (10** -7)	6.6E-01	6.0087E-07	8.7E-01	1
(STD. DEV.)/MEAN = 2.5E-01	2	7.5178 X (10** -14)	2.4E+00	6.3937E-07	3.0E+00	2
	3	5.1044 X (10** -20)	5.1E+00	6.7897E-07	7.5E+00	3

MOMENTS OF ENTIRE SOLUTION	J	MOMENT(J)	PERCENT ERROR	M(J)/M(J-1)	PERCENT ERROR	J
	-1	6.5602 X (10** 5)	1.0E+01			
	0	2.0193 X (10** -1)	7.0E-01	3.0781E-07	1.1E+01	0
	1	1.1772 X (10** -7)	6.6E-01	5.8299E-07	1.4E+00	1
(STD. DEV.)/MEAN = 3.1E-01	2	7.5182 X (10** -14)	2.4E+00	6.3863E-07	3.0E+00	2
	3	5.1044 X (10** -20)	5.1E+00	6.7894E-07	7.5E+00	3

In Table 4.3.1, K_2/K_1^2 values are also listed. These values are highly variable from run to run. Except for S-4, K_2/K_1^2 becomes smaller as concentration increases, probably because the quality of scattering data is better at higher concentration. Sample S-5, S-6 and S-7 show fairly large values of K_2/K_1^2. Since scattering intensity is proportional to the square of the molecular weight for a Rayleigh scatterer, this may be due to the weak scattering from these small molecular weight samples.

The K_2/K_1^2 value is a measure of the polydispersity of the sample. It can be expressed as (Brown et al, 1975)

$$\frac{K_2}{K_1^2} = \frac{\langle (D - <D>_z)^2 \rangle}{<D>_z^2} = \delta_z \qquad (4.3.29)$$

where δ_z is the relative dispersion in the diffusion coefficient (D) about its average ($<D>_z$). A very rough estimate of the polydispersity (M_w/M_n) from the δ_z value can be made for a narrowly distributed samples by the approximate formula (Selser, 1979);

$$\delta_z = \frac{\nu^2}{4} \frac{\delta_{2n}[4 + (1 - \nu)(\nu - 5)\delta_{2n}]}{[1 + [(2 - \nu)(1 - \nu)/2]\delta_{2n}]^2} \qquad (4.3.30)$$

where ν is the exponent in the power law expression of the diffusion coefficient as a function of molecular weight and δ_{2n} is the normalized (by number average molecular weight, M_n) second moment of the molecular weight distribution:

$$\delta_{2n} = \frac{\langle (M - <M>_n^2) \rangle_n}{\langle M \rangle_n^2} = \frac{M_w}{M_n} - 1 \qquad (4.3.31)$$

where M_w is the weight average molecular weight. The ν value for the system under study is 0.582, which is obtained from a plot of log M_w versus log D_0 as described in the next section. The

calculated polydispersity value is about 1.3 - 1.4 for samples S-1, S-3 and S-4, when the δ_z value obtained at the highest concentration, 0.08 or 0.09, is used. If the lowest value of δ_z obtained, 0.05 or 0.06, is used, the polydispersity is about 1.2. These polydispersity values (1.2 -1.3) are in good agreement with the usually accepted value of 1.3 for fractioned samples prepared by the fractional precipitation method (Mays et al, 1988). Experimentally, Selser (1979) obtained $\delta_z =$ 0.08 for a polystyrene sample with $M_w/M_n = 1.2$. The polydispersity values for S-2, S-5, S-6 and S-7 are larger than 1.3. The δ_z values for the first and second fraction were also measured, to provide a rough estimate of polydispersity. The first fraction has $\delta_z \approx 0.25$ - 0.3 indicating that the polydispersity of this fraction is much larger than that of the later fractions. The second fraction has $\delta_z \approx 0.14$ - 0.19. Thus, the polydispersity of the second fraction is rather larger than that of the 4th, 5th, 6th, and 7th fractions (sample S-1,S-2,S-3 and S-4, respectively), but is similar to those of the 8th, 9th and 10th fractions.

The diffusion coefficient measured from a polydispersed sample is a z-averaged quantity. The effect of polydispersity on the average diffusion coefficient can be calculated by expanding the z-averaged diffusion coefficient about M_w (Selser, 1979, 1981).

$$D_z = D_z^* \left\{ 1 - \frac{\nu(1-\nu)}{2} \left[\frac{M_z}{M_w} - 1 \right] \right\} \tag{4.3.32}$$

where D^* is the diffusion coefficient when polydispersity is 1, and M_z the z-average molecular weight. When ν is 0.582 and $M_z/M_w < 1.3$, as in the case of samples S-1, S-3 and S-4, the effect of polydispersity on the measured diffusion coefficient is less than 4%. The effects on D_z for samples S-2, S-5, S-6 and S-7 are expected to be less than 6% (calculated using $M_z/M_w = 1.5$). In a typical unfractionated polymer, $M_w/M_n \approx 2$ and $M_z/M_w \approx 1.5$ (Collins et al, 1973).

In Table 4.3.3, the calculated k_d values are given, together with the measured k_d values in parenthesis. The errors attached to the measured values are statistical uncertainties arising from least-squares fits to the D_z vs. concentration plots shown in Fig. 4.3.3. Theoretically calculated k_d values are in good agreement with the measured k_d values. Considering this point, the calculated k_d values used for the determination of D_0 values for S-5, S-6 and S-7 seem to be quite reasonable. Similar k_d values are obtained for the polystyrene-tetrahydrofuran system (Venkataswamy et al, 1986), where the k_d values are 14, 32 and 36 ml/g for samples with weight average molecular weight of 51,000, 110,000 and 180,000, respectively. In ethylbenzene, a value of 23.2ml/g was obtained for a sample with a weight average molecular weight of 100,000. This value is very close to the value obtained in this work, 24.2ml/g, for sample S-4.

4.4 Analysis of Data

4.4.1 Scaling Relationships and the Ratios between Sizes

The intrinsic viscosity [η] of a series of linear polymer homologs increases with molecular weight and follows a simple power law called the Mark-Houwink relation: (Yamakawa, 1971)

$$[\eta] = KM^{\nu} \tag{4.4.1}$$

where K and ν are constants for a given polymer-solvent system. Intrinsic viscosity values (Table 4.2.2) are plotted as a function of molecular weight in Fig. 4.4.1. The data can be described by

$$[\eta] = 2.06 \times 10^{-2} M^{0.662} \tag{4.4.2}$$

with an uncertainty in the exponent of $\pm$ 0.014. The molecular weight dependence of the second virial coefficient (A_2) for a series of flexible linear polymer homologs in a good solvent can be well-described by the empirical relation (Yamakawa, 1971, Morawetz, 1974)

$$A_2 = aM^{-\delta} \tag{4.4.3}$$

where a and δ are constants for a given polymer-solvent system. In Fig. 4.4.2, second virial coefficient values (Table 3.4.4) are plotted as a function of molecular weight. The data can be well-described by the power law

$$A_2 = 0.98 \times 10^{-2} M^{-0.260} \tag{4.4.4}$$
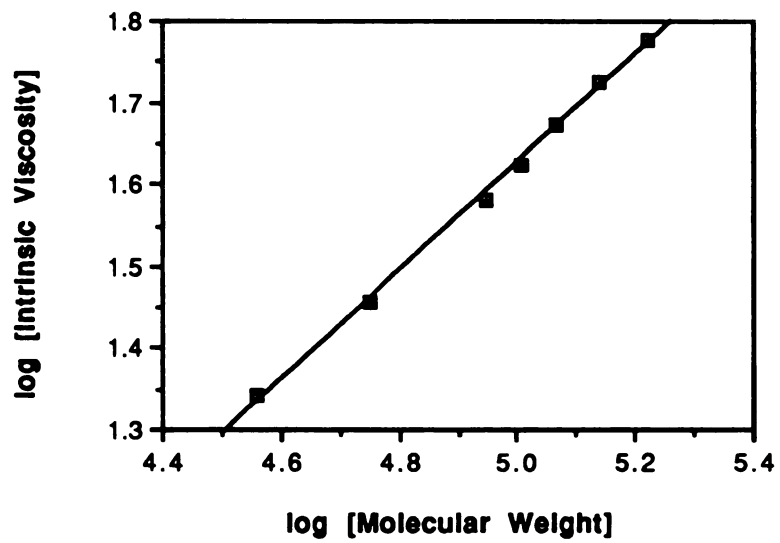
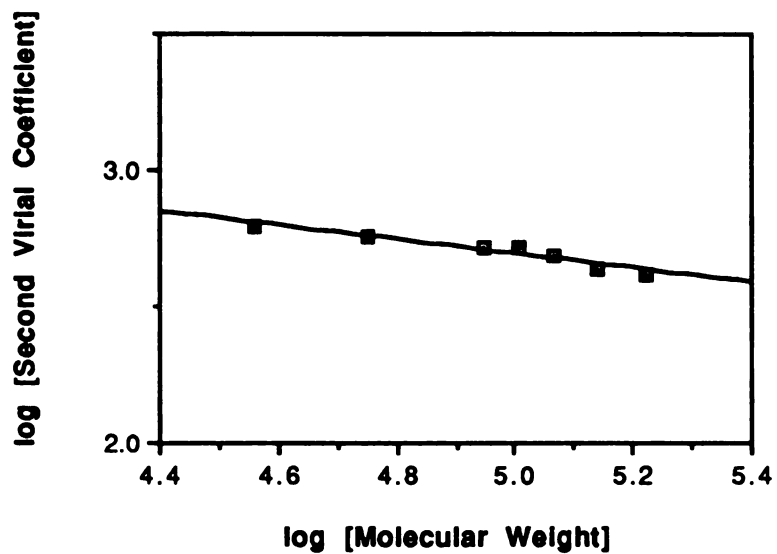Figure 4.4.1   Plot of the molecular weight dependence of intrinsic viscosity

Figure 4.4.2   Plot of the molecular weight dependence of second virial coefficient

with an uncertainty in the exponent of +/- 0.029.

Polymer molecules in good solvents are usually treated as impenetrable hard spheres both hydrodynamically and thermodynamically (Flory, 1953). For a hard sphere of volume V, $[\eta]$ can be described by Einstein's relationship

$$[\eta] = 2.5 N_A V/M \qquad (4.4.5)$$

where N_A is Avogadro's number and M the molecular weight. V can be written as $4/3\pi R_V^3$, where R_V is defined as the radius of an equivalent hard sphere showing the same viscosity as the coil. Hence, R_V is given by

$$R_V = 5.41 \times 10^{-9} ([\eta]M)^{1/3} \qquad (4.4.6)$$

From the thermodynamic consideration of the excluded volume, A_2 for a hard spherical molecule can be shown to be (Yamakawa, 1971)

$$A_2 = 4 N_A V/M^2 \qquad (4.4.7)$$

The thermodynamic radius, R_T, is defined

$$R_T = 4.63 \times 10^{-9} (A_2 M^2)^{1/3} \qquad (4.4.8)$$

Substituting for $[\eta]$ from (Eq. 4.4.2), and for A_2 from (Eq. 4.4.4), Eq. (4.4.6) and Eq. (4.4.8) can be rewritten in the following scaling expressions

$$R_V = 1.48 \times 10^{-2} M^{0.554} \qquad (4.4.9)$$

$$R_T = 0.99 \times 10^{-2} \, M^{0.580}$$ (4.4.10)

with uncertainties in the exponents of +/- 0.005 and +/- 0.01, respectively.

In Fig. 4.4.3, values of hydrodynamic radius (from Table 4.3.1) are plotted as a function of molecular weight. The data can be described by a power law (de Gennes, 1976)

$$R_H = 1.01 \times 10^{-2} \, M^{0.582}$$ (4.4.11)

with an uncertainty in the exponent of +/- 0.023. The values of R_V, R_T and R_H are collected in Table 4.4.1.

Table 4.4.1   Size of the molecules determined by various methods

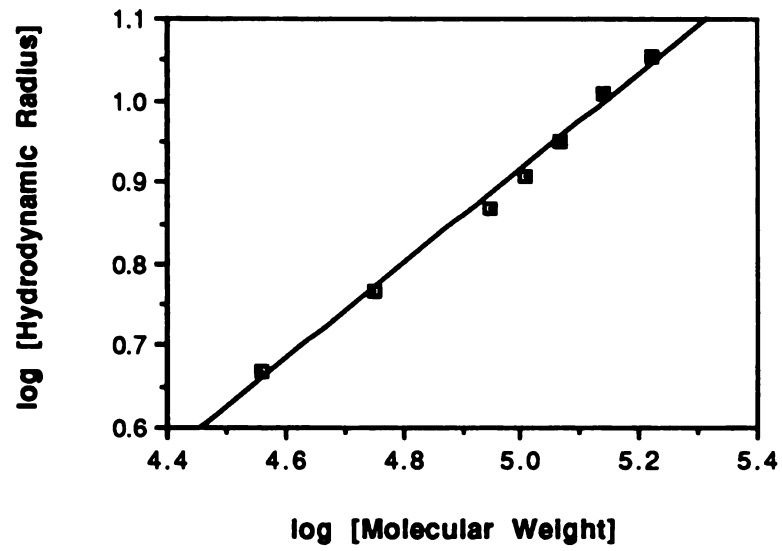| Sample	MW (g)	R_V, nm	R_T, nm	R_H, nm
S-1	166,500	11.7	10.4	11.3
S-2	138,600	10.5	9.4	10.2
S-3	116,700	9.5	8.7	8.9
S-4	101,600	8.8	8.1	8.0
S-5	88,800	8.1	7.4	7.4
S-6	56,200	6.4	5.6	5.8
S-7	36,400	5.0	4.3	4.7

The ratios between sizes are given in Table 4.4.2.

Figure 4.4.3 Plot of the molecular weight dependence of hydrodynamic radius

Table 4.4.2 Ratios between different radii for poly(MMA-co-AA)

Sample	MW (g)	R_V/R_H	R_T/R_H	R_V/R_T
S-1	166,500	1.04	0.92	1.13
S-2	138,600	1.03	0.92	1.12
S-3	116,700	1.07	0.98	1.09
S-4	101,600	1.10	1.01	1.09
S-5	88,800	1.10	1.00	1.09
S-6	56,200	1.10	0.97	1.14
S-7	36,400	1.07	0.92	1.16
	Average	1.07	0.96	1.12
	Standard Error	+/- 0.03	+/- 0.04	+/- 0.03

4.4.2   Discussion

The exponents obtained in this work should be treated qualitatively rather than quantitatively, because the molecular weights of the samples range over only one decade, and are not large enough to observe the asymptotic behavior of various physical and transport properties. Another reason for the qualitative interpretation of the exponents obtained is that the samples used are not monodisperse , as discussed in the previous section.

The exponent ν obtained for the Mark-Houwink equation (Eq. 4.4.1) is 0.662. A large amount of data indicates that ν is 0.5 in θ-solvents, and that ν takes values between 0.5 and 0.8 in non θ-solvents.   Generally, ν for a given polymer is larger for a better solvent (Polymer Handbook, 1989). In good solvents, ν is usually found to lie between 0.7 - 0.8. Actually, the good solvent limit of ν for flexible polymers is not yet established (Fujita, 1988). Einaga et al (1979) measured

[η] for polystyrene in benzene up to molecular weight 6×10^7 and obtained $v = 0.75$. Meyerhoff et al (1979) obtained $v = 0.724$ for polystyrene in toluene. These solvents (benzene and toluene) are typical good solvents for polystyrene. Kashiwagi et al (1980) studied [η] for poly(methyl methacrylate) in a good solvent, acetone, over a range of molecular weight up to 3×10^7 and found an even smaller value of 0.70 for v. The theoretically predicted good solvent limiting value of v is 0.8 (Oono et al, 1983, Flory, 1953). However, this value is seldom reported in well-documented experimental work (Fujita, 1988).

The v value obtained in this work is rather smaller than the values usually obtained in good solvents for other polymers. Einaga et al (1979) studied the intrinsic viscosity of polystyrene in benzene and plotted log [η] against log M_w. They found that the data points first follow a curve which is weakly bent upward and, beyond a M_w of about 4×10^5, they follow a straight line with a slope $v = 0.75$ as the molecular weight increases. The data points obtained in this work also follow a curve slightly bent upward at molecular weight lower than 88,800 (S-5) and follow a straight line with a slope $v = 0.728$ (Fig. 4.4.4). This v value is closer to the limiting value in a good solvent than the value $v = 0.662$ obtained by using the whole set of data points.

The exponent δ of Eq. 4.4.3 is usually in the range 0.2 -0.3, although the asymptotic value is predicted to be 0.2 (Flory, 1953, Yamakawa, 1971). However, it has been observed that log M vs. log A_2 plots show upward curvature in the low molecular weight region (Huber et al,1985, Miyaki et al, 1978). Fujita (1988) suggests that, in general, δ should be considered as a function of molecular weight. Fig. 4.4.2 shows the plot of log M vs. log A_2 for the data obtained in this work. The data are well fitted by a single straight line in the range of molecular weight studied. The value of δ obtained, 0.26, is well within the usual range of δ observed.
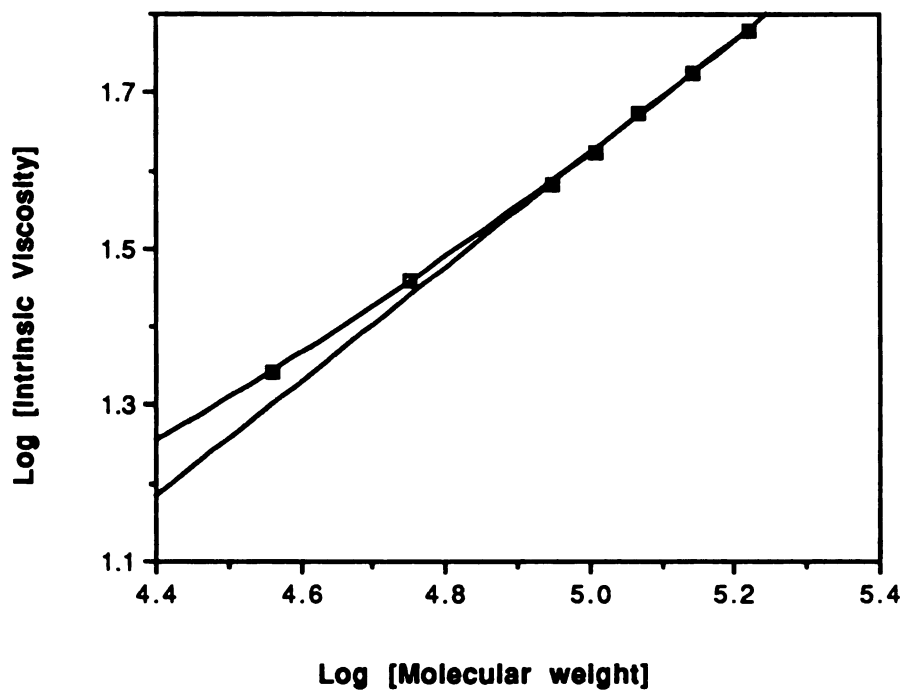
Figure 4.4.4 Plot of intrinsic viscosity against molecular weight. Intrinsic viscosities of the five largest molecular weight samples are used in the linear fit. A slight curvature is observed at lower molecular weight.

In Table 4.4.1, various sizes are listed. For sufficiently long flexible chains in good solvents, these radii (R_V, R_T and R_H) are expected to differ from one another, but to vary with molecular weight in the same way. Theory predicts that they exhibit power law scaling against molecular weight of the form,

$$\text{Radius} \propto M^V \tag{4.4.12}$$

where v is a characteristic exponent (De Gennes, 1976, Oono et al, 1983). In the asymptotic range of a strong excluded volume effect, Flory's theory (1953) predicts that $v = 0.6$. Renormalization group calculations (Le Guillou et al, 1977,1980) predict $v = 0.588$. Except for R_V, the exponents obtained in this work are close to these values, despite the low molecular weights of the samples examined.

Akcasu et al (1979) studied the molecular weight and temperature dependence of R_H and R_G, using the blob theory, and compared theoretical predictions with experimental data for polystyrene in different solvents and at different temperature. Their results show that, within the range of molecular weights studied ($2.04 \times 10^4 - 3.8 \times 10^6$), the experimental R_H values fall in the nonasymptotic region of the theoretical curve predicted, where a simple power law $R_H \sim M^V$ is not obeyed. It is also shown that any power law fit to the data is bound to yield an exponent less than 0.6. Similar results were reported by other authors (Weil et al, 1979), who also showed that R_H does not reach its asymptotic power law behavior within the range of experimental values of the molecular weight. On the other hand, they also showed that the experimental data on R_G fall in the asymptotic region at ordinary molecular weights studied.

Another possible reason for the lower exponent is suggested by other investigators (Freed et al, 1988, Wang et al, 1985, Douglas et al, 1984). They calculated the translational diffusion coefficient (or the hydrodynamic radius) for linear flexible polymers with the two-

parameter model, the Kirkwood approximation and the renormalization group method. They expressed the hydrodynamic radius in terms of the draining parameter and the excluded volume parameter. It was shown that an increase in the draining parameter decreases the ratio, R_H/R_G. They also showed that increasing the excluded volume interaction decreases this ratio. They suggested that this is due to the slower increase in R_H relative to that of R_G, which is dependent mainly on excluded volume interaction. Hence, the exponent in the scaling expression of R_H is smaller than that expected for R_G.

There are many experimental results which show significantly smaller exponents than the expected value, 0.6. Adam et al (1976) reported an exponent v=0.55+/- 0.02 for R_H for polystyrene in benzene in the molecular weight range 2.43×10^4 to 3.8×10^6. The same exponent was obtained by Nomoto et al (1984) . The exponent for R_G obtained in the polystyrene - benzene system is 0.595 (Miyaki et al, 1978). The exponents for R_H obtained for polystyrene in tetrahydrofuran and ethylbenzene are 0.556 and 0.551, respectively (Bhatt et al, 1989, Venkataswamy et al, 1986). Similar results were also observed from experiments on polystyrene in toluene (Utiyama et al, 1978).

Davidson et al (1987) suggest that such differences in exponent should perhaps not be strongly emphasized. They studied a dilute solution of polyisoprene in cyclohexane (good solvent) and obtained 0.584 for the exponent of R_H, which is very close to the expected value, 0.588, but the exponent obtained for R_G is 0.545. This result is contrary to observations on polystyrene in good solvents discussed above, where the R_G exponent agrees well with theoretical values. They suggested that specific solvent effects (Venkataswamy et al, 1986) may be important and may influence some size measurements more than others.

Considering the discussions above, it might be possible that the exponents obtained for R_H and R_T in this work with rather low molecular weight samples are fortuitous.

The ratios between sizes measured by different methods are shown in Table 4.4.2. The value of R_V/R_H varies between 1.03 and 1.10 with an average value of 1.07. The value of R_T/R_H varies between 0.92 and 1.01 with an average value of 0.96. The value of R_V/R_T varies between 1.09 and 1.16 with an average value of 1.12. Theoretical ratios of R_V/R_H, R_T/R_H and R_V/R_T for self-avoiding coils are listed in Table 4.4.3, along with the results obtained in the studies on various polymer systems in good solvents. R_G/R_H values are also listed for comparison. Theoretical predictions for hard spheres and coils in the θ-state are included.

The average values of R_V/R_H in various systems are generally in good agreement with theoretical prediction except for polystyrene in tetrahydrofuran, which shows an 11% difference from the predicted value of 1.12. Polystyrene samples in other solvents also show rather large differences (~8%). Poly(α-methylstyrene) and polyisoprene show very good agreement with the theoretical value. The value obtained in this work for poly(MMA-co-AA) is 1.07 +/- 0.03, which is about 4% different from the predicted value of 1.12.

The average values of R_T/R_H in various systems are also in good agreement with the theoretically predicted value 1.02. In contrast to R_V/R_T, the R_T/R_H values obtained for polystyrene in various solvents are in better agreement than poly(α-methylstyrene) and polyisoprene, which show about a 9% difference from the predicted value. The R_T/R_H value obtained for poly(MMA-co-AA) in N-methylformamide in this work is 0.96 +/- 0.04, in a good agreement with the theoretical value.

The theoretical value for R_V/R_T for self-avoiding coils is 1.10. The values of R_V/R_T in Table 4.4.3 show, in general, good agreement with this value, except for polystyrene in tetrahydryfuran which deviates by about 10% The value obtained in this work is 1.11 +/- 0.03, which is in excellent agreement with the theoretically predicted value.

134

Table 4.4.3 Theoretical and experimental ratios between various radii

Sample	Solvent	R_V/R_H	R_T/R_H	R_V/R_T	R_G/R_H	Reference
Spheres		1.0	1.0	1.0	0.775	Yamakawa(1971)
Gaussian coil	θ-solvent	1.23	0		1.24	Oono (1983)
Self-avoiding coils	Good solvent	1.12	1.02	1.10	1.56	Oono (1983)
Polystyrene	toluene	1.04	0.98	1.06	1.47	Roover (1980), Hubber (1985)
	benzene	1.03	1.02	1.01	1.55	Nemoto (1984), Einaga (1979) Miyaki (1978)
	ethylbenzene	1.21	1.07	1.13	1.61	Venkataswamy(1986)
	tetrahydrofuran	1.00	1.00	1.00	1.35	Bhatt(1988,1989)
Poly (α-methylstyrene)	toluene	1.09	0.94	1.16	1.50	Noda (1970,1977) Kato (1970) Cotts (1990) Selser (1981)
Polyisoprene	cyclohexane	1.11	0.94	1.18	1.39	Davidson (1987)
		1.06	0.97	1.09	1.50	Tsunashima(1988)
Poly (MMA-co-AA)	N-methylformamide	1.07	0.96	1.11		this work

Although R_G values were not measured for the samples prepared in this work, the average R_G/R_H values obtained for other systems are also listed in Table 4.4.3. Except for polystyrene in tetrahydrofuran and polyisoprene in cyclohexane, there is good agreement between experimental and theoretical values.

The values of R_V/R_H, R_T/R_H and R_V/R_T obtained in this work are close to the theoretical values even for the lowest molecular weight sample. Similar results are obtained by Davidson et al (1987). Table 4.4.4 shows the result of their work on polyisoprene in cyclohexane. The R_T/R_H values for samples with molecular weight 15,200 and 23,400 are 0.92 and 0.93 respectively, indicating that they are already close to the asymptotic value. In this work, the value of R_T/R_H for the sample of lowest molecular weight sample ($M_W = 36400$) is 0.92. The R_V/R_H value for lowest molecular weight sample in the dimensional study (47,000) is similar to thoseof the highest molecular weight samples. The average values obtained are in good agreement with theory. The R_V/R_H value obtained in this work for a sample of similar molecular weight (56200) is 1.10. The results of Cotts et al (1990) and Selser (1981) also show that the R_T/R_H values reach that typical of very high molecular weight samples, probably the asymptotic value, at $M_W = 30,000$. The results of Huber et al (1985) show that the R_T/R_H ratio reaches its asymptotic value at molecular weights as low as 10,000.

In conclusion, we find that the dilute solution properties (or the sizes) of a random copolymer, composed of two monomers with very different polarities, follow the scaling law against molecular weight in a good solvent in the same manner as the homopolymers, and that the ratios between the various radii agree well with the theoretically predicted values.

Table 4.4.4   Ratios between sizes obtained by different methods
for polyisoprene in cyclohexane (Davidson et al, 1987)

MW, 10^{-4}	R_V/R_H	R_T/R_H	R_G/R_H
1.52		0.92	
2.34		0.93	
4.70	1.13		
5.25	1.13		
6.20	1.11	0.95	
10.1		0.94	
12.9	1.11		
15.6	1.11	0.94	1.45
30.2	1.10	0.94	1.42
36.6	1.10		1.40
58.1	1.10	0.96	1.38
92	1.12	0.98	1.40
167	1.05	0.93	1.29
342		0.94	
Average	1.11	0.94	1.39

References

M. Adam and M. Delsanti, J. Phys. (Paris), 37, 1045, 1976

A. Z. Akcasu and C. C. Han, Macromolecules, 12, 276, 1979

H. R. Allcock and F. W. Lampe, Contemporary Polymer Chemistry, 1981

B. J. Berne and R. Pecora, Dynamic Light Scattering, John Wiley & Sons, New York, 1976

M. Bhatt and A. M. Jamieson, Macromolecules, 21, 3015, 1988

M. Bhatt and A. M. Jamieson, Macromolecules, 22, 2724, 1989

N. C. Billingham, Molar Mass Measurements in Polymer Science, John Wiley & Sons, New York, 1977

J. Brandrup and E. H. Immergut, Eds., Polymer Handbook, Wiley Interscience, New York, 1975

J. C. Brown and P. N. Pusey, J. Chem. Phys., 62, 1136, 1975

C. D. Cantrell, Phys. Rev. Al., 672, 1970

B.Chu, The application of laser light scattering to the study of biological motion, Ed., J. C. Earnshaw and M. W. Steer, Plenum Press, New York, N.Y., 1983

E. A. Collins, J. Bares and F. W. Billmeyer, Jr., Experiments in Polymer Science, John Wiley & Sons, New York, 1973

P. M. Cotts and J. C. Selser, Macromolecules, 23, 2050, 1990

N. S. Davidson, L. J. Fetters, W. G. Funk, N. Hadjichristidis and W. W. Graessley, Macromolecules, 20, 2614, 1987

P. G. de Gennes, Macromolecules, 9, 587, 1976

P. G. de Gennes, Scaling Concepts in Polymer Physics, Cornell Univ. Press, Ithaca, 1979

J. F. Douglas and K. F. Freed, Macromolecules, 17, 2354, 1984

Y. Einaga, Y. Miyaki and H. Fujita, J. Polym. Sci., Polym. Phys. Ed., 17, 2103, 1979

A. Flamberg and R. Pecora, J. Phys. Chem., 88, 3026, 1984

P. J. Flory, J. Chem. Phys. 17, 303, 1949

P. J. Flory, Principles of Polymer Chemistry, Cornell Univ. Press, Ithaca, 1953

N. C. Ford, Jr., in Dynamic Light Scateering, R. Pecora Eds., Plenum Press, New York, 1985

K. F. Freed, S. Q. Wang, J. Roovers and J. F. Douglas, Macromolecules, 21, 2219, 1988

Goniometer Instruction Manual, Brookhaven Instrument Co., 1984

A. J. Gordon, The Chemist Companion, John Wiley & Sons, New York, 1972

K. Huber, W. Burchard and A. Z. Akcasu, Macromolecules, 18, 2743, 1985

Y. Kashiwagi, Y. Einaga and H. Fujita, Polym. J., 12, 271, 1980

T. Kato, K. Miyaso, I. Noda, T. Fujimoto and M. Nagasawa, Macromolecules, 3, 777, 1970

D.E. Koppel, J. Chem. Phys., 57, 4814, 1972

M. Kurata, Y Tsunashima, M. Iwama and K. Kamada, Polymer Handbook, Chapter , 1975

J. C. Le Guillou and J. Zinn-Justin, Phys. Rev. Lett., 39, 95, 1977

J. W. Mays and N. Hadjichristidis, Rev. Mocromol. Chem. Phys., C28 (3 & 4), 371, 1988

G. Meyerhoff and B. Appelt, Macromolecules, 12, 968, 1979

Y. Miyaki, Y, Einaga and H. Fujita, Macromolecules, 11, 1978

H. Morawetz, Macromolecules in Solution, Wiley Interscience, New York, 1975

N. Nemoto, Y. Makita, Y. Tsunashima and M. Kurata, Macromolecules, 17, 425, 1984

I. Noda, K. Mizutani and T. Kato, Macromolecules, 10, 618, 1977

I. Noda, K. Mizutani, T. Kato, T. Fujimoto and M. Nagasawa, Macromolecules, 3, 787, 1970

Y. Oono and M. Komoto, J. Chem. Phys., 78(1), 520, 1983

R. Pecora, Stanford, Personal Communications

D. L. Phillips, J. Assoc. Comput. Mach., 9, 84, 1962

S. W. Provencher, Macromol. Chem., 180, 201, 1979

S. W. Provencher[1], Comput. Phys. Commun., 27, 213, 1982

S. W. Provencher[2], Comput. Phys. Commun., 27, 229, 1982

S. W. Provencher, J. Hendrix, L. De Maeyer and N. Paulussen., J. Chem. Phys., 69, 4273, 1978

S. W. Provencher, CONTIN (Version 2) Users Manual, 1984

J. Roovers and P. M. Toporowski, J. Polym. Sci., Polym. Phys. Ed., 18, 1907, 1980

D. W. Schaefer, G. B. Benedek, P. Schofield and E. Bradford, J. Chem Phys., 55, 3884, 1971

J. C. Selser, Macromolecules, 14, 346, 1981

J. C. Selser, Macromolecules, 12, 909, 1979

S. S. Sorlie and R. Pecora, Macromolecules, 21, 1437, 1988

R. S. Stock and W. H. Ray, J. Polym. Sci., Polym. Phys. Ed., 23, 1393, 1985

Y. Tsunashima, M. Hirata, N. Nemoto and M. Kurata, Macromolecules, 21, 1107, 1988

S. Twomey, J. Assoc. Comput. Mach., 10, 87, 1963

H. Utiyama, H. Utsumi, Y. Tsunashima and M. Kurata, Macromolecules, 11, 506, 1978

D. W. Van Krevelen, Properties of Polymer , Elsevier, 1976

K. Venkataswamy, A. M. Jamieson and R. G. Petschek, Macromolecules, 19, 124, 1986

S. Q. Wang, J. F. Douglas and K. F. Freed, Macromolecules, 18, 2464, 1985

G. Weil and J. des Cloizeaux, J. Phys. (Les Ulis. Fr.), 40, 99, 1979

H. Yamakawa, J. Chem. Phys., 36, 2995, 1962

H. Yamakawa, Modern Theory of Polymer Solutions, Harper and Row, New York, 1971

Chapter 5 CONCLUSIONS AND SUGGESTIONS FOR FUTURE WORK

5.1 CONCLUSIONS

A copolymer of methylmethacrylate and acrylamide has been prepared and characterized. It has been demonstrated that the distribution of each monomer in the chain molecule is random. Fractionation was carried out and each fraction was characterized in terms of molecular weight, second virial coefficient, intrinsic viscosity and diffusion coefficient. It has been shown that the exponents of the power expressions for the second virial coefficient, intrinsic viscosity and diffusion coefficient against molecular weight agree well with the theoretically predicted values in the asymptotic range, although these results are not conclusive due to the narrow range, and relatively low values of molecular weight investigated. It has also been shown that the ratio between the equivalent hard sphere radii calculated from the measured second virial coefficient, intrinsic viscosity and diffusion coefficient show good agreement with the theoretically predicted ratios for nondraining self-avoiding flexible linear chain molecules. These results indicate that random copolymers behave similarly, in their scaling behavior, to homopolymers.

5.2 SUGGESTIONS FOR FUTURE WORK

The measurement of dilute solution properties carried out in this work employed samples with rather low molecular weight that covers only one decade. The polydispersity of these samples was about 1.3. For the more quantitative exponent of power expression and better comparison with theory, the study should be extended to higher molecular weight samples that cover a wider range. Also the samples should have very low polydispersity. Anionic copolymerization has been used widely for the preparation of polystyrene standards (Odian, 1981). Polyisoprene with polydispersity less than 1.1 was also prepared by anionic

polymerization (Davidson et al, 1987). This method might also be a useful way for the preparation of poly(MMA-co-AA) with very low polydispersity, although a careful study of reactivity ratios would be required since the monomerreactivities may be different in anionic polymerization.

The radii of gyration for the samples studied in this work were not measured, because the molecular sizes were too small to observe the angular dependence of average scattered intensity. Measuring the radius of gyration using a short-wavelength scattering technique, such as neutron scattering, would provide complete set of experimental ratios for comparison with the theoretical predictions.

The polydispersities of the samples were roughly estimated from the second moment of cumulant analysis. Because the weight average molecular weight is already determined, only the measurement of number average molecular weight (by membrane osmometry) is necessary for the determination of polydispersity. The value thus obtained can then be used for a better evaluation of the effect of polydispersity on the various dilute solution properties measured in this work. It may be also interesting to compare the M_w/M_n obtained in this way with the results from the cumulant analysis.

The copolymer used in this work is similar to proteins, because it is composed of two monomers with very different polarities which are distributed randomly in the polymer chain. Methylmethacrylate and acrylamide in polymer chain can be considered as the hydrophobic and hydrophillic amino acids in the protein , respectively. Hence, it may be very interesting to study the dilute solution properties of these molecules in a bad solvent condition where the molecules may fold (collapse) like proteins. Recently, a theory for the folding and stability of a heteropolymer rmolecule was developed by Dill (1985). This theory predicts conditions under which molecular collapse occurs.

Some work has been tried in this direction, using the samples studied in this work, to detect the transition of the copolymer molecule from an unfolded (coil-like) state to a folded (collapsed) state, but the experiment was hampered by aggregates formed because the scattering intensity from these aggregates dominates over the intensity from other single molecules. It is thought that these aggregates are formed due to the distribution in composition and molecular weight of the samples used. For example, the highest molecular weight species in the polydispersed (although fractionated) sample may aggregate at the solvent condition where the other species may collapse. Similarly, some species with the largest deviation in composition may aggregte at the solvent condition where the other species may collapse. Actually Fields et al (1990) showed in their theory for protein aggregation that a small change in hydrophillicity or hydrophobicity may change the aggregation behavior substantially. Hence, it is thought to be very important to use a extremely narrowly-dispersed sample to study the folding behavior of these copolymer molecules.
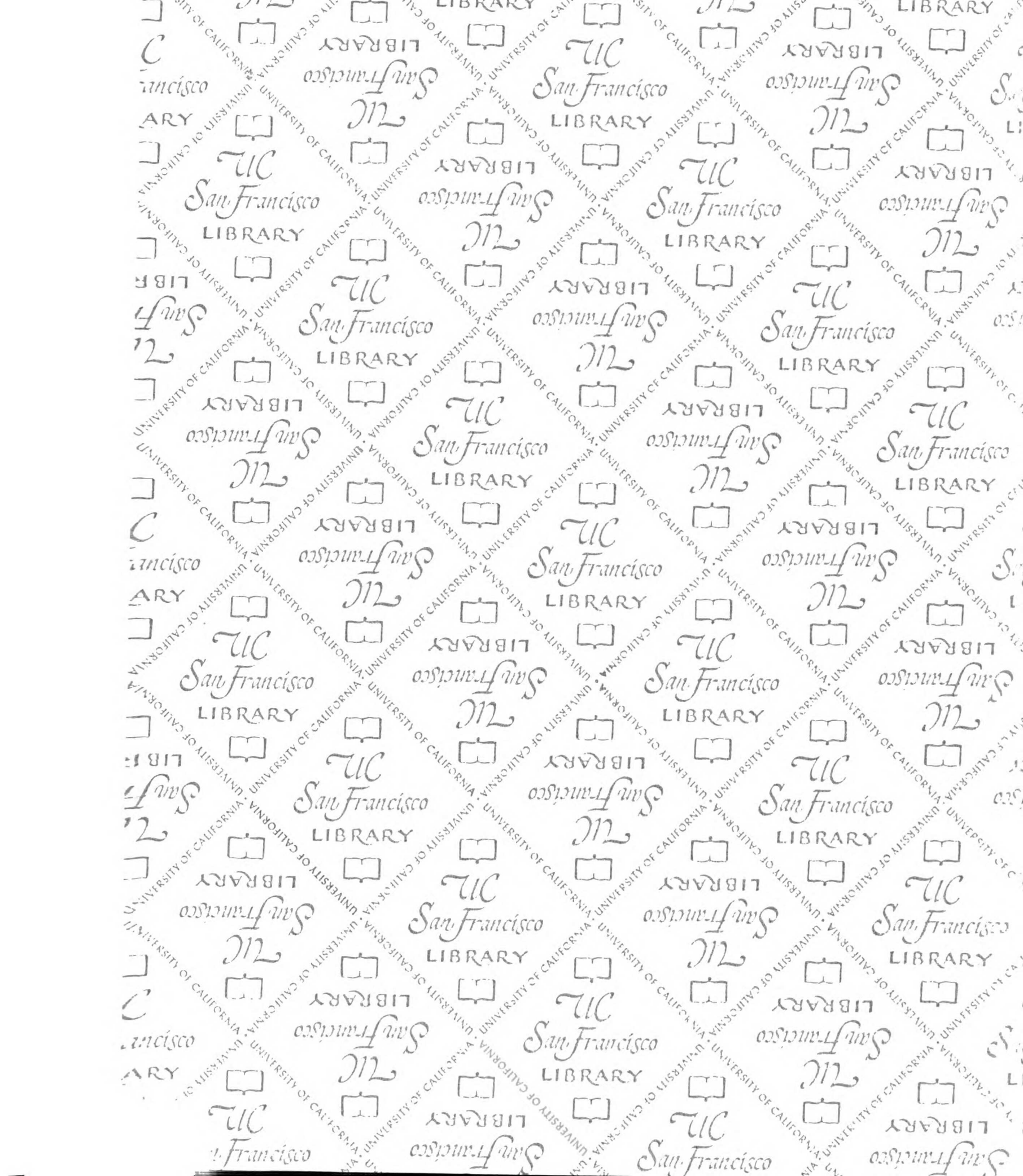
References

N .S. Davidson, L. J. Fetters, W. G. Funk, N. Hadjichristidis and W.W. Graessley, Macromolecules, 20, 2614, 1987

K. A. Dill, Biochemistry, 24, 1501, 1985

G. B. Fields, D. O. V. Alonso and K. A. Dill, personal communications, 1990

G. Odian, Principles of Polymerization, 2nd ed., John Wiley & Sons, New York,1981